Scalar–Fermion Theories on the Lattice

Mikhail Alexeevich Stephanov

Department of Physics
University of Oxford

A Thesis submitted for the degree of
Doctor of Philosophy

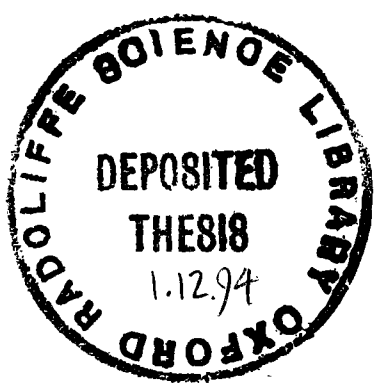

Jesus College

July 94

Abstract

We study scalar–fermion models with Yukawa interaction on a space–time lattice. Such models can describe the Higgs sector of the Standard Model in the case when the Higgs particle is very heavy (few hundred GeV) and there are very heavy fermions whose masses are due to their Yukawa interactions with the Higgs field. We study a realistic model with four component scalar field as well as simplified models with one and two component scalar fields. We use a mean field approximation to calculate equations for critical lines in the large d (dimension of space–time) limit. These lines are in very good agreement with available Monte Carlo data for the models at $d = 4$. We calculate fermion correlation functions in the mean field and large d approximations to study properties of different phases in the lattice models. We find two distinct phases with vanishing expectation values of the scalar field. One (at small Yukawa coupling Y) contains massless fermions, while in the other (at large Y) the fermions have masses larger than the scale given by the inverse lattice spacing. We find that in the latter phase fermions can form bosonic bound states. These states show up as poles in a four–fermion correlator. We discuss possible continuum limits in the lattice scalar–fermion models. In particular, we show that a theory defined near the critical line separating the disordered phase from the phase with antiferromagnetic order is not unitary.

Acknowledgements

I would like to express my gratitude to Mike Teper, my supervisor, for his constant support and encouragement. I enjoyed and I benefited very much from numerous discussions with him. His suggestions improved the style of the thesis considerably.

It is my pleasure to thank Maxim Tsypin, my colleague and friend. Many ideas presented in this work were born and shaped in our discussions.

I wish to thank Mikhail Voloshin for drawing my attention to the problem of a heavy Higgs and fermions, for encouragement and for many valuable suggestions.

I am very grateful to Vladimir Yakovlevich Fainberg under whose supervision I began my research back in Moscow.

My thanks also go to Jiri Jersák and his colleagues in Jülich for their interest in my work and many critical discussions. The numerical results obtained by this group were very valuable to this study.

I have enjoyed many helpful conversations with members of Theoretical Physics at Oxford.

The financial support of Jesus College Oxford and the Soros Foundation is acknowledged with gratitude.

Contents

Chapter 1

Introduction

1.1 Motivation

Scalar fields are one of the most important ingredients of the Weinberg–Salam–Glashow unified theory of weak and electromagnetic interactions [1]. These fields make the W and Z vector bosons massive via the Higgs mechanism [2].

The vector bosons mediating weak interactions appear naturally if one makes the $SU(2)$ symmetry which transforms particles in the weak isospin doublets (e.g., neutrino and left chirality electron) local. Local gauge invariance also ensures that the theory of vector gauge bosons is renormalisable. Renormalisability of the theory is important to enable us to make physical predictions using finite number of parameters. The problem of introducing masses for the W and Z bosons into the theory is that the mass term breaks the local gauge invariance explicitly and destroys renormalisability of the theory. The solution for this problem is the so–called Higgs mechanism.

One includes in the theory a scalar field which transforms under $SU(2)$ weak isospin symmetry as a doublet — the Higgs field. If one neglects the effect of gauge fields on the dynamics of the scalar field (which is often a good approximation as the electroweak coupling is small) one can distinguish two phases of the scalar field theory: symmetric and broken.

In the symmetric phase vacuum expectations of all the observables which are not invariant under the $SU(2)$ symmetry vanish. In other words the vacuum of the theory is symmetric. The spectrum of such a pure scalar theory consists of a complex doublet of scalar particles of the same mass (four degenerate real scalar particles). This phase is analogous to the paramagnetic phase of a ferromagnet.

The analogue of the broken phase is the ferromagnetic phase of a ferromagnet.

In this phase the vacuum of the theory is not invariant under the $SU(2)$ symmetry: the vacuum expectation value of the scalar field (mean magnetisation) in the limit of infinite volume of the system has nonzero value. Such a phenomenon, when the Lagrangian is invariant under some symmetry while the vacuum state is not, is called spontaneous breaking of the symmetry. The spectrum of the theory consists then of a triplet of massless particles (Goldstone particles [3]) and one massive real scalar particle.

It is the broken phase that is relevant for the electroweak theory. The interaction with the vector gauge fields removes massless Goldstone particles from the spectrum: each Goldstone field combines with two transverse components of the gauge vector field to form a massive vector field. The mass is proportional to the gauge coupling and the vacuum expectation value of the scalar field. The remaining fourth particle, neutral scalar, is the Higgs boson.

The mass of the Higgs boson is a free parameter of the theory. One of the interesting questions is: how heavy can this particle be? In the Standard Model the scalar sector of the theory is described by the Lagrangian:

$$\mathcal{L} = \frac{1}{2}\partial_\mu \Phi^\dagger \partial^\mu \Phi + \lambda(\Phi^\dagger \Phi - v^2)^2. \tag{1.1}$$

The Higgs field Φ is a complex doublet. The mass of the Higgs particle is related to the coupling λ at the tree level as $m_H = \sqrt{8\lambda}v$, where the vacuum expectation value $v = (\sqrt{2}G_F)^{-1/2} \simeq 246$ GeV is determined by the Fermi constant of the weak interactions G_F. Thus large m_H corresponds to large λ. In this case a nonperturbative treatment is desirable [7].

One of the most powerful non-perturbative approaches is the lattice regularisation. In this approach one replaces the continuous space–time by a discrete set of points — the sites of a lattice. This makes possible to apply methods of statistical mechanics to such a system, e.g., mean field, strong coupling, $1/d$, high temperature or other expansions, etc. A lattice theory in a finite volume has finite, although large, number of degrees of freedom. Physical quantities (masses, amplitudes, etc.) in such a system can be computed numerically using Monte Carlo method [8]. For example, it is possible to obtain an upper bound on the effective λ in the theory (1.1) and consequently a bound on the mass of the Higgs boson: $m_H \leq 700 - 800$ GeV [9–13] (see [14–19] for reviews).

The other important role of the Higgs field in the Standard Model is to provide fermions with masses. A mass term for the fermion (e.g., electron) mixes states with left and right chirality. The right chirality states do not participate in the weak interaction, i.e., they are singlets with respect to the weak isospin group $SU(2)$ (they have isospin 0). Left chirality states transform as doublets (isospin 1/2). Thus an

explicit mass term breaks $SU(2)$ gauge symmetry and destroys the renormalisability of the theory. Yukawa interaction with the Higgs field (which has isospin 1/2), however, is gauge invariant. In the broken phase the fermion acquires a mass which is proportional to the Yukawa coupling and the vacuum expectation value of the Higgs field.

The scenario with the heavy Higgs we described above contains only one large coupling constant λ. Then it is possible to retain only the Higgs sector and neglect interactions of Φ with gauge fields and fermions [7]. However, this is only possible if all fermion masses are much smaller than v. If this is not the case there are at least two large coupling constants in the theory: the Higgs self coupling λ and the Yukawa coupling. The interaction with the gauge fields and the Yukawa interactions with light fermions can again be neglected in the first approximation as they are governed by small couplings. The top quark with the mass around 170 GeV might be still light enough to treat its Yukawa coupling perturbatively also. However, if another generation of heavy fermions[1] with masses around few hundred GeV exists then their interaction with the Higgs field must be treated nonperturbatively.

An interesting question is then: how heavy can these fermions be? And also, how does the presence of a heavy fermion, or, in other words, a strong Yukawa interaction, affect the upper bound on the Higgs mass obtained in the study of the pure scalar model (1.1)? The answer to these questions requires understanding of the dynamics of the scalar–fermion Yukawa theories at strong Yukawa and Higgs self couplings. Thus one arrives at the idea to investigate such theories in nonperturbative lattice approach.

1.2 The model

Let us go back to the Lagrangian (1.1) for the Higgs sector of the Standard Model. Introducing real components ϕ^0, ϕ^1, ϕ^2, ϕ^3 of the complex Higgs doublet in the following way:

$$\Phi = \begin{pmatrix} \phi^0 + i\phi^3 \\ i\phi^1 - \phi^2 \end{pmatrix}, \tag{1.2}$$

one can rewrite this Lagrangian in the form:

$$\mathcal{L} = \frac{1}{2}\partial_\mu \phi^i \partial^\mu \phi^i + \lambda(\phi^i \phi^i - v^2)^2, \tag{1.3}$$

where the sum over repeating indices i is implied. One can see that the symmetry of the Higgs sector of the Standard Model described by (1.1) or (1.3) is in fact $O(4)$.

[1]The lightest fermion in that generation should be heavier than half of the mass of the Z boson to avoid contribution to the width of the Z resonance [5,6].

The potential of the Higgs field has an $O(4)$ symmetric valley of minima at $|\phi| \equiv \sqrt{\phi^i \phi^i} = v$. The spontaneous symmetry breaking occurs as the Higgs field vacuum expectation value assumes some direction in the $O(4)$ space, say ϕ^0, i.e., $\langle \phi^i \rangle = v\delta_{0i}$. The mass of the Higgs particle is determined by the curvature (second derivative) of the potential in the radial direction around the vacuum expectation value. That is: $m_H = \sqrt{8\lambda}v$.

Now let us consider a doublet of massive fermions in the Standard Model described by a doublet Ψ of Dirac fermion fields. The left-handed chirality component of this field: Ψ_L, is a doublet under the weak isospin:

$$\Psi_L = \begin{pmatrix} \psi_L^1 \\ \psi_L^2 \end{pmatrix}.$$

Each of the components ψ_L^1 and ψ_L^2 is a Weil spinor, or a Dirac spinor but with only two independent components, in other words, a chiral projection of the Dirac field Ψ:

$$\Psi_L = \frac{1}{2}(1 - \gamma_5)\Psi.$$

The right-handed components ψ_R^1 and ψ_R^2:

$$\Psi_R = \frac{1}{2}(1 + \gamma_5)\Psi,$$

are singlets under the weak isospin.

The interaction of the fermion doublet with the Higgs field Φ is described by the Lagrangian:

$$\mathcal{L}_F = i\bar{\Psi}_L \partial\!\!\!/ \Psi_L + i\bar{\psi}_R^1 \partial\!\!\!/ \psi_R^1 + i\bar{\psi}_R^2 \partial\!\!\!/ \psi_R^2 - y_1(\bar{\Psi}_L \Phi \psi_R^1 + h.c.) - y_2(\bar{\Psi}_L \tilde{\Phi} \psi_R^2 + h.c.). \quad (1.4)$$

where

$$\tilde{\Phi} \equiv -i\sigma_2 \Phi^* = \begin{pmatrix} 0 & -1 \\ 1 & 0 \end{pmatrix} \begin{pmatrix} \phi^0 - i\phi^3 \\ -i\phi^1 - \phi^2 \end{pmatrix} = \begin{pmatrix} i\phi^1 + \phi^2 \\ \phi^0 - i\phi^3 \end{pmatrix}, \quad (1.5)$$

is a conjugate of Φ which transforms under the $SU(2)$ group as a doublet (as Φ itself). The Yukawa term in a more explicit form is:

$$\mathcal{L}_Y = -y_1 \left[(\bar{\psi}_L^1, \psi_L^2) \begin{pmatrix} \phi^0 + i\phi^3 \\ i\phi^1 - \phi^2 \end{pmatrix} \psi_R^1 + h.c. \right] -$$
$$-y_2 \left[(\bar{\psi}_L^1, \psi_L^2) \begin{pmatrix} i\phi^1 + \phi^2 \\ \phi^0 - i\phi^3 \end{pmatrix} \psi_R^2 + h.c. \right], \quad (1.6)$$

where we introduced real components ϕ^i of the Higgs doublet according to (1.2) and (1.5). Let us assume again that the direction of the symmetry breaking is ϕ^0 and

$\langle\phi^0\rangle = v$. If we neglect fluctuations of the ϕ field around its vacuum expectation value we find for the masses of the fermions: $m_1 = y_1 v$, $m_2 = y_2 v$.

To simplify the model let us consider the case when $y_1 = y_2 \equiv y$.[2] Then one can simplify (1.6):

$$\mathcal{L}_Y = -y(\bar{\psi}_L^1, \bar{\psi}_L^2) \begin{pmatrix} \phi^0 + i\phi^3, & i\phi^1 + \phi^2 \\ i\phi^1 - \phi^2, & \phi^0 - i\phi^3 \end{pmatrix} \begin{pmatrix} \psi_R^1 \\ \psi_R^2 \end{pmatrix} + h.c. =$$
$$= -y\bar{\Psi}_L(\phi^0 + i\boldsymbol{\tau}\cdot\boldsymbol{\phi})\Psi_R + h.c., \qquad (1.7)$$

where we introduced the three component vector $\boldsymbol{\phi} = (\phi^1, \phi^2, \phi^3)$ and the column:

$$\Psi_R = \begin{pmatrix} \psi_R^1 \\ \psi_R^2 \end{pmatrix}.$$

The Pauli matrices are as usual: $\boldsymbol{\tau} = (\tau_1, \tau_2, \tau_3)$.

Note that in this limit ($y_1 = y_2$) the Lagrangian is symmetric under the $O(4)$ rotations of the 4-component scalar field ϕ^i. This symmetry is a product of $SU(2)_L$ which rotates doublets of left-handed fermion fields (local gauge symmetry in the electroweak theory) and $SU(2)_R$ which rotates the right-handed components of the fermion fields and is due to the degeneracy $y_1 = y_2$. Recalling that $\Psi_R + \Psi_L = \Psi$ and $\Psi_R - \Psi_L = \gamma_5\Psi$ one can rewrite the Lagrangian of the model in the form:

$$\mathcal{L}_F = i\bar{\Psi}\partial\!\!\!/\Psi - y\bar{\Psi}(\phi^0 + i\gamma_5\boldsymbol{\tau}\cdot\boldsymbol{\phi})\Psi, \qquad (1.8)$$

Next section explains how we obtain a lattice version of the model described by (the sum of) the Lagrangians (1.3) and (1.8).

1.3 The lattice model

1.3.1 Scalar sector

Let us start with the Higgs Lagrangian in the form (1.3). In fact, for the sake of simplicity, let us consider a scalar field with one real component ϕ first. The Lagrangian has the form:

$$\mathcal{L} = \frac{1}{2}\partial_\mu\phi\partial^\mu\phi + \lambda(\phi^2 - v^2)^2. \qquad (1.9)$$

[2] For a very heavy doublet (several hundred GeV) this could be a good approximation. There is an experimental upper bound on the mass splitting within the doublet. Radiative corrections to the ρ parameter ($\rho = m_W^2/(m_Z^2\cos^2\theta_W)$) become too large if $m_1 - m_2$ exceeds 200 GeV or so [4–6].

The field ϕ is a function of time argument t and three space arguments $\boldsymbol{x}$: $\phi = \phi(t, \boldsymbol{x})$.

To compute the amplitudes in the quantum theory (1.9) we need to sum over all "trajectories" $\phi = \phi(t, \boldsymbol{x})$. Each trajectory enters this sum with the weight proportional to e^{iS}, where

$$S = \int dt\, d^3\boldsymbol{x}\mathcal{L} \tag{1.10}$$

— is the action on a given trajectory $\phi(t, \boldsymbol{x})$. One of the most useful quantities is the generating functional for the Green functions:

$$Z[J] = \int \mathcal{D}\phi \exp\left\{iS + i\int dt\, d\boldsymbol{x}\, J(x)\phi(x)\right\}. \tag{1.11}$$

Here $x \equiv (t, \boldsymbol{x})$ is a 4-vector, and the sum over all configurations (trajectories) is denoted by $\int \mathcal{D}\phi$. Differentiating Z with respect to J one can obtain vacuum expectation values of products of the fields $\varphi(x)$ — the Green functions. For example, the vacuum expectation value of ϕ is:

$$\langle\phi(x)\rangle = \frac{1}{Z}\frac{\delta Z}{i\delta J(x)}.$$

The next step is to consider the analytical continuation of our model to pure imaginary time argument of the field $\phi(x)$. Here we assume that such a procedure (sometimes called Wick, or Euclidean, rotation) is well defined. We simply substitute: $t = -ix_4$. Then the space of 4-vectors (x_1, x_2, x_3, x_4) is simply a 4-dimensional Euclidean space with the metric (the distance between two points) given by:

$$(\Delta s)^2 = (\Delta x_1)^2 + (\Delta x_2)^2 + (\Delta x_3)^2 + (\Delta x_4)^2 \equiv \Delta x_i \Delta x_i.$$

Lorentz transformations of space–time become Euclidean rotations.

The reason for such a step is that Euclidean quantities are usually better defined. Also, the system in Euclidean space resembles to a great extent a statistical system in 4–dimensional space. Indeed, the generating function Z for the Green functions after rotation to the Euclidean space has the form:•

$$Z[J] = \int \mathcal{D}\varphi \exp\left\{-S_E + \int d^4x\, J(x)\varphi(x)\right\}, \tag{1.12}$$

where the Euclidean analogue of the action is:

$$S_E \equiv -iS(t = -ix_4) = \int d^4x \left[\frac{1}{2}\partial_\mu\varphi\partial_\mu\varphi + \lambda(\varphi^2 - v^2)^2\right]. \tag{1.13}$$

Notice that the Euclidean action S_E is nonnegative.

The functional Z has the form of a partition function of a (classical) statistical system in 4–dimensional space. The energy (actually, the energy divided by kT) in

this system is given by S_E.[3] This analogy becomes even more transparent after we put our theory on the lattice.

Such a correspondence between a quantum field theory and a statistical system allows us to employ methods developed in condensed matter theory such as mean field, high/low temperature expansions, duality transformations, etc. to gain information about the theory and compute some quantities. Finally, the Monte Carlo method can be used to study lattice field theories numerically.

So far, however, we do not really have a definition for the sum over all configurations of the field $\phi(x)$ in (1.12) which is symbolically denoted by $\int \mathcal{D}\phi$. One way to define this summation is to replace the continuous space–time by a discrete set of points of a lattice. Then we consider the field ϕ_x which is defined on the sites x of this lattice. The sum over all configurations of such a field is a multiple integral over the values ϕ_x in each site. If the volume of the system is finite so is the number of the integration variables ϕ_x and the procedure is well defined. In the limit when the lattice spacing a goes to zero such procedure will define for us the summation over all continuum field configurations.

To use this procedure to compute the partition function Z we also need to define the form of the action S for finite lattice spacing. This action should be a function of the lattice variables ϕ_x. An *a priori* requirement is that it should in the limit $a \to 0$ reproduce the continuum action (1.13).[4]

There is a considerable freedom in choosing the action that satisfies this requirement. In principle, there is no guarantee that the *quantum* theory resulting in the continuum limit will be the same for all such choices. Nevertheless, in most reasonable cases it is the same.

The situation is a bit more complicated, however. One should realise, that the continuum limit of a lattice theory is not simply a limit $a \to 0$. What is really needed to approximate a continuum theory by a lattice one is to make a much smaller than some physical scale, e.g., the Compton wavelength m^{-1} of a particle in such a theory. In practice this means that the limit $a \to 0$ is accompanied by tuning the parameters of the lattice action in such a way as to keep the physical scale fixed. The parameters of the lattice (bare) action of the model approach then a special (critical) point. Only in such points a continuum limit can be defined (see more on the question of the continuum limit in sections 1.3.2 and 3.4). With this in mind one can reformulate the question of the ambiguity of the lattice action as

[3]Note that S_E has nothing to do with the energy in the original quantum field theory in Minkowski space.

[4]The lattice action should also ensure that the integrals over ϕ_x exist. This is not a problem usually.

a question of choosing a critical point in the parameter space where the continuum limit is to be taken.

One way to deal with such an ambiguity is to employ some other definition of the path integral. Then one can use another, dynamical, *a posteriori*, requirement that the quantum theory produced by the lattice action in the continuum limit should map onto such a definition. However, practically, for most cases the only alternative definition of the path integral that can be used in such a way is based on perturbation theory: expansion in powers of a small coupling constant.

For strongly coupled theories the lattice regularisation is often the only available definition for the path integral. In such a situation the way one can proceed is to use some sensible lattice regularisation as a definition of a given quantum theory. The lattice actions that produce the same quantum theory in the continuum limit are then said to belong to the same *universality class.*

Now we turn to our pure scalar model where the situation is rather simple: practically any straightforward lattice approximation of (1.13) will give the same quantum theory in the continuum limit.

Let us assume the lattice to be a simple hypercubic one. The points of the lattice have coordinates $x \equiv (x_1, x_2, x_3, x_4) = (n_1 a, n_2 a, n_3 a, n_4 a)$, where n_μ are integer numbers. The discretisation of the potential term in (1.13) is straightforward. For the derivative in the gradient term we choose:

$$\partial_\mu \phi \to \frac{1}{a}(\phi_{x+\hat{\mu}a} - \phi_x), \tag{1.14}$$

where $\hat{\mu}$ is a unit vector in the μ–direction: e.g., $\hat{2} = (0,1,0,0)$. Finally, our lattice action for the scalar model (1.13) is:

$$S = \frac{1}{2a^2} a^4 \sum_{x,\mu} (\phi_{x+\hat{\mu}a} - \phi_x)^2 + \lambda a^4 \sum_x (\phi_x^2 - v^2)^2. \tag{1.15}$$

Factors a^4 are elements of the 4–volume.

The partition function is then:

$$Z = \int \prod_x d\phi_x \, \exp\left\{ -S + a^4 \sum_x J_x \phi_x \right\}. \tag{1.16}$$

where J_x is the source for the lattice field ϕ_x. It is convenient to rescale all dimensionful quantities: ϕ_x, v, x with appropriate powers of a to replace them by dimensionless quantities $\check{\phi}_x$, $\check{v}$, $\check{x}$:

$$\check{\phi}_x = a\phi_x, \quad \check{v} = av, \quad \check{x} = x/a. \tag{1.17}$$

We shall drop tildes in what follows. In other words, we use a as a unit of length in the lattice theory. This amounts to setting $a = 1$ in the formulas. We shall only

need to use some other (physical) units of length to discuss the continuum limit $a \to 0$. Thus our lattice action in lattice units takes the form:

$$S = \frac{1}{2}\sum_{x,\mu}(\phi_{x+\hat{\mu}} - \phi_x)^2 + \lambda\sum_x(\phi_x^2 - v^2)^2. \tag{1.18}$$

Now we simplify the model by considering the limit $\lambda = \infty$. The physical reason behind this is the following. As discussed above, larger Higgs masses correspond to larger values of the *bare* Higgs self coupling λ. For large λ the relation $m_H = \sqrt{8\lambda}v$ does not hold, but nonperturbative lattice studies of the Higgs sector show that the mass of the Higgs is an increasing function of λ for arbitrarily large λ and the limit $\lambda \to \infty$ is not singular [20].[5] Thus to estimate the upper bound on the Higgs mass one should consider the lattice model with $\lambda = \infty$.

In this limit the factor $\exp\{-\lambda\sum_x(\phi_x^2 - v^2)\}$ in the integrand of the partition function (1.16) restricts the integration over ϕ_x in each site to the summation over $\phi_x = \pm v$. The partition function of the scalar model takes the form:

$$\begin{aligned} Z &= \sum_{\{\phi_x = \pm v\}} \exp\left\{\sum_{x,\mu}\phi_{x+\hat{\mu}}\phi_x + \sum_x J_x\phi_x\right\} = \\ &= \sum_{\{\hat{\phi}_x = \pm 1\}} \exp\left\{v^2\sum_{x,\mu}\hat{\phi}_{x+\hat{\mu}}\hat{\phi}_x + \sum_x h_x\hat{\phi}_x\right\}, \end{aligned} \tag{1.19}$$

where we expanded $(\phi_{x+\hat{\mu}} - \phi_x)^2 = -2\phi_{x+\hat{\mu}}\phi_x + 2v^2$ and dropped the constant $2v^2$ from the action. We also introduced $\hat{\phi}_x = \phi_x/v$ and $h_x = vJ_x$.

The formula (1.19) is the partition function of the Ising model: a statistical system of spins (two state systems) $\hat{\phi}_x = \pm 1$ living on the sites of the lattice. The energy of the system is the sum of the energies of the interactions of the nearest neighbours. The energy of the interaction between two spins $\hat{\phi}_x$ and $\hat{\phi}_{x+\hat{\mu}}$ is $-\mathcal{J} < 0$ if they are in the same state and $+\mathcal{J}$ if they are in different states. Such a system (at zero external field h_x) can be in either of two phases depending on the value of $v^2 \equiv \mathcal{J}/kT$: symmetric or broken. The phases are distinguished by the order parameter, the mean magnetisation: $\sum_x \hat{\phi}_x/N$, where N is the total number of sites. As we know for the electroweak theory the broken phase is the relevant one.

The realistic theory with four component scalar field (1.3) can be discretised similarly. The limit $\lambda \to \infty$ corresponds to freezing the length of the vector ϕ^i: $\phi^i\phi^i = v^2$. Introducing unit vectors $\hat{\phi}_x^i = \phi_x^i/v$ we obtain for the partition function:

$$Z = \int\prod_x d\mu_x \exp\left\{v^2\sum_{x,\mu}\hat{\phi}_{x+\hat{\mu}}^i\hat{\phi}_x^i + \sum_x h_x^i\hat{\phi}_x^i\right\}. \tag{1.20}$$

[5] In the case when interaction with a heavy fermion is present this question was not studied nonperturbatively, to our knowledge. However, it is sensible to expect that larger Higgs masses correspond to larger λ's in this case also. This is true in perturbation theory [21,22].

The integration $\int d\mu_x$ in each site x is over the unit sphere covered by the vector $\hat{\phi}_x^i$.

1.3.2 Continuum limit

Now we can discuss the question of the continuum limit $a \to 0$. The lattice spacing a is a dimensionful quantity and we need to define some unit of length to measure it in. Clearly, it should be some physical scale in the theory, for example, the (inverse) mass of a particle in the spectrum (the Higgs in our case). It means we want to take the limit $am_H \to 0$. This is the same as to say that the mass measured in lattice units $\tilde{m}_H \equiv am_H$ goes to zero. In Euclidean space the mass determines exponential fall-off of the propagator (correlator): $\langle \phi_x \phi_y \rangle \to e^{-m_H|x-y|}$ at large distances $|x-y|$, i.e., $1/m_H$ is the correlation length. The limit $am_H \to 0$ means that the correlation length measured in the units of a: $\tilde{\xi} = 1/m_H a$ diverges. In statistical systems this happens when we approach the critical point of a second order phase transition.

The Ising model in 4 dimensions has a critical point at some (finite) value of $v^2 = v_c^2$. This point separates the symmetric and the broken phases. The transition is known to be of the second order, i.e., the correlation length in lattice units diverges as $v^2 \to v_c^2$. The continuum limit relevant for the Higgs sector of the electroweak theory is obtained by approaching the critical point from the broken phase ($v^2 \to v_c^2 + 0$).

The correlation length in the Ising model is a function of the parameter v^2: $\tilde{\xi} = \tilde{\xi}(v^2)$. Another way to say this is that the lattice spacing a in physical units ($1/m_H$) is a function of the parameter v^2 in the lattice action: $a = (m_H \tilde{\xi}(v^2))^{-1}$. We see that the role of the parameter v^2 is to determine how close we are to the continuum limit $a \to 0$ (more precisely: $am_H \to 0$). There are no more free parameters in the theory.

It is also useful to use the following terminology. The lattice introduces the cutoff for the minimum wavelength ($2a$) in the fluctuations of the fields. In other words, it cuts off the high frequency modes of the fields at the scale of $\Lambda \sim 1/a$. The limit $am_H \to 0$ can then be interpreted as the limit of infinite frequency or momentum cutoff: $\Lambda/m_H \sim (am_H)^{-1} \to \infty$.

It is interesting to see what happens if we consider the theory (1.18) at finite λ. The study of such ϕ^4 theories shows that for all $\lambda > 0$ there is a second order phase transition point at some $v^2 = v_c^2(\lambda)$ and the continuum limit is always the same: a noninteracting, free theory [24]. The role of the parameter λ is only to change the form of the dependence of the correlation length on v^2: $\tilde{\xi} = \tilde{\xi}(v^2, \lambda)$. One can also introduce other parameters into the lattice action (1.18), e.g., ϕ^6 terms or change

the form of the derivative terms. The continuum limit will still be the same and these parameters only change the relation between v^2 and $\tilde{\xi}$. This means that all such theories belong to the same universality class: the universality class of the Ising model. One can say that the critical point corresponding to this universality class has only one relevant parameter: v^2.

The phenomenon that the continuum limit of the ϕ^4 theory is a free theory is often called triviality [24]. Such a phenomenon was first discussed in the context of quantum electrodynamics [25]. It means that we cannot define a continuum limit for the interacting ϕ^4 theory. In other words, if we start with some bare ϕ^4 coupling λ then due to quantum fluctuations this coupling will be screened by a cloud of virtual scalar particles and the effective coupling λ_{eff} at some distance scale R (or momentum scale $\mu = 1/R$) will be smaller. The effective coupling will be a function of the scale at which it is measured and the cutoff: $\lambda_{\text{eff}}(\mu/m_H, \Lambda/m_H)$. It is convenient to define λ_{eff} at the scale $\mu = m_H$. This coupling is related to the Higgs mass via: $m_H = \sqrt{8\lambda_{\text{eff}}}(246 \text{ GeV})$. As we remove the cutoff: $\Lambda/m_H \to \infty$, the effective coupling λ_{eff} vanishes.

In this situation the best we can do to save the interaction is to say that the ϕ^4 theory can be defined only for energies/momenta below some cutoff scale of order Λ. Then we imagine that there are also other fields in the theory for which the lowest fluctuation frequencies are of order Λ, so that they are not excited by our low frequency experiments, but which change the behaviour of the theory in such a way that it becomes consistent for arbitrarily high energies. In other words, we view our ϕ^4 Higgs theory as an effective theory which one obtains by integrating out all fluctuations with frequencies greater than Λ. After all, we expect some new physics beyond the Standard Model to appear at some higher energy scale and the Standard Model to be an effective low energy theory which describes physics below this scale.

The upper bound on the Higgs mass arises when we demand that our effective theory for the Higgs particle is valid until some energy scale Λ. Then for given Λ (more precisely, Λ/m_H) the largest λ_{eff} and thus the largest Higgs mass is obtained for the bare theory with $\lambda = \infty$. This mass becomes larger as we decrease the cutoff. Clearly, when Λ is of the order m_H, the effective theory does not make sense anymore. The precise definition of the lowest ratio Λ/m_H is not obvious, but for $\Lambda/m_H > 3$ or so one obtains the upper bound: $m_H < 700 - 800$ GeV.

1.3.3 Adding fermions

We start from the continuum action (1.8). As in the scalar case we first need to make the rotation to the Euclidean space. We define this procedure as follows. As usual: $t = -ix_4$. The derivative term in the fermion action takes the form:

$$i\bar{\Psi}\partial\!\!\!/\Psi \equiv i\bar{\Psi}(\gamma_0\frac{\partial}{\partial t} - \gamma_m\frac{\partial}{\partial x^m})\Psi = i\bar{\Psi}(i\gamma_0\frac{\partial}{\partial x_4} - \gamma_m\frac{\partial}{\partial x^m})\Psi \equiv -\bar{\Psi}(\gamma_\mu^E\frac{\partial}{\partial x_\mu})\Psi, \quad (1.21)$$

where the summation over $m = 1,2,3$ and $\mu = 1,2,3,4$ is implied as usual and we introduced hermitian matrices γ_μ^E:

$$\gamma_m^E = i\gamma_m, \text{ for } m = 1,2,3; \quad \gamma_4^E = \gamma_0. \quad (1.22)$$

We shall omit indices E for these hermitian matrices in what follows.

We should note here that after Euclidean rotation the fields $\bar{\Psi}$ and Ψ are no longer related by complex conjugation: the relation $\bar{\Psi} = \Psi^\dagger\gamma_0$ does not exist in Euclidean space. The variables $\Psi(t,\boldsymbol{x})$ and $\bar{\Psi}(t,\boldsymbol{x})$ are independent for complex t. This is related to the fact that the group of rotations of Euclidean space $O(4)$ is a direct product of two independent groups of spinor rotations: $O(4) = SU(2) \times SU(2)$. The Lorentz group $O(3,1)$ can be also expressed as a direct product of two groups. However, these groups are not unitary and under hermitian conjugation transform into each other. Here we shall use this fact to flip the sign of one of the fields, say Ψ, to get rid of the overall minus sign in the expression for the Euclidean fermion action which then takes the form:

$$S_F^E = \int d^4x \left\{\bar{\Psi}\partial\!\!\!/\Psi + y\bar{\Psi}(\phi^0 + i\boldsymbol{\tau}\cdot\boldsymbol{\phi})\Psi\right\}. \quad (1.23)$$

Now we discretise this action. The discretisation of the Yukawa term is straightforward. For the derivative term we choose:

$$\partial_\mu\Psi \to \frac{\Psi_{x+\hat{\mu}a} - \Psi_{x-\hat{\mu}a}}{2a}. \quad (1.24)$$

The lattice action for the fermion field has the form:

$$S_F = \frac{1}{2a}a^4\sum_{x,\mu}\bar{\Psi}_x\gamma_\mu(\Psi_{x+\hat{\mu}a} - \Psi_{x-\hat{\mu}a}) + ya^4\sum_x\bar{\Psi}_x^\bullet(\phi_x^0 + i\gamma_5\boldsymbol{\tau}\cdot\boldsymbol{\phi}_x)\Psi_x. \quad (1.25)$$

We can introduce lattice units as usual (1.17) (fermion fields are rescaled by a factor $a^{3/2}$), i.e., set $a = 1$. Finally, the lattice partition function for the fermion is:

$$Z_F = \int\prod_x d\Psi_x\, d\bar{\Psi}_x\, \exp(-S_F) = \det M, \quad (1.26)$$

where integration over the anticommuting variables Ψ_x, $\bar{\Psi}_x$ produces the determinant of the fermion matrix:

$$M_{xz} = \frac{1}{2}\sum_\mu\gamma_\mu(\delta_{z,x+\hat{\mu}} - \delta_{z,x-\hat{\mu}}) + y(\phi_x^0 + i\gamma_5\boldsymbol{\tau}\cdot\boldsymbol{\phi}_x)\delta_{xz}. \quad (1.27)$$

1.3.4 Continuum limit, fermion doubling and staggered fermions

Here we shall discuss the "naive" continuum limit of the lattice fermion action (1.25). Let us regard ϕ_x^i as an external field and assume it to be constant over the lattice: $\phi_x^i = \phi\delta_{i0}$. The action (1.25) takes the form of the lattice action for a free Dirac fermion[6] with the mass $m_F = y\phi$. The continuum limit in such a theory corresponds to $am_F \to 0$ as we discussed in the case of the scalar sector. This goes well with the fact that at the continuum limit for the scalar theory (at the critical point): $\langle\phi\rangle \to 0$. Indeed, at the continuum limit which would describe a scalar–fermion theory the ratio of physical masses m_F/m_H should be a finite constant thus both am_H and am_F should go to zero.

If this were not the case, for example, if am_F did not go to zero while $am_H \to 0$, then obviously $m_F/m_H \to \infty$ in the limit $a \to 0$. In such a situation the fermion would not appear as a physical particle in the continuum limit. We say that it decouples from the physical spectrum, the scale for which is set by m_H. In other words, if we use the effective theory language, the fluctuations of the fermion field have typical frequencies of order Λ (wavelength $O(a)$) and are not excited by low energy (long wavelength) experiments. In fact, we do encounter such situation in lattice scalar–fermion models at large Yukawa coupling.

Now consider the lattice action for a free massless Dirac fermion ψ_x:

$$\frac{S}{a^4} = \frac{1}{2a}\sum_{x,\mu}\bar{\psi}_x\gamma_\mu(\psi_{x+\hat{\mu}a} - \psi_{x-\hat{\mu}a}) + m_F\sum_x\bar{\psi}_x\psi_x \equiv \frac{1}{a}\sum_{xy}\bar{\psi}_x(M_{am_F})_{xy}\psi_y \qquad (1.28)$$

where we introduced the free fermion matrix $(M_{am_F})_{xy}$ (compare to (1.27)). The propagator in this theory is:

$$\begin{aligned} a^3\left\langle\psi_x\bar{\psi}_y\right\rangle &= \left(M^{-1}_{am_F}\right)_{xy} = \\ &= a^4\int_{-\pi/a}^{+\pi/a}\frac{d^4p}{(2\pi)^4}e^{-ip(x-y)}\left[i\sum_\mu\gamma_\mu\sin(ap_\mu) + am_F\right]^{-1} = \\ &= a^4\int_{-\pi/a}^{+\pi/a}\frac{d^4p}{(2\pi)^4}e^{-ip(x-y)}\frac{-i\sum_\mu\gamma_\mu\sin(ap_\mu) + am_F}{\sum_\mu\sin^2(ap_\mu) + (am_F)^2}, \end{aligned} \qquad (1.29)$$

where we used the Fourier transform to invert the matrix M. The momentum p on the lattice takes values inside the Brillouin zone (a hypercube):

$$-\pi/a < p_\mu < +\pi/a, \qquad \mu = 1,2,3,4.$$

[6] More precisely, for a doublet of free Dirac fermions: $\Psi = \begin{pmatrix}\psi^1\\ \psi^2\end{pmatrix}$.

The exponential tail of the propagator $\left\langle \psi_x \bar{\psi}_y \right\rangle$ at large distances $|x-y| \gg (am_F)^{-1}$ is related to the position of the poles of the propagator in momentum space:

$$(\sum_\mu \sin^2(ap_\mu) + (am_F)^2)^{-1}.$$

The poles appear at complex values of p. At small $am_F \ll 1$ the pole near $p^2 \approx -m_F^2$ gives at large $|x-y|$ the term $\sim \exp\{-m_F|x-y|\}$. In other words, the typical wavelength of the fluctuations of the field ψ_x becomes large as $am_F \to 0$ and this field can define a continuum fermion field.

However, there are also 15 other poles near the corners of the Brillouin zone corresponding to the zeros of $\sum_\mu \sin^2(ap_\mu)$. For example, there is a pole at:

$$\{p - (\pi/a, 0, 0, 0)\}^2 \approx -m_F^2.$$

This pole gives a contribution to the propagator at long distances:

$$\sim (-1)^{x_1 - y_1} \exp\{-m_F|x-y|\}.$$

This means that the fluctuations of the field $(-1)^{x_1}\psi_x$ also acquire long wavelength. This field will define another fermion field in the continuum limit. Similarly, the soft modes of the fields $(-1)^{x_2}\psi_x$, $(-1)^{x_1+x_2}\psi_x$, ..., $(-1)^{x_1+x_2+x_3+x_4}\psi_x$ define another 14 fermion fields in the continuum limit. We can conclude that the fermion action (1.28) in the continuum limit defines a theory with 16 degenerate flavours of free fermions instead of one. This phenomenon is called fermion doubling [26]. On the hypercubic lattice in d dimensions the number of fermion flavours described by the action of the type (1.28) in the continuum limit is 2^d.

To understand the nature of the doubler fermions let us define a new field:

$$(\psi_1)_x = (-1)^{x_1}\psi_x \qquad \text{and} \qquad (\bar{\psi}_1)_x = (-1)^{x_1}\bar{\psi}_x.$$

The fermion action (1.28) in terms of the new field ψ_1 has exactly the same form, except that the γ_1 matrix has an additional minus sign. We can correct this by a unitary transformation of the fermion fields:

$$\psi_1 \to \gamma_5\gamma_1\psi_1 \qquad \text{and} \qquad \bar{\psi}_1 \to \bar{\psi}_1\gamma_1\gamma_5.$$

Such a transformation interchanges the left-handed and right-handed components of the Dirac spinor: it can be seen explicitly from the chiral representation of the γ-matrices (see Appendix A) or from the fact that $\gamma_5\gamma_1$ anticommutes with γ_5. It means that if the upper Dirac component of the fermion described by the long wavelength modes of the field ψ_x is right-handed then the upper component of the

continuum field $(-1)^{x_1}\psi_x$ will be left–handed. Similarly for the other 14 doublers: half of them will have left–handed upper Dirac components and the other half — right–handed.

The importance of this observation is that if we introduced some chiral interaction for the field ψ_x, i.e., coupled left– and right–handed components in a different way, the interaction for the doubler fermion $\gamma_5\gamma_1(-1)^{x_1}\psi_x$ would be a mirror reflection. The resulting theory would then be vectorlike, i.e.. left–right symmetric. This presents a problem for putting a chiral theory like the electroweak theory on the lattice [16,18,27]. The problem is very general and is not limited to the lattice discretisation we chose [28]. We will not attempt to tackle this problem here. We shall assume that for the questions we wish to study, such as the possible upper bound on the Higgs or fermion masses or the existence of a nontrivial (interacting) continuum limit of the scalar–fermion theory, this degeneracy does not play a crucial role.

There is, however, one way to improve the situation by reducing the number of doublers from 16 to 4 (to $2^{d/2}$ in d dimensions). The form of the doubler fields: $(\psi_1)_x = (-1)^{x_1}\psi_x$, $(\psi_2)_x = (-1)^{x_2}\psi_x$, $(\psi_3)_x = (-1)^{x_1+x_2}\psi_x$, etc. suggests to introduce 16 sublattices in the following obvious way. Take one unit hypercube which contains 16 sites. Then take each of these sites and translate it by steps of 2 lattice spacings in all directions. Each such sublattice contains 1/16 of all lattice sites. The lattice spacing in each sublattice is $2a$. Then define 16 fields ψ_{S0}, ψ_{S1}, ..., ψ_{S15} living on different sublattices: $(\psi_{Si})_x = \psi_x$ for $x \in i$-th sublattice. There are no doublers for these fields because the Brillouin zone shrinks to

$$-\pi/2a < p_\mu < \pi/2a.$$

There is only one pole: $p = 0$. in this interval. The original doublers ψ_i are now some certain linear combinations of the sublattice fields ψ_{Si}.

Unfortunately, the action (1.28) mixes the fields from different sublattices and we can not thin the degrees of freedom by considering only one of them. However, one can diagonalise the action in the *Dirac* indices by the following transformation [29]:

$$\psi_x = \gamma_1^{x_1}\gamma_2^{x_2}\gamma_3^{x_3}\gamma_4^{x_4}\ \chi_x \text{ and } \bar{\psi}_x = \bar{\chi}_x \cdot \gamma_4^{x_4}\gamma_3^{x_3}\gamma_2^{x_2}\gamma_1^{x_1}. \tag{1.30}$$

The lattice action (1.28) in terms of the new fields χ_x does not contain γ–matrices:

$$\frac{S}{a^4} = \frac{1}{2a}\sum_{x,\mu}\bar{\chi}_x\eta_{x,\mu}(\chi_{x+\hat{\mu}a} - \chi_{x-\hat{\mu}a}) + m_F\sum_x \bar{\chi}_x\chi_x, \tag{1.31}$$

where

$$\eta_{x,\mu} = (-1)^{x_1+\ldots+x_{\mu-1}} \text{ for } \mu > 1 \text{ and } \eta_{x,1} = 1. \tag{1.32}$$

This sign factor arises from the anticommutation of γ–matrices, for example:

$$\eta_{x,2} = \gamma_4^{x_4}\gamma_3^{x_3}\gamma_2^{x_2}\gamma_1^{x_1} \cdot \gamma_2 \cdot \gamma_1^{x_1}\gamma_2^{x_2+1}\gamma_3^{x_3}\gamma_4^{x_4} = (-1)^{x_1}.$$

The action (1.31) does not mix the Dirac components of the spinor χ. One can now thin the degrees of freedom by considering only one of these components. Such a one component fermion field with the action (1.31) is called staggered fermion [30]. It describes 4 (=16/4) Dirac fermions in the continuum limit. The Dirac components of these continuum fermions are linear combinations of the 16 χ_{Si} fields living on different sublattices.

We shall use staggered fermions to reduce the degeneracy due to the fermion doubling. For a small number of doublers one can even imagine, that this lattice degeneracy might coincide with some physically real degeneracy (or approximate degeneracy) of the fermions we want to describe.

1.4 Notations and the outline

The models we study in this work are described by the sum of the actions (1.18) with $\lambda = \infty$ and (1.25). Such and similar scalar–fermion models attracted considerable interest recently [31–54]. For reviews see, e.g., [15–19,55]. Both analytical and numerical (Monte Carlo) techniques were used to study their phase diagrams. The Monte Carlo study of theories with dynamical fermions is notoriously difficult and computer time consuming. Thus it is very helpful to have an approximate analytical method to determine the structure of the phase diagram which can be then compared with Monte Carlo results. We used the mean field method to determine the lines of the phase transitions and to study the properties of different phases in lattice scalar–fermion models. Our results are in remarkable agreement with the available Monte Carlo data (see section 3.3).

Some simplified models with two component scalar field ($O(2)$, or $U(1)$, symmetry instead of $O(4)$) [40–47] and one component scalar field (Z_2 symmetry) [31–39] were also subject to various investigations recently. The results obtained in these models are similar. We study such simplified theories as well.

In Chapter 2 we develop the mean field approximation for scalar–fermion theories. This chapter is devoted to finding the approximate equations for the phase transition lines in the scalar–fermion theories with Z_2, $U(1)$ and $O(4)$ symmetry.

In Chapter 3 we study the phase structure of the models and properties of the phases. In particular, we compute some fermionic observables, such as the fermion condensate $\langle\bar{\psi}\psi\rangle$ and the fermion propagator. We use this information to distinguish two different symmetric phases: with massless fermions and without them (section 3.1). We study the phase structure and the phase diagrams of the scalar–fermion theories in section 3.2. We compare our analytical mean field results for the phase diagrams to numerical Monte Carlo results and find a good agreement (section 3.3). We discuss continuum limits in scalar–fermion theories in section 3.4. In section 3.5 we study some four–fermion correlators at large Yukawa coupling and find poles which can be interpreted as bound states of fermion–antifermion or fermion–fermion pairs. In section 3.6 we discuss the continuum limit at the critical line separating para– and antiferromagnetic phases and argue that such a theory is not unitary.

Finally, we make concluding remarks in Chapter 4. The results presented in this work are published in [37,42,54,57].

In this section we define the models we are studying. We define and explain the notations which are used in the rest of the work. This section can be used for

reference.

1.4.1 One component scalar field — Z_2 symmetry

The action of the model is:

$$S = S_B + S_F. \tag{1.33}$$

The pure bosonic (scalar) part of the action: S_B, is the action of the Ising model:

$$S_B = -2\kappa \sum_{x,\mu} \sigma_x \phi_{x+\hat{\mu}}$$
$$\sigma_x = \pm 1. \tag{1.34}$$

We dropped the hat from the variable $\hat{\phi}_x$ compared to (1.19) and also used a standard (historically accepted) notation 2κ instead of v^2.

The fermionic part of the action is:

$$S_F = \frac{1}{2} \sum_{x,\mu} \bar{\psi}_x \gamma_\mu (\psi_{x+\hat{\mu}} - \psi_{x-\hat{\mu}}) + Y \sum_x \bar{\psi}_x \psi_x \phi_x, \tag{1.35}$$

where ψ_x is a Dirac spinor. The action (1.33) is symmetric under the Z_2 transformation:

$$\phi_x \to -\phi_x, \quad \psi_x \to i\gamma_5 \psi_x \quad \text{and} \quad \bar{\psi}_x \to i\bar{\psi}_x \gamma_5. \tag{1.36}$$

Performing the spin diagonalisation (1.30) we can rewrite this action in the form of a sum of 4 identical actions for 4 staggered fermions χ_x. Each staggered fermion action has the form:

$$S_F^{\text{st}} = \frac{1}{2} \sum_{x,\mu} \bar{\chi}_x \eta_{x,\mu} (\chi_{x+\hat{\mu}} - \chi_{x-\hat{\mu}}) + Y \sum_x \bar{\chi}_x \chi_x \sigma_x. \tag{1.37}$$

where $\eta_{x,\mu}$ is the standard sign factor for the staggered fermions (1.32).

The partition function of the model (dropping the source terms) is:

$$Z = \sum_{\{\sigma_x = \pm 1\}} \int \prod_x d\psi_x \, d\bar{\psi}_x \, e^{-(S_B + S_F)}. \tag{1.38}$$

We can integrate over the fermion variables to obtain:

$$Z = \sum_{\{\sigma_x = \pm 1\}} \exp(-S_B + \ln \det M), \tag{1.39}$$

where M is the fermion matrix:

$$M_{xy} = \frac{1}{2} \sum_\mu \gamma_\mu (\delta_{y,x+\hat{\mu}} - \delta_{y,x-\hat{\mu}}) + Y \sigma_x \delta_{xy}. \tag{1.40}$$

The model (1.39) is a model with only bosonic degrees of freedom ϕ_x and the action:

$$S_{\text{eff}} = S_B - \ln \det M. \tag{1.41}$$

We can also rewrite the fermion action using staggered fermions and then integrate over the staggered fermion fields χ_x. Then we obtain for $\det M$ in (1.39):

$$\det M = (\det M^{\text{st}})^4. \tag{1.42}$$

where the staggered fermion matrix is:

$$M^{\text{st}}_{xy} = \frac{1}{2}\sum_{\mu} \eta_{x,\mu}(\delta_{y,x+\hat{\mu}} - \delta_{y,x-\hat{\mu}}) + Y\phi_x\delta_{xy}. \tag{1.43}$$

Equations (1.42) and (1.43) show that $\det M$ is nonnegative. This allows the interpretation of $S_{\text{eff}} = S_B - \ln \det M$ as the energy of a 4 dimensional statistical system. The interaction in this system is nonlocal due to nonlocality of $\ln \det M$. This is the main source of difficulties in simulating such systems by Monte Carlo method.

We can also thin the fermionic degrees of freedom by considering only 2 instead of 4 species of staggered fermions χ_x. We can not consider one (or, indeed, any odd number of) species because $\det M^{\text{st}}$ is not necessarily positive.[7] More generally, we can consider any even number D of species of staggered fermions. The action for such a model is:

$$S_{\text{eff}} = S_B - D \ln \det M^{\text{st}}. \tag{1.44}$$

Obviously, it coincides with (1.41) if $D = 4$. The model with D staggered fermions describes $4D$ Dirac fermions in the "naive" continuum limit.

1.4.2 Two component scalar field — $U(1)$ symmetry

The action is again:

$$S = S_B + S_F. \tag{1.45}$$

The bosonic part is now the action of the 4 dimensional XY model:

$$\begin{aligned} S_B &= -2\kappa \sum_{x,\mu} \phi^i_x \phi^i_{x+\hat{\mu}}, \\ \phi^0_x &= \cos\theta_x, \\ \phi^1_x &= \sin\theta_x, \end{aligned} \tag{1.46}$$

where summation over $i = 0, 1$ is implied. The length of the two component field ϕ_x is again fixed in each site to unity: $\phi^i_x \phi^i_x = 1$.

[7] For example, for $Y \gg 1$: $\det M^{\text{st}} \approx \prod_x (Y\phi_x)^N$ This can be negative if an odd number of sites have $\phi_x = -1$.

The fermion part of the action is:

$$S_F = \frac{1}{2}\sum_{x,\mu} \bar{\psi}_x \gamma_\mu (\psi_{x+\hat{\mu}} - \psi_{x-\hat{\mu}}) + Y \sum_x \bar{\psi}_x (\phi_x^0 + i\gamma_5 \phi_x^1)\psi_x \equiv \sum_{xy} \bar{\psi}_x M_{xy} \psi_y, \quad (1.47)$$

where we defined a new matrix M. The Yukawa term can be also written as:

$$Y \sum_x \bar{\psi}_x \exp(i\gamma_5 \theta_x)\psi_x.$$

The model is invariant under the $U(1)$ group of transformations:

$$\theta_x \to \theta_x + \alpha, \quad \psi_x \to \exp(-i\gamma_5 \frac{\alpha}{2})\psi_x \quad \text{and} \quad \bar{\psi}_x \to \bar{\psi}_x \exp(-i\gamma_5 \frac{\alpha}{2}). \quad (1.48)$$

This transformation acts on the fermion field ψ_x as a chiral transformation: it rotates the phases of the right- and left-handed components in opposite directions. However, due to the fermion doubling the whole transformation is vectorlike (i.e. left–right symmetric) as it rotates the components of half of the doublers the opposite way.

We can introduce staggered fermions as usual using transformation (1.30). The action in terms of the field χ is diagonal with respect to its Dirac components $\chi^1, \chi^2, \chi^3, \chi^4$ if we choose chiral representation for Dirac matrices, in which $\gamma_5 = \mathrm{diag}(1, 1, -1, -1)$. Two staggered fields χ^1 and χ^2 have the action:

$$S_F^{\mathrm{st}} = \frac{1}{2}\sum_{x,\mu} \bar{\chi}_x^\alpha \eta_{x,\mu} (\chi_{x+\hat{\mu}}^\alpha - \chi_{x-\hat{\mu}}^\alpha) + Y \sum_x \bar{\chi}_x^\alpha (\phi_x^0 + i\zeta_x \phi_x^1)\chi_x^\alpha \equiv \sum_{xy} \bar{\chi}_x^\alpha M_{xy}^{\mathrm{st}} \chi_y^\alpha, \quad (1.49)$$

where the sign factor

$$\zeta_x = (-1)^x, \qquad x \equiv x_1 + x_2 + x_3 + x_4 \quad (1.50)$$

arises after we anticommute the γ–matrices with γ_5:

$$\gamma_4^{x_4}\gamma_3^{x_3}\gamma_2^{x_2}\gamma_1^{x_1} \cdot \gamma_5 \cdot \gamma_1^{x_1}\gamma_2^{x_2}\gamma_3^{x_3}\gamma_4^{x_4} = (-1)^x \cdot \gamma_5.$$

The other two staggered fields χ^3 and χ^4 have additional minus sign in front of ζ_x (i.e., $M^{\mathrm{st}} \to (M^{\mathrm{st}})^*$) in (1.49).

We can again generalize our theory to any even number D of staggered fermion fields. After integrating over the fermion fields we obtain the pure bosonic model with the action:

$$S_{\mathrm{eff}} = S_B - \frac{D}{2} \ln\det M^{\mathrm{st}} - \frac{D}{2} \ln\det (M^{\mathrm{st}})^* = S_B - D\,\mathrm{Re}\,\ln\det M^{\mathrm{st}}. \quad (1.51)$$

As in the Z_2 case we see that the action S_{eff} is real. Finally, the partition function of the model has the form:

$$Z = \int \prod_x d\theta_x \, \exp\{-S_{\mathrm{eff}} + \textstyle\sum_x h_x^i \phi_x^i\}, \quad (1.52)$$

where h^i $(i = 0, 1)$ is a two component external source for the field ϕ_x^i.

1.4.3 Four component scalar field — $O(4)$ symmetry

The notations are very similar. The action is again:

$$S = S_B + S_F. \tag{1.53}$$

with

$$S_B = -2\kappa \sum_{x,\mu} \phi_x^k \phi_{x+\hat{\mu}}^k ,$$
$$\phi_x^k \phi_x^k = 1, \tag{1.54}$$

and the sum over $k = 0, 1, 2, 3$ implied. The fermion action is:

$$S_F = \frac{1}{2} \sum_{x,\mu} \bar{\Psi}_x \gamma_\mu (\Psi_{x+\hat{\mu}} - \Psi_{x-\hat{\mu}}) + Y \sum_x \bar{\Psi}_x (\phi_x^0 + i\gamma_5 \boldsymbol{\tau} \cdot \boldsymbol{\phi}_x) \Psi_x \equiv \sum_{xy} \bar{\Psi}_x M_{xy} \Psi_y, \tag{1.55}$$

Here each Dirac component of Ψ_x and $\bar{\Psi}_x$ is a complex doublet. The Pauli matrices $\boldsymbol{\tau}$ act on these doublets. The $O(4)$ symmetry of this model rotates the 4 component field ϕ_x^k. It is a direct product of two $SU(2)$ symmetries: $O(4) = SU(2)_1 \times SU(2)_2$. The corresponding transformations are described by two independent $SU(2)$ matrices U_1 and U_2:

$$(\phi_x^0 + i\boldsymbol{\tau} \cdot \boldsymbol{\phi}_x) \to U_2 (\phi_x^0 + i\boldsymbol{\tau} \cdot \boldsymbol{\phi}_x) U_1;$$
$$\Psi_x \to U_1^\dagger \Psi_x; \quad \bar{\Psi}_x \to \bar{\Psi}_x U_2^\dagger. \tag{1.56}$$

As usual we shall be using staggered fermions. We apply the transformation (1.30) and use $\gamma_5 = \mathrm{diag}(1, 1, -1, -1)$. Similar to the $U(1)$ case we obtain the action for the first two Dirac components χ_x^1 and χ_x^2 of the field χ in the form:

$$S_F^{\mathrm{st}} = \frac{1}{2} \sum_{x,\mu} \bar{\chi}_x^\alpha \eta_{x,\mu} (\chi_{x+\hat{\mu}}^\alpha - \chi_{x-\hat{\mu}}^\alpha) + Y \sum_x \bar{\chi}_x^\alpha (\phi_x^0 + i\zeta_x \boldsymbol{\tau} \cdot \boldsymbol{\phi}_x) \chi_x^\alpha \equiv \sum_{xy} \bar{\chi}_x^\alpha M_{xy}^{\mathrm{st}} \chi_y^\alpha, \tag{1.57}$$

Note again that each field χ_x^1 and χ_x^2 in this case is an $SU(2)$ doublet. The matrix M has corresponding $SU(2)$ indices as well which we also suppress. The other two staggered fields, χ^3 and χ^4, have the action (1.57) with $\zeta_x \to -\zeta_x$. However, one can make the following transformation of these fields:

$$\chi_x \to \zeta_x \tau_2 \bar{\chi}_x^T \qquad \text{and} \qquad \bar{\chi}_x \to \chi_x^T \tau_2 \zeta_x, \tag{1.58}$$

and the action in terms of the new fields takes the same form as (1.57). As in the Z_2 and $U(1)$ cases we can consider a theory with D staggered fermions χ: D doublets under $SU(2)$. The number of the doublets D can be odd if $\det M^{\mathrm{st}} > 0$ for all configurations of the field ϕ_x. One can see that $\det M^{\mathrm{st}}$ is real which follows from

the identity: $(M^{\rm st})^* = \tau_2 M^{\rm st} \tau_2$. We argue that it is positive in appendix B. The partition function of the model is:

$$Z = \int \prod_x d\mu_x \, \exp\{-S_{\rm eff} + \textstyle\sum_x h_x^k \phi_x^k\}. \tag{1.59}$$

where the integration $\int d\mu_x$ in each site x is over the unit sphere covered by the vector ϕ_x^k and h^k is an external source. The effective action in (1.59) has the form:

$$S_{\rm eff} = S_B - D \ln \det M^{\rm st}. \tag{1.60}$$

We use only staggered fermion formulation of the scalar–fermion models in the $U(1)$ and $O(4)$ cases. Then we will not write the index "st" for the matrix $M^{\rm st}$ for the sake of simplicity.

Chapter 2

Mean field theory and the phase transition lines

To study the continuum limit of a lattice model we need to find the position of critical points (points of second order phase transition) in the space of parameters of the lattice action. Near the critical points the correlation length (in units of the lattice spacing) diverges and a continuum limit can be defined. Numerical investigation of the scalar–fermion theories with dynamical fermions is very difficult and computer time consuming. Thus it is very helpful to have some approximate analytical method to study the structure of the phase diagram, to determine the position of the critical points. An analytical approach is necessary to analyse the numerical results obtained by Monte Carlo method.

It is known that the mean field method can predict the point of the phase transition in the Ising and similar spin models with a precision of about 20%. In this work we apply the mean field approximation to the scalar–fermion theories to study the structure of their phase diagrams. This chapter is devoted to finding the equations for the second order phase transition lines [37,42,54].

2.1 Mean field approximation in the Ising model

Let us start with the simplest case of the Ising model to illustrate the basic idea of the mean field method. We shall consider the Ising model on a hypercubic lattice in d dimensions. The partition function of the model in a homogeneous external field h is given by:

$$Z = \sum_{\{\phi_x=\pm 1\}} \exp\left(2\kappa \sum_{x,\mu} \phi_x \phi_{x+\hat{\mu}} + h \sum_x \phi_x\right). \qquad \mu = 1, 2, \ldots, d. \tag{2.1}$$

One can notice that each given spin, say ϕ_x, interacts with a sum of $2d$ nearest neighbour spins. Indeed, the terms in the energy of the interaction which contain ϕ_x can be written as: $-2\kappa\phi_x \sum_\mu (\phi_{x+\hat{\mu}} + \phi_{x-\hat{\mu}})$. If the number of nearest neighbours $2d$ gets large one can expect that the fluctuations of the spins in the sum become relatively small. Then one can approximate this sum by $2d$ times the average magnetisation in the system σ. After that the partition function factorises and one obtains:

$$Z = \sum_{\{\phi_x=\pm 1\}} \exp\left(4d\kappa\sigma \sum_x \phi_x + h \sum_x \phi_x\right) = (2\cosh(4d\kappa\sigma + h))^N. \tag{2.2}$$

where N is the total number of lattice sites.

Now one can determine the average magnetisation σ as a function of the external magnetic field h self consistently:

$$\sigma \equiv \left\langle \frac{1}{N} \sum_x \phi_x \right\rangle = \frac{1}{N} \frac{1}{Z} \frac{\partial Z}{\partial h} = \tanh(4d\kappa\sigma + h), \tag{2.3}$$

where N is the total number of sites on the lattice. This is the well known self consistency equation of the mean field method. Note that without interaction: $\kappa = 0$, the partition function is: $Z = (2\cosh h)^N$ and thus: $\sigma = \tanh h$. The effect of the interaction between spins is to produce an effective mean field $4d\kappa\sigma$ acting on each spin as an additional external field. The total (mean) field acting on each spin is: $H = 4d\kappa\sigma + h$. The self consistency equation can be also written in terms of this mean field:

$$\frac{H - h}{4d\kappa} = \tanh H. \tag{2.4}$$

Now consider the case of zero external field h. Then the mean field H is determined by the equation:

$$\frac{H}{4d\kappa} = \tanh H. \tag{2.5}$$

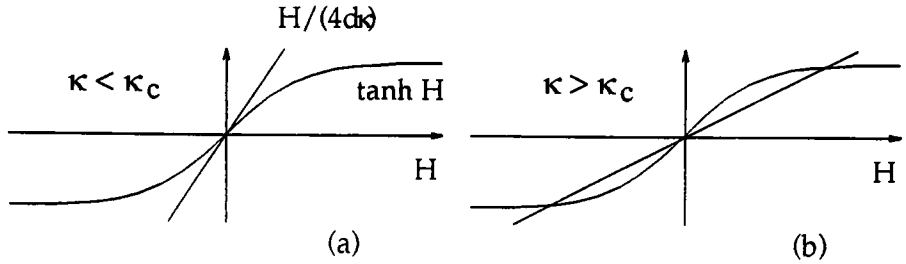

Figure 2.1: The mean field self consistency equation (2.5).

One can easily see (fig. 2.1a) that for $\kappa < 1/4d$ this equation has only one solution: $H = 0$, which means that $\sigma = 0$. This corresponds to the symmetric phase of the Ising model. For $\kappa > 1/4d$ (fig. 2.1b) the value $H = 0$ is still a solution, but two nonzero solutions also appear. These solutions correspond to the broken phase of the model, i.e. $\sigma \neq 0$. We shall see that the trivial solution is unstable in this case. Thus the mean field approximation predicts a phase transition between symmetric and broken phases in the Ising model at $\kappa = 1/4d$. One can see that the transition is of second order: the magnetisation σ behaves continuously with κ. Indeed expanding: $\tanh H \approx H + H^3/3$ for small H in (2.5), we find near the critical point $\kappa \approx \kappa_c \equiv 1/4d$:

$$\sigma \approx H \approx \sqrt{12d(\kappa - \kappa_c)} \tag{2.6}$$

The mean field approximation is better if the number of neighbours interacting with each spin, $2d$, is larger. Indeed, the average of a larger number of random variables $\phi_{x\pm\hat{\mu}}$ which form the mean field fluctuates less. We are not aware of any systematic proof but it looks very plausible that the mean field approximation becomes exact as d goes to infinity. One can actually compute corrections to the leading mean field result and write an expansion for κ_c in powers of $1/d$. The leading correction is given by: $4d\kappa_c = 1 + \frac{1}{2d} + O(\frac{1}{(2d)^2})$, in accordance with our expectations. Numerically, for $d = 4$ the critical point in the Ising model is at $\kappa_c \approx 0.075$ and the leading mean field result is 0.0625.

There are different ways to implement the idea of the mean field method and we demonstrated the most straightforward one. However, for the scalar-fermion theories another, variational, approach proves to be more appropriate. We shall demonstrate it on the Ising model first.

The free energy (per site) of the statistical system defined as: $W(h) = -\frac{1}{N}\ln Z$, equals the thermodynamic energy minus the entropy (and divided by N). The thermodynamic energy is the average of the microscopic energy: $-2\kappa\sum_{x,\mu}\phi_x\phi_{x+\hat{\mu}} - h\sum_x\phi_x$, over the fluctuations of the field ϕ_x. We can not calculate this average exactly because the fluctuations of ϕ_x in different sites are correlated. The mean

field approximation corresponds to neglecting the correlations of the field ϕ_x. In other words, we average over the fluctuations of the *uncorrelated* random field ϕ_x with the probability distribution: $P(\phi) = Z_H^{-1} \exp(H \sum_x \phi_x)$:

$$\langle \ldots \rangle_H = \frac{1}{Z_H} \sum_{\{\phi_x = \pm 1\}} \exp(H \textstyle\sum_x \phi_x)(\ldots). \tag{2.7}$$

where

$$Z_H = \sum_{\{\phi_x = \pm 1\}} \exp(H \textstyle\sum_x \phi_x) = (2 \cosh H)^N. \tag{2.8}$$

The average over this test distribution can be computed and we get for the energy:

$$\text{"energy"} \approx \left\langle -2\kappa \sum_{x,\mu} \phi_x \phi_{x+\hat{\mu}} - h \sum_x \phi_x \right\rangle_H = -2dN\kappa (\tanh H)^2 - Nh \tanh H. \tag{2.9}$$

where we used the fact that:

$$\langle \phi_x \phi_{x+\hat{\mu}} \rangle_H = \langle \phi_x \rangle_H \langle \phi_{x+\hat{\mu}} \rangle_H \quad \text{and} \quad \langle \phi_x \rangle_H = \tanh H. \tag{2.10}$$

The entropy of the system with probability distribution $P(\phi)$ will give us the estimate for the entropy then:

$$\text{"entropy"} \approx \langle -\ln P(\phi) \rangle_H = N \ln(2 \cosh H) - NH \tanh H. \tag{2.11}$$

For $H = 0$ the entropy is $N \ln 2$ which corresponds to two states, $\varphi_x = \pm 1$, with equal probability, per site. For $H \to \infty$ the entropy goes to zero as all spins are frozen along the field H. The mean field estimate $\tilde{W}(h, H)$ for the free energy is then:

$$W(h) \approx -2d\kappa (\tanh H)^2 + (H - h) \tanh H - \ln(2 \cosh H) \equiv \tilde{W}(h, H). \tag{2.12}$$

One can make more formal derivation of this estimate [56]. The procedure is based on the so–called Peierls inequality:

$$\langle \exp A \rangle \geq \exp \langle A \rangle . \tag{2.13}$$

which reflects the convexity property of exponential function. One rewrites Z in the following way:

$$Z = Z_H \cdot \frac{1}{Z_H} \sum_{\{\phi_x = \pm 1\}} \exp(H \textstyle\sum_x \varphi_x) \exp\left(2\kappa \textstyle\sum_{x,\mu} \varphi_x \phi_{x+\hat{\mu}} + (h - H) \sum_x \phi_x\right). \tag{2.14}$$

Then one can use the definition of the average over uncorrelated field ϕ_x (2.7) and apply the Peierls inequality to it to get:

$$\begin{aligned} Z = Z_H \left\langle \exp\left(2\kappa \textstyle\sum_{x,\mu} \phi_x \phi_{x+\hat{\mu}} + (h-H)\sum_x \phi_x\right)\right\rangle_H \geq \\ \geq Z_H \exp\left\langle 2\kappa \textstyle\sum_{x,\mu} \phi_x \phi_{x+\hat{\mu}} + (h-H)\sum_x \phi_x \right\rangle_H = \\ = \exp(-N\tilde{W}(h,H)), \end{aligned} \tag{2.15}$$

with $\tilde{W}(h,H)$ as in (2.12). Taking logarithms of both sides of (2.15) one obtains the estimate:

$$W(h) \leq \tilde{W}(h,H). \tag{2.16}$$

Now we can optimise the choice of the test distribution $P(\phi)$ by minimising the mean field free energy $\tilde{W}(h,H)$ with respect to H. The condition $\partial\tilde{W}(h,H)/\partial H = 0$ coincides with the self consistency equation (2.4). Now, however, we can also see that for $h = 0$ the two $H \neq 0$ solutions appearing at $\kappa > 1/4d$ are minima of the free energy $\tilde{W}(h=0,H)$, while $H = 0$ is a local maximum. Indeed,

$$\left.\frac{\partial^2 \tilde{W}(h=0,H)}{\partial H^2}\right|_{H=0} = 1 - 4\kappa d, \tag{2.17}$$

i.e. the solution $H = 0$ becomes unstable when $\kappa > 1/4d$.

We also see from the idea of the variational approach that the mean field approximation works better when the correlations of the field ϕ_x are small. Then the approximation by the uncorrelated random field is good. This is the case when the system is not very close to a critical point (second order phase transition). Near the critical point the correlations become large and cannot be neglected. However, even then the mean field can provide a good approximation if the number of dimensions d is large enough.

2.2 Mean field approximation for scalar–fermion theory: Z_2 case

We start with the simplest case of the one component scalar field (see sect. 1.4.1). The action of the model has the form (as in (1.33), (1.34), (1.35)):

$$\begin{aligned} S &= S_B + S_F; \\ S_B &= -2\kappa \sum_{x,\mu} \varphi_x \phi_{x+\hat{\mu}}, \qquad \phi_x = \pm 1; \\ S_F &= \frac{1}{2} \sum_{x,\mu} \bar{\psi}_x \gamma_\mu (\psi_{x+\hat{\mu}} - \psi_{x-\hat{\mu}}) + Y \sum_x \bar{\psi}_x \psi_x \varphi_x. \end{aligned} \tag{2.18}$$

To apply the mean field method to the scalar–fermion theory (2.18) we first integrate over the fermionic variables in the partition function (1.38) to obtain the pure bosonic theory with the contribution of the fermion determinant in the action:

$$Z = \sum_{\{\phi_x = \pm 1\}} \exp(-S_B + \ln \det M). \tag{2.19}$$

where S_B is the action of the Ising model given by (1.34). The matrix M is given by (1.40). It will be also convenient to introduce the matrix of the fermion kinetic term:

$$K_{xy} = \frac{1}{2} \sum_\mu \gamma_\mu (\delta_{y,x+\hat{\mu}} - \delta_{y,x-\hat{\mu}}), \tag{2.20}$$

so that

$$M_{xy} = K_{xy} + Y \phi_x \delta_{xy}. \tag{2.21}$$

We also generalise the model to arbitrary (even) number of dimensions d for we know that $1/d$ controls the quality of the mean field approximation. This generalisation is rather straightforward. We extend the summation over Euclidean space indices μ in the formulas to $\mu = 1, 2, \ldots, d$. Also, the number of the Dirac components of the fermion becomes $2^{d/2}$. The generalised γ–matrices obey the same anticommutation algebra as in 4 dimensions. The formulation of the model in terms of staggered fermions proves to be very useful in this respect, because it does not need γ–matrices at all. We shall demonstrate the method on the model with one Dirac fermion ψ_x. However, the results are easily generalised to a theory with any even number D of staggered fermions. The case of one Dirac fermion corresponds to $D = 2^{d/2}$.

Now we can apply the variational mean field method to the model (2.19). The only difference is that $\ln \det M$ contributes additional term to the mean field free energy $\tilde{W}(h, H)$:

$$\tilde{W}(h, H) = -2d\kappa (\tanh H)^2 + (H - h) \tanh H - \ln(2 \cosh H) - \frac{1}{N} (\ln \det M)_H. \tag{2.22}$$

We shall study $\tilde{W}(h,H)$ as a function of parameters κ and Y to determine the phase structure of the model. It would be ideal to compute $\langle \ln\det M\rangle_H$ as a function of Y exactly, using the fact that ϕ_x do not correlate with each other. However, we have been able to compute it only for small and large values of Y. This nevertheless provides very useful information about the phase diagram.

Let us go back one step and analyse the behaviour of the model (2.19) at very small and very large Y without the mean field approximation.

First of all, one can see that at $Y=0$ the dependence on ϕ in the term $\ln\det M$ disappears and the model (2.19) at $Y=0$ becomes simply the Ising model. When $Y\to\infty$ one can neglect the kinetic term K_{xy} in M_{xy} (see (2.21)) and then $\det M\to \prod_x (Y\phi_x)^D = Y^{D}$ due to the constraint $\phi_x^2=1$. Thus in the limit $Y\to\infty$ the fermions also do not contribute and we again recover the Ising model. The Ising model (at $h=0$) has a transition at $\kappa=\kappa_c$ which separates the symmetric $\kappa<\kappa_c$ and the broken $\kappa>\kappa_c$ phases. Thus we expect lines of the phase transition to begin at points $(Y,\kappa)=(0,\kappa_c)$ and (∞,κ_c). These lines must continue into the (Y,κ) plane to separate the phases with $\langle\phi\rangle=0$ and $\langle\phi\rangle\neq 0$. To find the equations for these lines will be the main goal of this chapter.

Next, we can expand $\ln\det M$ in (2.19) in powers of $1/Y$ for large $Y\gg 1$ (using the identity $\ln\det M = \mathrm{tr}\,\ln M$)[1] :

$$\begin{aligned}\ln\det M_{xy} &= \ln\det(Y\phi_x\delta_{xy}+K_{xy}) = \\ &= \ln\det(Y\phi_x\delta_{xy}) + \mathrm{tr}\,\ln(\delta_{xy}+\frac{1}{Y}K_{xy}\phi_y) = \\ &= \ln Y^{ND} - \frac{1}{2Y^2}\,\mathrm{Tr}\sum_{xy} K_{xy}\varphi_y K_{yx}\phi_x + O(1/Y^4). \end{aligned} \tag{2.23}$$

We used the fact that $1/\phi_x=\phi_x$. The trace "Tr" is over the Dirac spinor indices only: e.g., $\mathrm{Tr}\;1 = D$. Using the explicit form of K_{xy} (2.20) we find:

$$\sum_{xy} K_{xy}K_{yx}\phi_x\phi_y = -\frac{1}{2}\sum_{x,\mu}\phi_x\phi_{x+\hat{\mu}}. \tag{2.24}$$

Thus the action $S_{\rm eff} = S_B - \ln\det M$ in (2.19) up to the power $1/Y^2$ at large Y takes the form (ignoring constants):

$$S_{\rm eff} = -2\kappa\sum_{x,\mu}\phi_x\phi_{x+\mu} - \frac{D}{4Y^2}\sum_{x,\mu}\phi_x\phi_{x+\hat{\mu}} + O(1/Y^4). \tag{2.25}$$

[1] This expansion contains only even powers of $1/Y$. This is due to the symmetry of the model (2.18): $Y\to -Y$. Indeed, the sign in front of Y can be changed by the redefinition of the fermion fields: $\psi_x\to\zeta_x\psi_x$, $\bar{\psi}_x\to-\zeta_x\bar{\psi}_x$.

We see that up to this order in $1/Y^2$ the action has still the form of the action of the Ising model. The effect of the fermion determinant is to shift the coupling κ to

$$\kappa^* = \kappa + \frac{D}{8Y^2}. \tag{2.26}$$

This tells us that the line of the phase transition which starts at (∞, κ_c) in the (Y, κ) plane for large Y follows the equation:

$$\kappa = \kappa_c - \frac{D}{8Y^2} + O(1/Y^4) \qquad (Y \gg 1). \tag{2.27}$$

We can also expand $\ln\det M$ in powers of Y^2 for small $Y \ll 1$.[2] We get:

$$\begin{aligned} \ln\det M_{xy} &= \ln\det(K_{xy} + Y\phi_x\delta_{xy}) = \\ &= \ln\det K_{xy} + \operatorname{tr}\ln(\delta_{xy} + Y(K^{-1})_{xy}\phi_y) = \\ &= \ln\det K - \frac{1}{2}Y^2 \operatorname{Tr}\sum_{xy}(K^{-1})_{xy}\varphi_y(K^{-1})_{yx}\varphi_x + O(Y^4). \end{aligned} \tag{2.28}$$

Now, however, the term $O(Y^2)$ couples not only the nearest neighbour spins ϕ_x, ϕ_y: the matrix $(K^{-1})_{xy}$ is nonlocal. Thus we cannot obtain the exact result in the order $O(Y^2)$ similar to (2.27). Nevertheless, we can calculate $\langle\ln\det M\rangle_H$ to this order in Y^2 and use the mean field approximation to determine the phase transition line for small Y.

Recalling that (see (2.10)):

$$\langle\varphi_x\varphi_y\rangle_H = \begin{cases} (\tanh H)^2 & \text{for} \quad x \neq y; \\ 1 & \text{for} \quad x = y; \end{cases} \tag{2.29}$$

we obtain from (2.28):

$$\begin{aligned} \langle\ln\det M\rangle_H &= \text{const} - \frac{1}{2}Y^2(\tanh H)^2 \operatorname{Tr}\sum_x (K^{-2})_{xx} + O(Y^4) = \\ &= \text{const} + \frac{1}{2}ND c Y^2(\tanh H)^2 + O(Y^4), \end{aligned} \tag{2.30}$$

We used the fact that $\sum_y (K^{-1})_{xy}(K^{-1})_{yx} = (K^{-2})_{xx}$ does not depend on x due to translational invariance ($x \to x + \hat{\mu}$), and defined a constant:

$$c \equiv -(K^{-2})_{xx} = \int_{-\pi}^{+\pi} \frac{d^d p}{(2\pi)^d}\Big(\sum_\mu \sin^2 p_\mu\Big)^{-1} \tag{2.31}$$

For $d = 4$, numerically $c = 0.6197\ldots$.

[2] See footnote 1 on page 31.

Thus we obtain for the mean field free energy:

$$\tilde{W}(h,H) = -2d\kappa(\tanh H)^2 + (H-h)\tanh H - \ln(2\cosh H) - \\ -\frac{1}{2}DcY^2(\tanh H)^2 + O(Y^4) + \text{const.} \qquad (2.32)$$

The mean field equation $d\tilde{W}/dH = 0$ takes the form:

$$H - h = (4d\kappa + DcY^2)\tanh H. \qquad (2.33)$$

The solution $H = \langle\phi\rangle = 0$ at $h = 0$ is stable if

$$\left.\frac{\partial^2\tilde{W}(0,H)}{\partial H^2}\right|_{H=0} = 1 - 4d\kappa - DcY^2 > 0. \qquad (2.34)$$

Thus the second order phase transition line separating the symmetric $\langle\phi\rangle = 0$ and the broken $\langle\phi\rangle \neq 0$ phases in the (Y,κ) plane follows the following equation for small Y:

$$\kappa = \frac{1}{4d}(1 - DcY^2) + O(Y^4) \qquad (Y \ll 1). \qquad (2.35)$$

We see that the effective interaction between spins ϕ_x induced by the fermion determinant favours ferromagnetic ordering: the value of κ above which the symmetric (paramagnetic) phase $\langle\phi\rangle = 0$ is unstable becomes smaller compared to the Ising model. It is also obvious from the explicit form of the contribution of the fermion determinant at large Y (2.25).

2.3 The fermion determinant to leading order in $1/d$

In this section we improve the computation of the phase transition lines. We take into account the following two considerations.

First, the (local) stability of the $\langle\phi\rangle = 0$ solution of the mean field self consistency equation is determined by the sign of $\partial^2\tilde{W}(0,H)/\partial H^2|_{H=0}$. Thus it should be sufficient to compute $\tilde{W}(0,H)$ up to terms of order H^2 or, which is the same, to the order σ^2 where

$$\sigma \equiv \langle\phi\rangle_H = \tanh H. \tag{2.36}$$

Second, we expect that the mean field theory, being approximate in general, becomes exact when $d \to \infty$. It is correct in the leading order in $1/d$. We shall retain only leading $1/d$ term in each order in $1/Y$ or Y expansions of $\ln\det M$. Then we are able to sum up these expansions and obtain the equations for the phase transition lines to the leading order in $1/d$. This is analogous to the well known $1/N$ expansion: one keeps only leading $1/N$ term in each order in the expansion in powers of the coupling constant. The leading $1/N$ terms can be also summed then.

2.3.1 Large Y

We begin with the $1/Y$ expansion:

$$\begin{aligned}\langle\ln\det M\rangle_H &= \langle\ln\det(Y\phi_x\delta_{xy})\rangle_H + \langle\,\mathrm{tr}\,\ln(\delta_{xy} + \frac{1}{Y}K_{xy}\varphi_y)\rangle_H = \\ &= \ln Y^{ND} - \frac{1}{2Y^2}\,\mathrm{Tr}\sum_{xy} K_{xy}K_{yx}\langle\phi_x\varphi_y\rangle_H - \ldots - \\ &-\frac{1}{nY^n}\,\mathrm{Tr}\sum_{x_1x_2\ldots x_n} K_{x_1x_2}\ldots K_{x_nx_1}\langle\phi_{x_1}\varphi_{x_2}\ldots\phi_{x_n}\rangle_H - \ldots .\end{aligned} \tag{2.37}$$

Terms in this expansion can be represented by diagrams. Each term in the sum $\sum_{x_1x_2\ldots x_n}$ in (2.37) can be depicted as a closed chain with vertices in the points $x_1x_2\ldots x_n$. The matrix elements $K_{xy} \neq 0$ only when x and y are nearest neighbours (see (2.20)). Thus the links of the chain connecting vertices $x_1x_2\ldots x_n$ for nonzero diagram should be links of the lattice. Typical diagrams in the order $1/Y^6$ are shown in fig. 2.2. When the chain passes a site an odd number of times this site contributes a factor σ. The sites passed an even number of times contribute a factor 1. This follows from the properties:

$$\varphi_x\varphi_x = 1 \quad\text{and}\quad \langle\phi_x\rangle_H = \sigma. \tag{2.38}$$

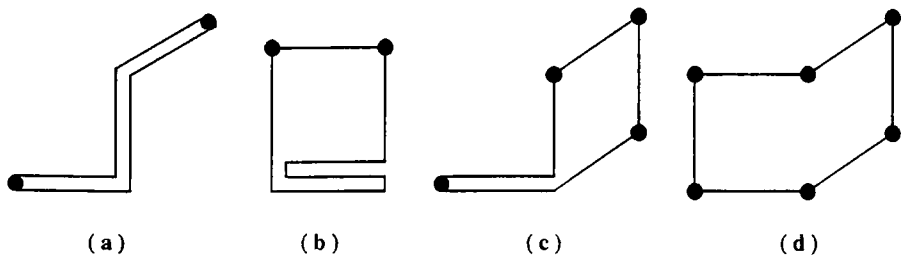

Figure 2.2: Typical diagrams in the order $1/Y^6$ for the expansion (2.37). The full circles mark unpaired vertices. Each of them contributes a factor σ. The diagrams (a), (b) are proportional to σ^2; (c) is of order σ^4; (d) is of order σ^6.

The value of a diagram does not depend on its position and orientation on the lattice. We represent all such diagrams obtained by translations and rotations of one diagram by a single diagram. Each such diagram is accompanied then by a factor equal to the number of possible ways to place this diagram on the lattice.

Obviously, there are different types of diagrams which contribute terms of order σ^2 to $\langle \ln \det M \rangle_H$. The most interesting type of diagrams is shown in fig. 2.2a. These are various *double chains*. The ends of these double chains do not coincide, so that they contribute the necessary factor σ^2. To the leading order in $1/d$ the number of the diagrams of this type is $(2d)^{n/2}N/2$.[3]

It seems very plausible that for all other diagrams contributing terms of order σ^2 this factor has lower order in d. Indeed, consider n fixed and $d \gg n$. Then the leading contribution, which is proportional to $(2d)^{n/2}$, is exhausted by diagrams with first $n/2$ steps made in $n/2$ different directions. Among these only the contribution of the double chains is proportional to σ^2.

With this very plausible assumption we can compute the part of the $\langle \ln \det M \rangle_H$ of order σ^2 to the leading order in $1/d$. In every order in $1/Y$ the leading term in the $1/d$ expansion is:

$$-\frac{1}{n}\frac{1}{Y^n} D\sigma^2 \left(\frac{1}{2}\right)^n (-1)^{n/2} n\,(2d)^{n/2}\,\frac{N}{2}. \tag{2.39}$$

where the factor $\left(\frac{1}{2}\right)^n (-1)^{n/2}$ is the product of the matrix elements of K_{xy} along the chain and the factor n accounts for different ways to enumerate the vertices of a given diagram with $x_1 x_2 \ldots x_n$. Thus the $O(\sigma^2)$ contribution to $\frac{1}{N}\langle \ln \det M \rangle_H$ to the leading order in $1/d$ is:

$$-\sigma^2 D \sum_{n=2,4,6,\ldots}^{\infty} \frac{1}{n}\frac{1}{Y^n}\left(\frac{1}{2}\right)^n (-1)^{n/2} n\,(2d)^{n/2}\,\frac{N}{2} = \frac{\sigma^2}{2} D \frac{d}{d+2Y^2}. \tag{2.40}$$

[3]In the large d limit one can neglect self crossings.

Now we can substitute this into the equation (2.22) for the mean field free energy $\tilde{W}(h, H)$ and calculate $\partial^2 \tilde{W}(0, H)/\partial H^2|_{H=0}$. The condition

$$\left.\frac{\partial^2 \tilde{W}(0, H)}{\partial H^2}\right|_{H=0} = 1 - 4d\kappa - \frac{Dd}{d + 2Y^2} = 0 \tag{2.41}$$

will determine the phase transition line:

$$\kappa = \frac{1}{4d}\left(1 - \frac{Dd}{d + 2Y^2}\right) \tag{2.42}$$

(see figure 3.2: the line separating PM and FM regions).

In what region of the phase diagram is this formula applicable? First, we can see that it agrees with (2.27) at large $Y^2 \gg d$ ($\kappa_c = 1/4d$ in our approximation). However, it is obviously wrong at small Y. It is sensible to assume that (2.42) is applicable in the domain of convergence of the series (2.40), that is for $Y^2 > d/2$.

2.3.2 Small Y

For small Y we can expand $\langle \ln \det M \rangle_H$ in powers of Y:

$$\begin{aligned}\langle \ln \det M \rangle_H &= \ln \det K + \operatorname{tr} \ln(\delta_{xy} + Y(K^{-1})_{xy}\phi_y) = \\ &= \ln \det K - \frac{1}{2}Y^2 \operatorname{Tr} \sum_{xy} (K^{-1})_{xy}(K^{-1})_{yx} \langle \phi_x \phi_y \rangle_H - \ldots - \\ &- \frac{1}{n} Y^n \operatorname{Tr} \sum_{x_1 x_2 \ldots x_n} (K^{-1})_{x_1 x_2} \ldots (K^{-1})_{x_n x_1} \langle \phi_{x_1} \phi_{x_2} \ldots \phi_{x_n} \rangle_H - \ldots .\end{aligned} \tag{2.43}$$

We can similarly represent the terms in this expansion by diagrams: closed chains with vertices in points $x_1 x_2 \ldots x_n$. The matrix $(K^{-1})_{xy}$ is nonlocal, and the diagrams do not have such a simple form as the ones in the $1/Y$ expansion. The links of the chains are not links of the lattice, they can be arbitrarily long. However, the matrix elements $(K^{-1})_{xy}$ are suppressed by additional powers of $1/d$ for larger distances between x and y.

Indeed, we can compute $(K^{-1})_{xy}$ using a trivial identity: $K^{-1} = K(K^{-2})$. We write:

$$(K^{-1})_{x0} = \sum_y K_{xy}(K^{-2})_{y0} = \frac{1}{2}\sum_\mu \gamma_\mu \left[(K^{-2})_{x+\hat{\mu},0} - (K^{-2})_{x-\hat{\mu},0}\right] \tag{2.44}$$

The matrix (K^{-2}) can be easily computed through its Fourier transform:

$$-(K^{-2})_{y0} = \int \frac{d^d p}{(2\pi)^d} e^{-ipy} \left(\sum_\nu \sin^2 p_\nu\right)^{-1} = \int_0^\infty d\alpha \prod_\nu \left(\int_{-\pi}^{+\pi} \frac{dp_\nu}{2\pi} e^{-\alpha \sin^2 p_\nu - i\alpha y_\nu}\right). \tag{2.45}$$

This is nonzero only when *all* the coordinates of the point y: $y_1, y_2, \ldots, y_d$, are *even*. Then it equals to:

$$-(K^{-2})_{y0} = \int_0^\infty d\alpha\, e^{-\frac{\alpha d}{2}} \prod_\nu I_{\frac{y_\nu}{2}}(\alpha/2). \tag{2.46}$$

Using the expansion of the modified Bessel function of integer order n at small argument x:

$$I_n(x) = \frac{x^{|n|}}{2^{|n|}|n|!} + O(x^{|n|+2}),$$

we can find the leading $1/d$ behaviour of a given matrix element $(K^{-2})_{y0}$:

$$(K^{-2})_{y0} \propto \begin{cases} \left(\frac{1}{d}\right)^{1+\frac{1}{2}\sum_\nu |y_\nu|}, & \text{all } y_\nu \text{ are even;} \\ 0, & \text{any of } y_\nu \text{ is odd.} \end{cases} \tag{2.47}$$

Comparing this and (2.44) we find that matrix elements of the matrix K^{-1}_{y0} are nonzero only when exactly one coordinate y_{μ_0} is *odd* and the rest are even. Such matrix elements depend on d for large d as:[4]

$$(K^{-1})_{y0} \propto \gamma_{\mu_0} \left(\frac{1}{d}\right)^{\frac{1}{2}+\frac{1}{2}\sum_\nu |y_\nu|} \qquad \text{(all but one } y_\nu \text{ are even)}, \tag{2.48}$$

We see that for $d \to \infty$ the matrix elements $(K^{-1})_{xy}$ with x, y being nearest neighbours are the leading ones. Using (2.44) we can calculate them:

$$(K^{-1})_{xy} = \mp\frac{c}{2}\gamma_\mu, \quad \text{for} \quad y = x \pm \hat{\mu}\ , \tag{2.49}$$

where c is as in (2.31):

$$c \equiv -(K^{-2})_{00} = \int_0^\infty d\alpha\, e^{-\frac{\alpha d}{2}} \left(I_0(\alpha/2)\right)^d = \frac{2}{d} + O(\frac{1}{d^2}). \tag{2.50}$$

Finally, we see that the matrix $(K^{-1})_{xy}$ becomes more and more local as $d \to \infty$. The leading behaviour at large d is:

$$(K^{-1})_{xy} = -\frac{1}{d}\sum_\mu \gamma_\mu(\delta_{y,x+\hat{\mu}} - \delta_{y,x-\hat{\mu}}) + O(\frac{1}{d^2}) \overset{\bullet}{=} -\frac{2}{d}K_{xy} + O(\frac{1}{d^2}). \tag{2.51}$$

We assume that the corrections $O(\frac{1}{d^2})$ in this formula can be neglected when calculating the terms in (2.43) to the leading order in d. For example, the exact calculation in the order Y^2 gives (see (2.30) and (2.31)):

$$\langle \ln \det M \rangle_H = \text{const} + \frac{1}{2} N D c Y^2 \sigma^2 + O(Y^4), \tag{2.52}$$

[4]Note that this is the behaviour at *fixed* y and $d \to \infty$. Of course, if we fix d then for $y \to \infty$ the propagator $(K^{-1})_{y0} \propto \sum_\mu \gamma_\mu y_\mu / (\sum_\nu y_\nu^2)^{d/2}$

while the substitution $K^{-1} \to -\frac{2}{d}K$ into (2.43) gives:

$$\langle \ln \det M \rangle_H = \text{const} + \frac{1}{d} NDY^2\sigma^2 + O(Y^4), \tag{2.53}$$

i.e. the correct result in the leading order in $1/d$ (see (2.50)). Similarly, we verified this assumption explicitly in the order Y^4.

If we make the substitutions $K^{-1} \to -\frac{2}{d}K$ together with $Y \to \frac{d}{2Y}$ in (2.43) this series takes the same form as (2.37) which we already calculated. Using (2.41) and substituting $Y \to \frac{d}{2Y}$ we obtain the equation for the phase transition line at small y:

$$\left.\frac{\partial^2 \tilde{W}(0,H)}{\partial H^2}\right|_{H=0} = 1 - 4d\kappa - \frac{Dd}{d + 2(d/2Y)^2} = 0.$$

or

$$\kappa = \frac{1}{4d}\left(1 - \frac{2DY^2}{d + 2Y^2}\right) \tag{2.54}$$

(the line between PM and FM regions on figure 3.2).

The situation with the region of applicability of this formula is analogous to that for the formula (2.42). It is correct at small Y and is obviously wrong at $Y \to \infty$. Again, it is sensible to assume (2.54) to be applicable in the region of convergence of the series in (2.43), i.e. $Y^2 < d/2$.

One can notice that the regions of applicability of the formulae (2.54) and (2.42) complement each other and merge at $Y^2 = d/2$.[5] At this point both formulas give the same result:

$$\kappa = \frac{1}{4d}\left(1 - \frac{D}{2}\right).$$

[5] The value $Y^2 = d/2$ is also remarkable because the fermion determinant $\det M$ vanishes for some configurations of the field ϕ near $Y^2 \approx d/2$. This is an exact result (see appendix C).

2.4 Antiferromagnetic phase

So far we have considered the phase transition from the paramagnetic $\langle\phi\rangle = 0$ to the ferromagnetic $\langle\phi\rangle \neq 0$ phase. The ferromagnetic ordering corresponds to the configuration: $\phi_x = 1$. However, at negative κ in the Ising model (2.1) antiferromagnetic ordering becomes favourable. This ordering corresponds to the configuration: $\phi_x = \zeta_x$, where $\zeta_x = (-1)^{x_1+\ldots+x_d}$. A convenient way to study the corresponding phase transition in the Ising model is to make in (2.1) the following substitution:

$$\kappa \to -\kappa \quad , \qquad \phi_x \to \zeta_x \phi_x. \tag{2.55}$$

It is easy to see that the action of the Ising model in terms of the new variables has the same form. The ferromagnetic order in the new variables corresponds to antiferromagnetic order in terms of the old ones. Thus there is a paramagnetic–antiferromagnetic phase transition in the Ising model at $\kappa = -\kappa_c$. This transition is characterised by the order parameter, staggered magnetisation:

$$\langle\phi_{\rm st}\rangle \equiv \langle\frac{1}{N}\sum_x \zeta_x\phi_x\rangle. \tag{2.56}$$

On the phase diagram of the scalar–fermion model (2.18) the transition separating the paramagnetic $\langle\phi_{\rm st}\rangle = 0$ from the antiferromagnetic $\langle\phi_{\rm st}\rangle \neq 0$ phase in the (Y, κ) plane should occur on the lines beginning in the points: $(0, -\kappa_c)$ and $(\infty, -\kappa_c)$. We can derive the equations for these lines using the same approximations.

One can check that the action of the model (2.18) is invariant under the following substitution:

$$\begin{aligned} &\kappa \to -\kappa, && \phi_x \to \zeta_x \phi_x, \\ &Y \to -iY, && \psi_x \to \exp(i\zeta_x\tfrac{\pi}{4})\psi_x, \qquad \bar{\psi}_x \to \exp(i\zeta_x\tfrac{\pi}{4})\bar{\psi}_x. \end{aligned} \tag{2.57}$$

Thus we do not need to repeat our computation for the case of the antiferromagnetic phase transition. It is sufficient to make this substitution in (2.42) and (2.54) to obtain the equations for the para–antiferro phase transition lines:

$$\kappa = -\frac{1}{4d}\left(1 + \frac{2DY^2}{d - 2Y^2}\right), \qquad Y^2 < d/2; \tag{2.58}$$

$$\kappa = -\frac{1}{4d}\left(1 - \frac{Dd}{d - 2Y^2}\right), \qquad Y^2 > d/2. \tag{2.59}$$

(See figure 3.2: the PM–AM and PM'–AM lines.)

In a bit more detail, transformation (2.57) maps the ferromagnetic order parameter $\langle\phi\rangle$ onto the the parameter of antiferromagnetic ordering $\langle\phi_{\rm st}\rangle$. The free energy as a function of the antiferromagnetic external source $h_x = h'\zeta_x$ has the same form as it has as a function of the homogeneous source $h_x = h$ but with $\kappa \to -\kappa$ and $Y^2 \to -Y^2$. The antiferromagnetic transition is characterised by the divergence of $(\partial^2 W/\partial h'^2)_{h'=0}$ (the susceptibility to h'). Thus the equations for the para-ferro and para–antiferro phase transition lines should be related by the transformation $\kappa \to -\kappa$ and $Y^2 \to -Y^2$. It is also sensible to assume that the regions of applicability of the formulae (2.58) and (2.59) are similar to those of (2.54) and (2.42).

2.5 Mean field approximation in the $U(1)$ scalar–fermion model

We study the model with a two component scalar field for which it is more convenient to use a complex notation: $\phi_x = \phi_x^0 + i\phi_x^1 = e^{i\theta_x}$. The action of the model is:

$$\begin{aligned} S &= S_B + S_F; \\ S_B &= -2\kappa \sum_{x,\mu} \mathrm{Re}\, \phi_x^* \phi_{x+\hat{\mu}}, \qquad |\phi_x|^2 = 1; \\ S_F &= \sum_{\alpha=1}^{D} \sum_{x,\mu} \frac{1}{2} \bar{\chi}_x^\alpha \eta_{x,\mu} (\chi_{x+\hat{\mu}}^\alpha - \chi_{x-\hat{\mu}}^\alpha) + \\ &+ \sum_{\alpha=1}^{D/2} \sum_x Y \bar{\chi}_x^\alpha e^{i\zeta_x \theta_x} \chi_x^\alpha + \sum_{\alpha=D/2+1}^{D} \sum_x Y \bar{\chi}_x^\alpha e^{-i\zeta_x \theta_x} \chi_x^\alpha, \end{aligned} \tag{2.60}$$

where we used staggered fermions as in (1.49). We can introduce the fermion matrix M^{st} as in (1.49):

$$M_{xy}^{\mathrm{st}} = \frac{1}{2} \sum_\mu \eta_{x,\mu} (\delta_{y,x+\hat{\mu}} - \delta_{y,x-\hat{\mu}}) + Y e^{i\zeta_x \theta_x} \delta_{xy} = K_{xy}^{\mathrm{st}} + Y e^{i\zeta_x \theta_x} \delta_{xy}, \tag{2.61}$$

and write:

$$S_F = \sum_{\alpha=1}^{D/2} \sum_{xy} \bar{\chi}_x^\alpha M_{xy}^{\mathrm{st}} \chi_y^\alpha + \sum_{\alpha=D/2+1}^{D} \sum_{xy} \bar{\chi}_x^\alpha (M^{\mathrm{st}})_{xy}^* \chi_y^\alpha. \tag{2.62}$$

The partition function of the model is:

$$\begin{aligned} Z &= \int \prod_x d\theta_x \int \prod_{y,\alpha} d\chi_y^\alpha \, d\bar{\chi}_y^\alpha \, e^{-S} = \\ &= \int \prod_x d\theta_x \, \exp(-S_B + D \,\mathrm{Re}\, \ln \det M^{\mathrm{st}}), \end{aligned} \tag{2.63}$$

where we set the external sources to zero.

We shall drop the index "st" from M^{st} and K^{st} in what follows. The properties of these matrices are very similar to matrices (1.40) and (2.20).

Following the procedure described in the sections 2.1 and 2.2 we can estimate the free energy of the pure bosonic theory with the action $S_B - D \,\mathrm{Re}\, \ln \det M$:

$$W \le \tilde{W}(H) = \frac{1}{N} \left[\left\langle S_B - D \,\mathrm{Re}\, \ln \det M + \sum_x \mathrm{Re}\, H^* \phi_x \right\rangle_H - \ln Z_H \right], \tag{2.64}$$

where $H \equiv H^0 + iH^1$ is a complex notation for the mean field acting on each ϕ_x,

$$Z_H = \int \prod_x d\theta_x \, \exp\left(\textstyle\sum_x \mathrm{Re}\, H^* \phi_x\right) = (2\pi I_0(|H|))^N, \tag{2.65}$$

and the average over the uncorrelated random field ϕ_x is:

$$\langle \ldots \rangle_H = \frac{1}{Z_H} \int \prod_x d\theta_x \, \exp\left(\textstyle\sum_x \mathrm{Re}\, H^* \phi_x\right) (\ldots) \,. \tag{2.66}$$

Using the averaging rules:

$$\langle \phi_x \phi_{x+\hat{\mu}} \rangle_H = \langle \phi_x \rangle_H \langle \phi_{x+\hat{\mu}} \rangle_H \quad \text{and} \quad \langle \phi_x \rangle_H \equiv \sigma = u'(|H|) e^{i \arg H}. \tag{2.67}$$

where

$$u(|H|) = \frac{1}{N} \ln Z_H = \ln(2\pi I_0(|H|)) \quad \text{and} \quad u'(|H|) = \frac{I_1(|H|)}{I_0(|H|)} = \frac{|H|}{2} + O(|H|^3), \tag{2.68}$$

we find:

$$\tilde{W}(H) = -2d\kappa (u'(|H|))^2 + |H| u'(|H|) - u(|H|) - \frac{1}{N} \langle D \, \mathrm{Re} \ln \det M \rangle_H \,. \tag{2.69}$$

The best estimate for the W is $\min_H \tilde{W}(H)$ and the corresponding H is the self consistent mean field. The symmetric phase $H = \langle \phi \rangle = 0$ becomes unstable if:

$$\left. \frac{\partial^2 \tilde{W}(H)}{\partial |H|^2} \right|_{H=0} < 0. \tag{2.70}$$

Similar to the Z_2 case the dependence on ϕ_x disappears from $\det M$ at $Y = 0$ and $Y = \infty$. The model (2.63) reduces to the d dimensional XY model with the action S_B. This model for large κ is in the broken phase $\langle \phi \rangle \neq 0$ and is in the symmetric phase $\langle \phi \rangle = 0$ at small κ. The mean field equation $\partial \tilde{W}(H)/\partial H = 0$ has the form:

$$|H| = 4d\kappa u'(|H|). \tag{2.71}$$

It is very similar to the mean field equation (2.5) in the Ising model. Using (2.68) we find that for $\kappa < 1/2d$ the only solution is $H = 0$. For $\kappa > 1/2d$ a nonzero solution $|H| \neq 0$ appears. This corresponds to a degenerate set of solutions $H \neq 0$ due to the $U(1)$ symmetry of the model. The symmetric solution becomes unstable (2.70) at $\kappa > 1/2d$. Thus the mean field estimate for the phase transition point in the XY model is: $\kappa = 1/2d$. Numerically, in $d = 4$ dimensions the transition occurs at $\kappa_c \approx 0.15$, while the mean field estimate is 0.125.

2.5.1 Para–ferromagnetic phase transition lines

To calculate $\langle \mathrm{Re} \ln \det M \rangle_H$ we first observe using (2.66) and (2.61) that:

$$\langle \ln \det M^* \rangle_H = \langle \ln \det M \rangle_{H^*} \,. \tag{2.72}$$

Then we expand $\langle \ln \det M \rangle_H$ in powers of Y:

$$\langle \ln \det M \rangle_H = \ln \det K + \operatorname{tr} \ln(\delta_{xy} + Y(K^{-1})_{xy} e^{i\zeta_y \theta_y}) =$$
$$= \ln \det K - \frac{1}{2} Y^2 \sum_{xy} (K^{-1})_{xy} (K^{-1})_{yx} \left\langle e^{i\zeta_x \theta_x} e^{i\zeta_y \theta_y} \right\rangle_H - \ldots -$$
$$- \frac{1}{n} Y^n \sum_{x_1 x_2 \ldots x_n} (K^{-1})_{x_1 x_2} \ldots (K^{-1})_{x_n x_1} \left\langle e^{i\zeta_{x_1} \theta_{x_1}} e^{i\zeta_{x_2} \theta_{x_2}} \ldots e^{i\zeta_{x_n} \theta_{x_n}} \right\rangle_H - \ldots . \tag{2.73}$$

One can see that a term of order Y^n contributes $O(|H|^n)$ for small H. Indeed, if all the sites $x_1, x_2, \ldots, x_n$ are distinct then using (2.67), (2.68) we find that

$$\left\langle e^{i\zeta_{x_1} \theta_{x_1}} e^{i\zeta_{x_2} \theta_{x_2}} \ldots e^{i\zeta_{x_n} \theta_{x_n}} \right\rangle_H = O(|H|^n). \tag{2.74}$$

If, however, some site x appears k times in this set then using (2.66) we find:

$$\left\langle e^{ik\theta_x} \right\rangle_H = \frac{I_k(|H|)}{I_0(|H|)} e^{ik \arg H} = O(H^k), \tag{2.75}$$

One can see that (2.74) holds in this case also.

Thus only the Y^2 term contributes to the equation (2.70) which determines the stability of the symmetric phase $H = \langle \phi \rangle = 0$. Calculating this term we find:

$$\left. \frac{\partial^2 \tilde{W}(|H|)}{\partial |H|^2} \right|_{H=0} = \frac{1}{2} - d\kappa - \frac{DcY^2}{4}, \tag{2.76}$$

where c is the same as in (2.31), (2.50). The phase transition line that begins at the point $(0, \kappa_c)$ follows the equation:

$$\kappa = \frac{1}{2d}(1 - \frac{DcY^2}{2}). \tag{2.77}$$

As in the Z_2 case we see that this formula is correct at $Y = 0$ but is obviously wrong at $Y = \infty$.

For large Y we can expand $\ln \det M$ in powers of $1/Y$:

$$\langle \ln \det M \rangle_H = \langle \ln \det(Y e^{i\zeta_x \theta_x} \delta_{xy}) \rangle_H + \langle \operatorname{tr} \ln(\delta_{xy} + \frac{1}{Y} K_{xy} Y e^{i\zeta_y \theta_y} \delta_{xy}) \rangle_H =$$
$$= \ln Y^N - \frac{1}{2Y^2} \sum_{xy} K_{xy} K_{yx} \left\langle e^{i\zeta_x \theta_x} e^{i\zeta_y \theta_y} \right\rangle_H - \ldots -$$
$$- \frac{1}{nY^n} \sum_{x_1 x_2 \ldots x_n} K_{x_1 x_2} \ldots K_{x_n x_1} \left\langle e^{i\zeta_{x_1} \theta_{x_1}} e^{i\zeta_{x_2} \theta_{x_2}} \ldots e^{i\zeta_{x_n} \theta_{x_n}} \right\rangle_H - \ldots . \tag{2.78}$$

Similar to the expansion (2.73) only the $1/Y^2$ terms contribute $O(|H|^2)$ at small H. The equation for the phase transition line takes the form:

$$\left. \frac{\partial^2 \tilde{W}(|H|)}{\partial |H|^2} \right|_{H=0} = \frac{1}{2} - d\kappa - \frac{Dd}{4Y^2} = 0$$

or

$$\kappa = \frac{1}{2d}(1 - \frac{Dd}{4Y^2}). \tag{2.79}$$

This formula is correct at $Y = \infty$ but is wrong at $Y = 0$. We assume that similar to the Z_2 model the regions of applicability of the equations (2.77) and (2.79) complement each other and merge at some intermediate value of $Y = Y_*$. We recall again that the mean field approximation should give correct leading $1/d$ results. We can get a self consistent large d picture if we neglect $O(1/d^2)$ terms in $c = 2/d + O(1/d^2)$ in (2.77) and take $Y_* = \sqrt{d/2}$. At this value of Y the lines (2.77) and (2.79) come to the same point[6] :

$$\kappa = \frac{1}{2d}\left(1 - \frac{D}{2}\right).$$

Finally, we find approximate phase transition lines separating the symmetric $\langle\phi\rangle = 0$ and broken $\langle\phi\rangle \neq 0$ phases in the $U(1)$ scalar–fermion model:

$$\kappa = \frac{1}{2d}\left(1 - \frac{DY^2}{d}\right), \qquad Y^2 < d/2; \tag{2.80}$$

$$\kappa = \frac{1}{2d}\left(1 - \frac{Dd}{4Y^2}\right), \qquad Y^2 > d/2. \tag{2.81}$$

(See figure 3.3: the PM–FM and PM'–FM lines.)

2.5.2 Antiferromagnetic phase

In the XY model at negative κ the antiferromagnetic ordering becomes favourable. Total antiferromagnetic order corresponds to $\phi_x = \zeta_x$ (up to a global complex phase) as in the Ising model. The transformation (2.55) maps the ferromagnetic phase onto the antiferromagnetic one and κ onto $-\kappa$. Thus there is a para–antiferro phase transition at $\kappa = -\kappa_c$ in the XY model.

In the scalar–fermion model we expect lines of the phase transition separating the paramagnetic from the antiferromagnetic phase to begin in the points $(0, -\kappa_c)$ and $(\infty, -\kappa_c)$. We can, as in the Z_2 case, simplify the derivation of these phase transition lines using the transformation similar to (2.57):

$$\begin{array}{lll} \kappa \to -\kappa, & & \varphi_x \to \zeta_x \varphi_x, \\ Y \to -iY, & \psi_x \to \exp(i\zeta_x \frac{\pi}{4})\psi_x, & \bar{\psi}_x \to \exp(i\zeta_x \frac{\pi}{4})\bar{\psi}_x. \end{array} \tag{2.82}$$

[6]The value $Y = \sqrt{d/2}$ has some other remarkable features: see footnote 5 on page 38 and appendix C.

This transformation does not change the action of the model. The para–antiferro phase transition lines can be obtained from (2.80), (2.81) by substituting $\kappa \to -\kappa$ and $Y^2 \to -Y^2$:

$$\kappa = -\frac{1}{2d}\left(1 + \frac{DY^2}{d}\right), \qquad Y^2 < d/2; \tag{2.83}$$

$$\kappa = -\frac{1}{2d}\left(1 + \frac{Dd}{4Y^2}\right), \qquad Y^2 > d/2. \tag{2.84}$$

(See figure 3.3: the PM–AM and PM'–AM lines.)

2.6 Mean field approximation in the $O(4)$ scalar–fermion model

Now we shall discuss the more realistic model with four component scalar field. The action of the model has the form:

$$\begin{aligned} S &= S_B + S_F; \\ S_B &= -2\kappa \sum_{x,\mu} \phi^k_x \phi^k_{x+\hat{\mu}}, \qquad \phi^k_x \phi^k_x = 1; \\ S_F &= \sum_{\alpha=1}^{D} \sum_{x,\mu} \eta_{x,\mu} \bar{\chi}^\alpha_x (\chi^\alpha_{x+\hat{\mu}} - \chi^\alpha_{x-\hat{\mu}}) + Y \sum_x \bar{\chi}^\alpha_x \Phi_x \chi^\alpha_x \equiv \\ &\equiv \sum_{\alpha=1}^{D} \sum_{xy} \bar{\chi}^\alpha_x M_{xy} \chi^\alpha_y; \end{aligned} \tag{2.85}$$

where the summation over $k = 0, 1, 2, 3$ is implied. We use a convenient $SU(2)$ notation for the scalar field in the Yukawa term:

$$\Phi_x = \phi^0_x + i\zeta_x \boldsymbol{\tau} \cdot \boldsymbol{\phi}_x \tag{2.86}$$

The model contains D species of staggered fermions χ^α. Each of them is an $SU(2)$ doublet.

The partition function of the model has the form:

$$Z = \int \prod_x d\mu_x \, \exp(-S_B + D \ln \det M). \tag{2.87}$$

where we integrated over the fermion fields and dropped external sources. The integration $\int d\mu_x$ in each site x is over the unit sphere covered by the vector ϕ^k_x.

Now as in the Z_2 and the $U(1)$ cases we use the mean field approximation to compute the partition function and/or the free energy in this theory. We neglect correlations of the field ϕ^i_x and use a test probability distribution:

$$P(\phi) = Z_H^{-1} \exp(\textstyle\sum_x H^k \phi^k_x), \tag{2.88}$$

where H^k is the 4 component mean field and the normalisation factor Z_H is:

$$Z_H \equiv \int \prod_x d\mu_x \exp(\textstyle\sum_x H^k \phi^k_x) = \{2\pi^2 (I_0(H) - I_2(H))\}^N. \tag{2.89}$$

where $H = \sqrt{H^k H^k}$. The mean field estimate for the free energy per site is:

$$\tilde{W}(H) = \frac{1}{N} (\langle S_B - D \ln \det M \rangle_H + \langle \textstyle\sum_x H^k \phi^k_x \rangle_H - \ln Z_H). \tag{2.90}$$

The self consistent value of the mean field H is a minimum of the mean field free energy $\tilde{W}(H)$. The mean field free energy is symmetric under $O(4)$ rotations of H due to the symmetry of the theory (2.85). Thus $H = 0$ is always an extremum of (2.90). Whether it is a (local) minimum depends on the sign of the $\partial^2\tilde{W}/\partial H^2|_{H=0}$. The phase transition between symmetric and broken phases occurs when:

$$\left.\frac{\partial^2\tilde{W}(H)}{\partial H^2}\right|_{H=0} = 0. \tag{2.91}$$

One can compute $\tilde{W}(H)$ *exactly* in the limits $Y = 0$ or $Y = \infty$, where $\det M$ does not depend on ϕ_x and the model reduces to the $O(4)$ spin model with the action S_B. Using the relations:

$$\langle\phi^k_x\phi^k_{x+\hat{\mu}}\rangle_H = \langle\phi^k_x\rangle_H\langle\phi^k_{x+\hat{\mu}}\rangle_H, \qquad \langle\phi^k_x\rangle_H = \frac{\partial u(H)}{\partial H^k} = \frac{H^k}{4} + O(H^3),$$
$$u(H) \equiv \frac{1}{N}\ln Z_H = \text{const} + \frac{H^2}{8} + O(H^4) \tag{2.92}$$

and the condition for the phase transition (2.91) one can find that the second order phase transition in such a model occurs at $\kappa = 1/d$.

To compute $\langle\ln\det M_{xy}\rangle_H$ we expand this quantity in powers of Y for small Y and in powers of $1/Y$ for large Y.

2.6.1 Large Y

Consider first the case of large Y , then:

$$\begin{aligned}\langle\ln\det M_{xy}\rangle_H &\equiv \langle\ln\det(K_{xy} + Y\Phi_x\delta_{xy})\rangle_H = \\ &= \langle\ln\det(Y\Phi_x\delta_{xy})\rangle_H + \langle\,\mathrm{tr}\,\ln(\delta_{xy} + Y^{-1}K_{xy}\Phi_y)\rangle_H = \\ &= \ln Y^{2N} - \frac{1}{2Y^2}\sum_{xy}K_{xy}K_{yx}\langle\,\mathrm{Tr}\,\Phi_x\Phi_y\rangle_H - \ldots - \\ &- \frac{1}{nY^n}\sum_{x_1\ldots x_n}K_{x_1x_2}\ldots K_{x_nx_1}\langle\,\mathrm{Tr}\,\Phi_{x_1}\Phi_{x_2}\ldots\Phi_{x_n}\rangle_H - \ldots .\end{aligned} \tag{2.93}$$

where "Tr" denotes the trace over the $SU(2)$ indices. We used the fact that $\Phi^{-1} = \Phi^\dagger$, and also that $\det M(\Phi^\dagger) = \det M(\Phi)$, which follows from the reality of the $\det M$.

Terms in (2.93) can be represented by diagrams: closed chains with links connecting neighbouring sites $x_1, x_2, \ldots, x_n$: exactly as in the Z_2 case. Each type of the diagrams is associated with a factor

$$\langle\,\mathrm{Tr}\,\Phi_{x_1}\Phi_{x_2}\ldots\Phi_{x_n}\rangle_H \equiv F_n \tag{2.94}$$

and a factor equal to the number of possible ways to put the diagram of this type on the lattice.

To study the *local* stability of the symmetric phase we need only $O(H^2)$ terms in (2.93). As we shall see, unlike the case of $U(1)$ symmetry, it is not only the $1/Y^2$ term in the expansion of $\langle \ln \det M_{xy} \rangle_H$ which contributes $O(H^2)$, i.e. the situation resembles the Z_2 case. We proceed as in the Z_2 case and calculate $O(H^2)$ terms in each order in $1/Y$ to the leading order in $1/d$. These terms can be summed up then.

First, we need to calculate the factor F_n: it gives the H dependence. We shall write it in the form:

$$F_n = \mathrm{Tr}\left(T^{k_1}\bar{T}^{k_2}T^{k_3}\dots\bar{T}^{k_n}\right)\langle\phi_{x_1}^{k_1}\phi_{x_2}^{k_2}\phi_{x_3}^{k_3}\dots\phi_{x_n}^{k_n}\rangle_H, \tag{2.95}$$

where $T^k = (1, i\tau)$ and $\bar{T}^k = (1, -i\tau)$. The T's alternate with $\bar{T}$'s because the links of the diagrams connect neighbouring sites and $\zeta_{x+\hat{\mu}} = -\zeta_x$.

Each site that the chain passes only once contributes a factor:

$$\langle\phi_x^k\rangle_H = \frac{H^k}{4} + O(H^3). \tag{2.96}$$

A site passed twice contributes

$$\langle\phi_x^k\phi_x^m\rangle_H = \frac{1}{4}\delta^{km} + O(H^2). \tag{2.97}$$

One can see that a site passed an odd number of times contributes a factor $O(H)$ and a site passed an even number of times contributes a factor $O(1)$. This situation resembles the Z_2 case where we had $\tanh H$ for the sites passed an odd number of times and 1 for the sites passed an even number of times. Similarly, we can assume that the leading contribution in the limit $d \to \infty$ to the terms of order $O(H^2)$ for given order in $1/Y$ is exhausted by diagrams of the *double chain* type (like the diagram on fig. 2.3).

We can easily compute the factor (2.95) for a double chain diagram to the order $O(H^2)$. We substitute (see fig. 2.3):

$$\begin{aligned} &\langle\phi_{x_{n/2}}^k\rangle_H \to \frac{H^k}{4} \qquad \text{and} \qquad \langle\phi_{x_n}^k\rangle_H \to \frac{H^k}{4}; \\ &\langle\phi_{x_i}^k\phi_{x_{n-i}}^m\rangle_H \to \frac{\delta^{km}}{4} \qquad \text{for} \qquad i = 1, \dots, \frac{n}{2} - 1. \end{aligned} \tag{2.98}$$

Take for definiteness a chain with an odd number $n/2$ of double links. Then:

$$\begin{aligned} F_n = \mathrm{Tr}\left(T^{k_1}\dots\bar{T}^{k_{n/2-1}}T^{k_{n/2}}\bar{T}^{k_{n/2+1}}\dots T^{k_{n-1}}\bar{T}^{k_n}\right)\frac{H^{k_{n/2}}}{4}\frac{H^{k_n}}{4}\cdot \\ \cdot\left(\frac{1}{4}\right)^{n/2-1}\delta^{k_1,k_{n-1}}\dots\delta^{k_{n/2-1},k_{n/2+1}} + O(H^4). \end{aligned} \tag{2.99}$$

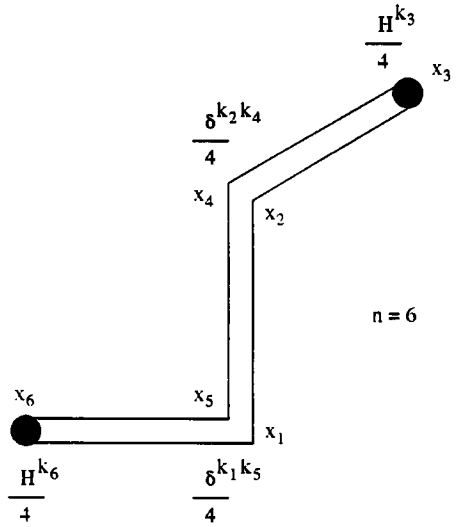

Figure 2.3: An example of a double chain diagram for $n = 6$. The sites of the lattice passed by the chain are: $x_1 = x_5$, $x_2 = x_4$, x_3 and x_6. The contributions to the factor $\langle \phi_{x_1}^{k_1} \phi_{x_2}^{k_2} \dots \phi_{x_6}^{k_6} \rangle_H$ from each site are written next to the sites. The identity (2.100) is used to calculate F_n (2.99) in the following way: $\mathrm{Tr}\,(T^{k_1}\bar{T}^{k_2}T^{k_3}\bar{T}^{k_4}T^{k_5}\bar{T}^{k_6})\delta^{k_1 k_5}\delta^{k_2 k_4} = -2\,\mathrm{Tr}\,(T^{k_1}\bar{T}^{k_3}T^{k_5}\bar{T}^{k_6})\delta^{k_1 k_5} = (-2)^2\,\mathrm{Tr}\,(T^{k_3}\bar{T}^{k_6})$.

One can check that:

$$\bar{T}^m T^k \bar{T}^m = (1 - 1 - 1 - 1)\bar{T}^k = (-2)\bar{T}^k. \tag{2.100}$$

Using this identity and its hermitian conjugate we can cancel all T's except $T^{k_{n/2}}$ and $\bar{T}^{k_n}$. Finally, we obtain neglecting terms $O(H^4)$:

$$F_n = (-2)^{n/2-1}\,\mathrm{Tr}\,\left(T^k \bar{T}^m\right)\left(\frac{1}{4}\right)^{n/2-1}\frac{H^k}{4}\frac{H^m}{4} = \frac{H^2}{8}\left(-\frac{1}{2}\right)^{n/2-1}. \tag{2.101}$$

One can repeat this procedure for the case of even $n/2$ and arrive again at (2.101).[7]

Comparing this result with the case of Z_2 model we note that besides obvious difference in numbers there is an essential additional sign factor $(-1)^{n/2-1}$ which changes the result for the phase transition lines qualitatively (see sect. 3.2.2). One can trace the appearance of this factor to (2.100). We can also recall the result from the $U(1)$ model where we found that only $1/Y^2$ term contributed $O(H^2)$. To compare the case of $O(4)$ and $U(1)$ models it is helpful to use 2 component $O(2)$ notations for the complex field ϕ in the Yukawa term in (2.60): $e^{i\theta} = \phi^0 + i\phi^1 \equiv \sum_{i=0,1} T^i \varphi^i$, i.e., $T^i = (1, i)$ and $\bar{T}^i = (1, -i)$. Then the algebra is very similar to the $O(4)$ case except that the identity analogous to (2.100) is:

$$O(2): \qquad \bar{T}^j T^i \bar{T}^j = (1 - 1)T^i = 0. \tag{2.102}$$

[7] Only the formula (2.99) changes: $T^{k_{n/2}}$ and T^{k_n} are then both T's or both $\bar{T}$'s.

Thus the site passed twice by the chain contributes a factor $O(H^2)$ rather than $O(1)$ as one could expect from: $\langle \phi_x^i \phi_x^j \rangle_H = \frac{1}{2}\delta^{ij} + O(H^2)$. Therefore in the $U(1)$ model only the shortest chain: with 2 vertices, gives $O(H^2)$ term.

Finally, we collect all the factors corresponding to a given n, i.e.:

$-1/(nY^n)$ - see (2.93);

F_n - as in (2.101);

n - the number of ways to enumerate the vertices;

$(-1/4)^{n/2}$ - the product of the K's matrix elements;

$N(2d)^{n/2}/2$ - the number of different double chains on the lattice in the leading order in d (we neglect self crossings).

Summing over all (even) n we obtain the $O(H^2)$ contribution to $\langle \ln \det M \rangle_H$ in the leading order in $1/d$ expansion. Substituting this in (2.90) we find the mean field free energy to order $O(H^2)$:

$$\tilde{W}(H) = \frac{H^2}{8} - d\kappa \frac{H^2}{8} - D\frac{d}{4Y^2 - d}\frac{H^2}{8} + O(H^4), \qquad \text{large } Y. \tag{2.103}$$

Using (2.91) we find the equation for the phase transition line beginning in the point $(Y = \infty, \kappa = 1/d)$:

$$\kappa = \frac{1}{d}\left(1 - D\frac{d}{4Y^2 - d}\right), \qquad \text{large } Y. \tag{2.104}$$

2.6.2 Small Y

For small Y we expand $\langle \ln \det M \rangle_H$ in powers of Y:

$$\begin{aligned}\langle \ln \det M_{xy} \rangle_H &\equiv \langle \ln \det K_{xy} \rangle_H + \langle \operatorname{tr} \ln(\delta_{xy} + Y \left(K^{-1}\right)_{xy} \Phi_y) \rangle_H = \\ &= \ln \det K_{xy} - \frac{1}{2}Y^2 \sum_{xy} \left(K^{-1}\right)_{xy} \left(K^{-1}\right)_{yx} \langle \operatorname{Tr} \Phi_x \Phi_y \rangle_H - \ldots - \\ &- \frac{1}{n}Y^n \sum_{x_1 \ldots x_n} \left(K^{-1}\right)_{x_1 x_2} \ldots \left(K^{-1}\right)_{x_n x_1} \langle \operatorname{Tr} \Phi_{x_1} \Phi_{x_2} \ldots \Phi_{x_n} \rangle_H - \ldots .\end{aligned} \tag{2.105}$$

A diagrammatic representation is again possible. But now links of the closed chains connect not only neighbouring sites since the matrix $(K^{-1})_{xy}$ is nonlocal. The situation is exactly the same as in the Z_2 model. We can again simplify the

problem keeping only leading contribution in the $d \to \infty$ limit to $O(H^2)$ terms in a given order in Y. In this limit

$$\left(K^{-1}\right)_{xy} = -\frac{2}{d}K_{xy} + O(1/d^2)$$

(see (2.51)). As in the Z_2 model we substitute:

$$K^{-1} \to -\frac{2}{d}K \quad \text{and} \quad Y \to \frac{d}{2Y}$$

into (2.105). Then this series takes the same form as the series for large Y (2.93).

Thus we can obtain the leading large d contribution to the mean field free energy to the order $O(H^2)$ substituting $d/2Y$ for Y into the expression (2.103):

$$\tilde{W}(H) = \frac{H^2}{8} - \kappa d\frac{H^2}{8} - D\frac{Y^2}{d-Y^2}\frac{H^2}{8} + O(H^4), \qquad \text{small } Y. \tag{2.106}$$

Using (2.91) we find the equation for the second order phase transition line which begins in the point $(0, \frac{1}{d})$ in the (Y, κ) plane:

$$\kappa = \frac{1}{d}\left(1 - D\frac{Y^2}{d-Y^2}\right), \qquad \text{small } Y. \tag{2.107}$$

2.6.3 Para–antiferro phase transition lines

To study the second order phase transition from the paramagnetic to the antiferromagnetic phase where $\langle\phi_{\rm st}\rangle \equiv \langle\sum_x \varphi_x\zeta_x/N\rangle \neq 0$ we can use the transformation similar to (2.82). Again (see sect. 2.4), we can obtain equations for the second order para–antiferro phase transition lines by substituting $\kappa \to -\kappa$, $Y^2 \to -Y^2$ into the equations (2.107) and (2.104):

$$\kappa = -\frac{1}{d}\left(1 + D\frac{Y^2}{d+Y^2}\right), \qquad \text{small } Y. \tag{2.108}$$

and

$$\kappa = -\frac{1}{d}\left(1 + D\frac{d}{4Y^2+d}\right). \qquad \text{large } Y. \tag{2.109}$$

We shall discuss the regions of applicability of the formulae for the phase transition lines in the next chapter where we study the properties of the phases in the scalar–fermion theories. The phase diagram of the $O(4)$ theory for different values of D is described in section 3.2.2: see figure 3.4.

Chapter 3

Properties of the phases

In this chapter we extend our methods to study the properties of different phases. In the previous chapter we studied the phase structure of scalar–fermion models using the vacuum expectation of the scalar field $\langle\phi\rangle$ as an order parameter. It, however, does not provide any information about the properties of the fermions in the theory. As was first pointed out in [34] fermions display quite different behaviour at small and large values of Y in the broken phase near the critical line. For small Y the masses of the fermions behave as $m_F \approx Y\langle\phi\rangle$ and vanish on the critical line. At large Y the fermion masses grow as one approaches the critical line. The crossover occurs at around $Y \approx 1.4$ in $d = 4$ [34]. Therefore it is interesting to study different fermionic correlation functions. We compute the fermion condensate $\langle\bar{\psi}\psi\rangle$ and the fermion propagator in the mean field approximation in the symmetric phase and near the critical line. We find that the region $\langle\phi\rangle = 0$ is not a single phase. It is separated into two phases by a transition around $Y \approx \sqrt{d/2}$. The phases are distinguished by the properties of the fermions.

The symmetric phase at large Y is interesting because fermions are massive there. This contradicts the tree level relation $m_F = Y\langle\phi\rangle$. On the other hand, at large values of the Yukawa coupling one can expect some nonperturbative phenomena to occur. In particular, the fermions can form bound states. To check this hypothesis we calculate the four–fermion correlator in the mean field approximation. We see that it has poles which do not correspond to fundamental fields in the theory. We also address the question of whether one can define a continuum limit where these bound states are in the physical (low energy) spectrum. This might be possible near the PM–PM' line.

Finally, one can perform continuum limit at the critical line between the symmetric and antiferromagnetic phases. We study this continuum limit and discover that in the resulting theory unitarity is violated.

3.1 Behaviour of the fermions

3.1.1 Fermion condensate: $\langle\bar{\psi}\psi\rangle$

We begin with computing the fermion condensate, or the fermion propagator in coinciding points, $\langle\bar{\psi}_x\psi_x\rangle$.

Consider the Z_2 model. Let us introduce an additional parameter m (the bare fermion mass) in the action (2.18). The partition function is then:

$$Z(m) \equiv e^{-NW(m)} = \sum_{\{\phi_x=\pm1\}} \int \prod_x d\psi_x\, d\bar{\psi}_x\, e^{-S-m\sum_x \bar{\psi}_x\psi_x} = \\ = \sum_{\{\phi_x=\pm1\}} \exp(-S_B + \ln\det M'), \tag{3.1}$$

where

$$M'_{xy} = K_{xy} + Y\phi_x\delta_{xy} + m\delta_{xy}. \tag{3.2}$$

Obviously, m acts as a source for $\bar{\psi}\psi$. The partition function $Z(m)$ can be estimated in the framework of mean field theory as before. The formula (2.22) becomes:

$$\tilde{W}(h,H,m) = -2d\kappa(\tanh H)^2 + (H-h)\tanh H - \ln(2\cosh H) - \frac{1}{N}\langle\ln\det M'\rangle_H. \tag{3.3}$$

We have already calculated $\langle\ln\det M'\rangle_H$ up to terms $O(\sigma^2)$ at $m=0$, where $\sigma \equiv \langle\phi\rangle_H = \tanh H$. One can calculate the σm and m^2 terms analogously.

At large Y we expand in powers of $1/Y$:

$$\langle\ln\det M'\rangle_H = \langle\ln\det(Y\phi_x\delta_{xy})\rangle_H + \langle\,\mathrm{tr}\,\ln(\delta_{xy} + \frac{1}{Y}(m\delta_{xy}+K_{xy})\phi_y)\rangle_H = \\ = \ln Y^{ND} + \frac{1}{Y}\,\mathrm{Tr}\sum_x (m\delta_{xx}+K_{xx})\langle\phi_x\rangle_H - \\ -\frac{1}{2Y^2}\,\mathrm{Tr}\sum_{xy}(m\delta_{xy}+K_{xy})(m\delta_{yx}+K_{yx})\langle\phi_x\phi_y\rangle_H + \ldots + \\ +\frac{(-1)^{n+1}}{nY^n}\,\mathrm{Tr}\sum_{x_1x_2\ldots x_n}(m\delta_{x_1x_2}+K_{x_1x_2})\cdot\ldots\cdot(m\delta_{x_nx_1}+K_{x_nx_1})\cdot \\ \cdot\langle\phi_{x_1}\phi_{x_2}\cdots\phi_{x_n}\rangle_H - \ldots. \tag{3.4}$$

The contribution of each term in this expansion proportional to m^2 can be illustrated by diagrams similar to those considered in the previous chapter. The diagrams are closed chains with vertices in points $x_1, x_2, \ldots, x_n$. In fact, there are $n-2$ vertices because two pairs of points x_i coincide due to two factors $m\delta_{xy}$. The typical diagrams in the order $1/Y^8$ are shown in fig. 3.1.

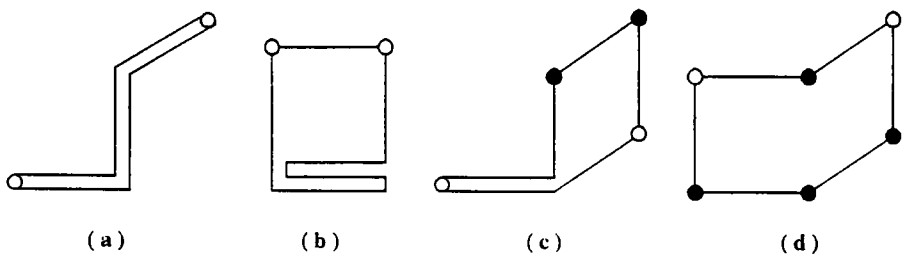

Figure 3.1: Typical diagrams in the order $1/Y^8$ for the expansion (3.4) which contribute terms of order m^2. The unfilled circles denote the vertices contributing a factor m each. The filled circles are for the unpaired vertices which contribute a factor σ each.

As before, we can argue that to calculate the contribution proportional to m^2 to the leading order in $1/d$ it is sufficient to take into account only *double chain* diagrams (fig. 3.1a). The contribution of these diagrams to order $1/Y^n$ ($n = 2, 4, 6, \ldots$) is:

$$-\frac{1}{nY^n} m^2 \frac{n}{2} (2d)^{n/2-1} \left(-\frac{1}{4}\right)^{n/2-1} ND. \tag{3.5}$$

Summing over $n = 2, 4, 6, \ldots$ we obtain the contribution proportional to m^2 to the $\langle \ln \det M' \rangle_H$:

$$-m^2 \frac{1}{d + 2Y^2} ND. \tag{3.6}$$

The contribution proportional to $m\sigma$ in the expansion (3.4) can be described by the same diagrams as the contribution of order m^2. There is an unpaired ϕ_x vertex in the place of one of the m vertices (see fig. 3.1 — these diagrams now describe the contribution of order $1/Y^7$). The contribution of the *double chain* diagrams in the order $1/Y^n$ ($n = 1, 3, 5, \ldots$) is equal to:

$$\frac{1}{nY^n} m\sigma n (2d)^{\frac{n-1}{2}} \left(-\frac{1}{4}\right)^{\frac{n-1}{2}} ND. \tag{3.7}$$

Summing over odd n we obtain the contribution of order $m\sigma$ to $\langle \ln \det M' \rangle_H$:

$$m\sigma \frac{2Y}{d + 2Y^2} ND. \quad \bullet \tag{3.8}$$

At small Y we use the expansion:

$$\begin{aligned}
\langle \ln \det M' \rangle_H &= \operatorname{tr} \ln K + \langle \operatorname{tr} \ln(\delta_{xy} + (K^{-1})_{xy}(Y\phi_y + m)) \rangle_H = \\
&= \operatorname{tr} \ln K - \frac{1}{2} \operatorname{Tr} \sum_{xy} (K^{-1})_{xy} (K^{-1})_{yx} \langle (Y\phi_x + m)(Y\phi_y + m) \rangle_H - \ldots - \\
&- \frac{1}{n} \operatorname{Tr} \sum_{x_1 x_2 \ldots x_n} (K^{-1})_{x_1 x_2} \cdots (K^{-1})_{x_n x_1} \\
&\cdot \langle (Y\phi_{x_1} + m)(Y\phi_{x_2} + m) \cdots (Y\phi_{x_n} + m) \rangle_H - \ldots .
\end{aligned} \tag{3.9}$$

The diagrams representing the terms in this expansion are similar to the ones in the small Y expansion of $\langle \ln \det M \rangle_H$ (2.43). We can again argue (see sect. 2.3.2) that at large d the matrix K^{-1} becomes local and one can substitute in (3.9):

$$K^{-1} \to -\frac{2}{d} K.$$

Assuming again that the leading large d result in each order in Y is given by the double chain diagrams we can calculate the m^2 terms in each order n in (3.9):

$$-\frac{m^2 Y^{n-2}}{n} \frac{n}{2} (2d)^{n/2} \left(-\frac{1}{d^2}\right)^{n/2} ND \tag{3.10}$$

Summing over $n = 2, 4, 6, \ldots$ we obtain:

$$m^2 \frac{1}{d + 2Y^2} ND. \tag{3.11}$$

The $m\sigma$ terms are described by similar diagrams but with one m vertex replaced by $Y\phi_x$. The contribution of the double chains in order n in (3.9) is:

$$-\frac{m\sigma Y^{n-1}}{n} n (2d)^{n/2} \left(-\frac{1}{d^2}\right)^{n/2} ND. \tag{3.12}$$

The sum over $n = 2, 4, 6, \ldots$ gives:

$$m\sigma \frac{2Y}{d + 2Y^2} ND. \tag{3.13}$$

Finally, we obtain for the derivatives of $\tilde{W}(h = 0, H, m)$:

$$\left.\frac{\partial^2 \tilde{W}(h = 0, H, m)}{\partial m^2}\right|_{m=0} = \varepsilon(2Y^2 - d) \frac{2D}{d + 2Y^2} + O(\sigma^2). \tag{3.14}$$

and

$$\left.\frac{\partial \tilde{W}(h = 0, H, m)}{\partial m}\right|_{m=0} = -D \frac{2Y}{d + 2Y^2} \sigma + O(\sigma^3), \tag{3.15}$$

where $\varepsilon(x) = +1$ for $x > 0$ and -1 for $x < 0$. Taking into account that

$$\langle \bar{\psi}\psi \rangle = -\frac{1}{N} \frac{1}{Z} \frac{\partial Z}{\partial m} = \frac{\partial W}{\partial m}. \tag{3.16}$$

one can write the mean field estimate for the fermion condensate (more accurately: the fermion propagator in coinciding points):

$$\langle \bar{\psi}\psi \rangle\Big|_{m=0} = -D \frac{2Y}{d + 2Y^2} \sigma + O(\sigma^3). \tag{3.17}$$

3.1.2 Two different phases with $\langle\phi\rangle = 0$

Let us now consider the formula (3.14). The derivative $\partial^2 W/\partial m^2$ describes the response (susceptibility) of the fermion condensate to m and can be also expressed as a four fermion correlator:

$$\frac{\partial^2 W}{\partial m^2} = \frac{\partial}{\partial m}\langle\bar{\psi}\psi\rangle = -\sum_y \left(\langle\bar{\psi}_x\psi_x\bar{\psi}_y\psi_y\rangle - \langle\bar{\psi}_x\psi_x\rangle^2\right). \tag{3.18}$$

The discontinuous behaviour of this quantity in our approximation (3.14) in the domain where $\sigma = 0$ suggests that there is a phase transition at $Y = \sqrt{d/2}$.[1] The line of this phase transition divides the region where $\sigma = 0$ into two phases with different signs of the quantity (3.14).

To understand what happens to the fermions at this transition one can calculate $\partial^2 W/\partial m^2$ in the theory of free massive fermions (i.e., $Y = 0$):

$$\frac{\partial^2 W}{\partial m^2} = -D\int_{-\pi}^{+\pi} \frac{d^d p}{(2\pi)^d} \frac{-\sum_\mu \sin^2 p_\mu + m^2}{(\sum_\mu \sin^2 p_\mu + m^2)^2} \approx -2D\frac{d - 2m^2}{(d + 2m^2)^2}, \tag{3.19}$$

where we have used a large d approximation. One can see that a positive value for this quantity corresponds to very large fermion masses $m > \sqrt{d/2} \gg 1$. In other words, the masses are much larger than the inverse lattice spacing (lattice momentum cutoff).

At small Y, however, the perturbation theory applies and gives: $m_F \approx Y\langle\phi\rangle$, i.e., the fermions are massless in the symmetric phase $\langle\phi\rangle = 0$ at small Y.

We conclude that the theory at $Y^2 < d/2$ contains massless fermions in the symmetric phase, while at $Y^2 > d/2$ the fermions are very massive. In other words, the fermions do not exist as low energy degrees of freedom in the theory at large Y.

One can do similar calculations in the $U(1)$ and $O(4)$ models and arrive to the same conclusions. Also, in the $U(1)$ case it is possible to calculate the fermion propagator in the symmetric phase in the mean field approximation.

The fermion propagator is given by: $\langle\chi_x\bar{\chi}_y\rangle$. One can integrate over fermion variables exactly and obtain: $\langle\chi_x\bar{\chi}_y\rangle = \langle(M^{-1})_{xy}\rangle$, where M is the fermion matrix:

$$M_{xy} = K_{xy} + Ye^{i\zeta_x\theta_x}\delta_{xy}. \tag{3.20}$$

[1] Strictly speaking, (3.14) is the mean field estimate for the one particle irreducible part of the correlator (3.18). Taking the derivative of $\tilde{W}(H, m)$ with respect to m one should take into account that the mean field H depends on m via the self consistency condition $\partial\tilde{W}(H, m)/\partial H = 0$. The corresponding additional term in the mean field estimate for (3.18) is: $-(\partial^2\tilde{W}/\partial H^2)^{-1}(\partial^2\tilde{W}/\partial m\partial H)^2$ It describes the contribution of the intermediate state of one ϕ particle. However, this term is continuous at $Y = \sqrt{d/2}$.

The mean field approximation means that we neglect the correlations of the field $\phi_x = e^{i\zeta_x\theta_x}$, i.e., the propagator is given by $\langle (M^{-1})_{xy}\rangle_H$. We can compute this quantity expanding it in powers of Y at small Y:

$$(M^{-1})_{xy} = (K^{-1})_{xy} - \sum_z (K^{-1})_{xz} Y\phi_z (K^{-1})_{zy} + \ldots + \\ +(-1)^n \sum_{z_1\ldots z_n} (K^{-1})_{xz_1} Y\phi_{z_1} (K^{-1})_{z_1 z_2} \cdots Y\phi_{z_n} (K^{-1})_{z_n y} + \ldots . \qquad (3.21)$$

In the symmetric phase $\langle\phi_x\rangle_{H=0} = 0$. It is very helpful that in the $U(1)$ model also the average of any power of ϕ_x is zero for $H = 0$ (2.75). Using the fact that there are no correlations in our approximation we conclude that the only nonzero contribution to $\langle (M^{-1})_{xy}\rangle_{H=0}$ comes from the first term in (3.21). Thus in the region of applicability of the Y expansion we have:

$$\langle (M^{-1})_{xy}\rangle_{H=0} = (K^{-1})_{xy}, \qquad (3.22)$$

i.e., the fermions are massless.

For large Y we expand in powers of $1/Y$:

$$(M^{-1})_{xy} = \frac{\phi_x^*}{Y}\delta_{xy} - \frac{\phi_x^*}{Y} K_{xy} \frac{\phi_y^*}{Y} + \ldots + \\ +(-1)^{n+1} \sum_{z_1\ldots z_n} \frac{\phi_x^*}{Y} K_{xz_1} \frac{\phi_{z_1}^*}{Y} K_{z_1 z_2} \cdots \frac{\phi_y^*}{Y}, \qquad (3.23)$$

where we used the fact that $1/\phi_x = \phi_x^*$. The average of each term in this expansion over the uncorrelated random field ϕ_x at $H = 0$ is zero. Therefore in the region of applicability of the $1/Y$ expansion[2] :

$$\langle (M^{-1})_{xy}\rangle_{H=0} = 0. \qquad (3.24)$$

This means that fermions do not propagate: their mass is infinitely large in the symmetric phase at large Y.

[2] A simple analogy of such a discontinuous behaviour of the fermion propagator (compare (3.22) and (3.24)) is the integral:

$$\int_0^{2\pi} d\theta\, (1 - a\exp i\theta)^{-1}$$

It is equal to 2π for $|a| < 1$ and is zero for $|a| > 1$. This can be verified by expanding in powers of a for $|a| < 1$ and $1/a$ for $|a| > 1$. It can be also expressed as a contour integral in the complex plane:

$$-i \oint \frac{dz}{z(1-z)},$$

where the contour is a circle of radius $|a|$ around $z = 0$. Then the result is obvious from Cauchy's theorem.

Finally, we conclude from the behaviour of the four fermion correlator (3.18) and the fermion propagator that the symmetric phase $\langle\phi\rangle = 0$ is divided by a phase transition along the vertical line $Y^2 = d/2$ into two distinct phases. The phase at smaller Y contains massless fermions as one would expect from perturbation theory: $m_F = Y\langle\phi\rangle = 0$. In the phase at large Y the fermions do not exist as low energy degrees of freedom.

3.2 The phase diagrams of the scalar–fermion models

Now we put together our results on the equations for the phase transition lines from Chapter 2 and the structure of the symmetric phase and discuss the mean field (large d) phase diagrams of the scalar–fermion models.

3.2.1 The Z_2 model

The phase diagram of the model (2.18) is shown in figure 3.2a. The number of Dirac components of the fermion field ψ is D=4: as in four space–time dimensions. The phase diagram for the smallest number of staggered fermions $D = 2$ is shown in figure 3.2b for comparison.

We rescaled the parameters κ and Y so that the diagrams fig. 3.2 look the same for all large d and given D. One can see that a natural large d limit corresponds to keeping $Y/\sqrt{d}$ and κd fixed. This is analogous to the $1/N$ expansion in the scalar ϕ^4 theories with N component fields: the natural large N limit corresponds to keeping λN fixed.

There are four phases:

FM – the phase with ferromagnetic ordering: $\langle\phi\rangle \neq 0$, or the broken phase;

PM – paramagnetic, or disordered, symmetric phase $\langle\phi\rangle = 0$; in this phase the fermions are massless;

PM' – another paramagnetic phase $\langle\phi\rangle = 0$; there are no massless fermions in this phase, instead the fermions are very massive ($m_F \gg 1/a$);

AM – the phase with antiferromagnetic ordering: $\langle\phi_{\rm st}\rangle \equiv \langle\sum_x \zeta_x\phi_x\rangle \neq 0$.

The two symmetric phases PM and PM' are separated by a phase transition along the vertical line $Y = \sqrt{d/2}$. This transition is characterised by a discontinuous behaviour of fermion correlation functions, for example, see (3.14), (3.18). We expect that fermion correlation functions depend continuously on σ at the second order phase transition where σ vanishes (e.g., as in (3.14)). In this case the line of the discontinuous transition at $Y = \sqrt{d/2}$ should continue into the broken phase. The position of its final point in the broken phase is beyond our approximations: we could calculate (3.14) only for small σ.

We studied only the local stability of the symmetric phase to determine the lines of the second order phase transitions. This means that some first order transition

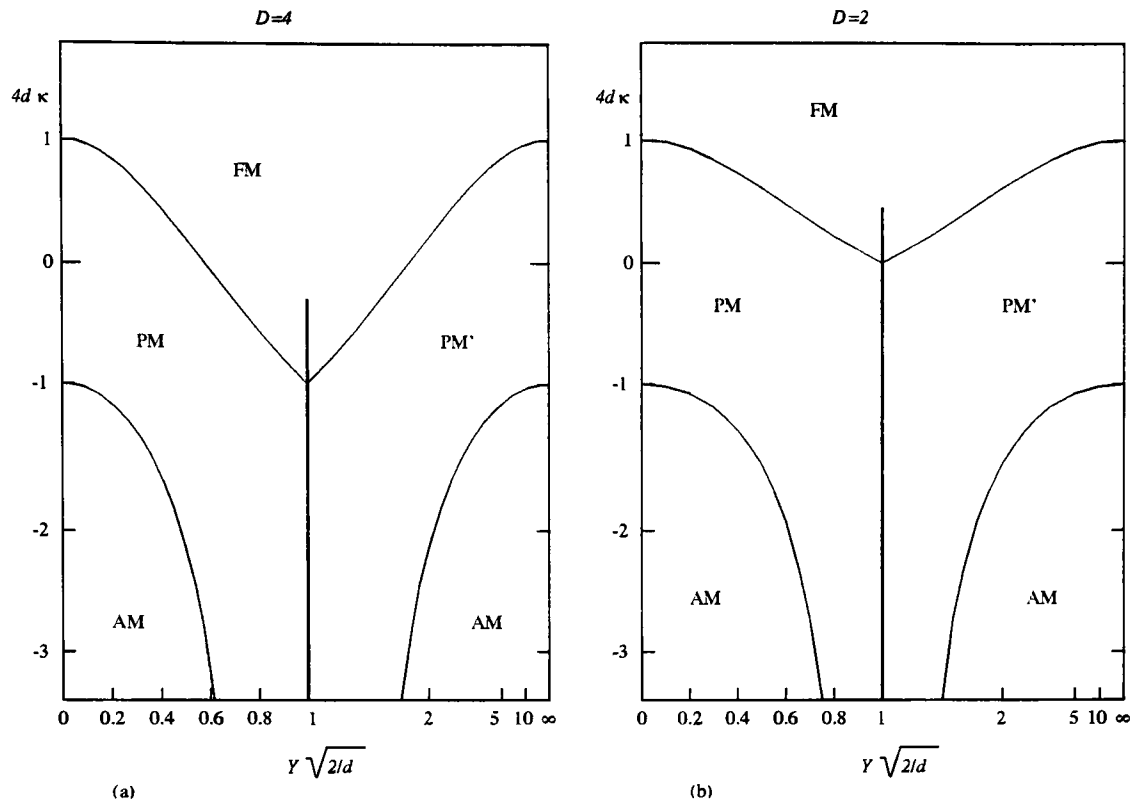

Figure 3.2: The phase diagram of the Z_2 model with 4 (part a) and 2 (part b) staggered fermions. The scale along the horizontal axis is chosen in such a way that the transformation $Y \to d/2Y$ corresponds to simple reflection. The curves are second order phase transition lines: equations (2.42), (2.54), (2.58) and (2.59). The thick vertical line at $Y\sqrt{2/d} = 1$ is the phase transition separating two symmetric phases: with massless fermions and without them. We do not know the position of its end point in the FM phase.

lines can exist on the phase diagram. In the mean field theory this could correspond to additional minima of the mean field free energy $W(H)$ at nonzero H which become deeper than the minimum at $H = 0$.

The diagram fig. 3.2a (or fig. 3.2b) is obtained in the leading order in the $1/d$ expansion. It could be used as a large d approximation to the real phase diagram in $d = 4$. The real phase diagram can have some deviations from the large d one. For example, the lines of the PM–FM and PM'–FM transitions might cross the line of the PM–PM' transition in two different points. It is also possible that the PM-AM and PM'–AM lines do not go to $\kappa = -\infty$, but terminate on the PM–PM' line. Another possibility is that the PM and PM' phases do not touch along a vertical line, but are separated by a region of some other phase.

The precise form of the phase diagram at $d = 4$ is a task for Monte Carlo

simulations. Unfortunately, we are not aware of any Monte Carlo computation of the phase diagram of such a Z_2 model. One technical difficulty is the discrete nature of the scalar variables: $\phi_x = \pm 1$. The algorithm of simulating the action with the contribution of the fermion determinant is based on making small changes of ϕ_x.[3]

The quenched approximation corresponds to neglecting the contribution of the fermion determinant to the action. This simplifies the numerical task considerably. It is much easier to generate the statistical ensemble with the weight $\exp(-S_B)$, because S_B couples only neighbouring sites, than with the weight $\exp(-S_B + \ln\det M)$, where the contribution of the fermion determinant is nonlocal. The Z_2 models were studied in one of the first papers on the scalar–fermion lattice models [34] in the quenched approximation. It was noticed there that fermions behave in a different way at large and small Y. A discontinuous jump of the fermion mass was also observed in the broken phase at $Y \approx 1.4$.

The $U(1)$ and $O(4)$ models were studied extensively by several groups. We shall now describe the phase diagrams in these models in the large d approximation. We shall compare our mean field results with the Monte Carlo data in section 3.3.

3.2.2 The $U(1)$ and $O(4)$ models

The phase diagram of the $U(1)$ model (2.60) is shown in figure 3.3. We chose the smallest number of the staggered fermions: $D = 2$. Similarly to the Z_2 model we rescaled the parameters κ and Y to obtain a universal large d phase diagram. The phase structure is very similar to the phase structure of the Z_2 model. There are four phases: FM, PM, PM' and AM with the same properties as in the Z_2 case.

The situation in the $O(4)$ model is more interesting. Note that the lines of the PM–FM and PM–AM transitions diverge in the Z_2 model as Y increases from zero. These lines in the $U(1)$ model are parallel. In the $O(4)$ models the PM–FM and PM–AM lines converge.

The lines are parallel in the $U(1)$ case because the terms of order Y^4 and higher are absent in the equations for the phase transition lines: see (2.80). Indeed, if there was a Y^4 term in the equation $\kappa = \kappa(Y)$ for the PM–FM line then due to the symmetry $\kappa \to -\kappa$ and $Y^2 \to -Y^2$ between the PM–FM and PM–AM lines this term must be present with the *opposite* sign in the equation for the PM–AM line. Thus the phase transition lines must diverge or converge at small Y depending on the sign of the Y^4 term. In the Z_2 and $O(4)$ models the $O(Y^4)$ term is present: see

[3]The restriction $\phi_x = \pm 1$ results in the limit $\lambda \to \infty$. Some Z_2 models with small scalar self coupling λ have been studied by Monte Carlo [32,39].

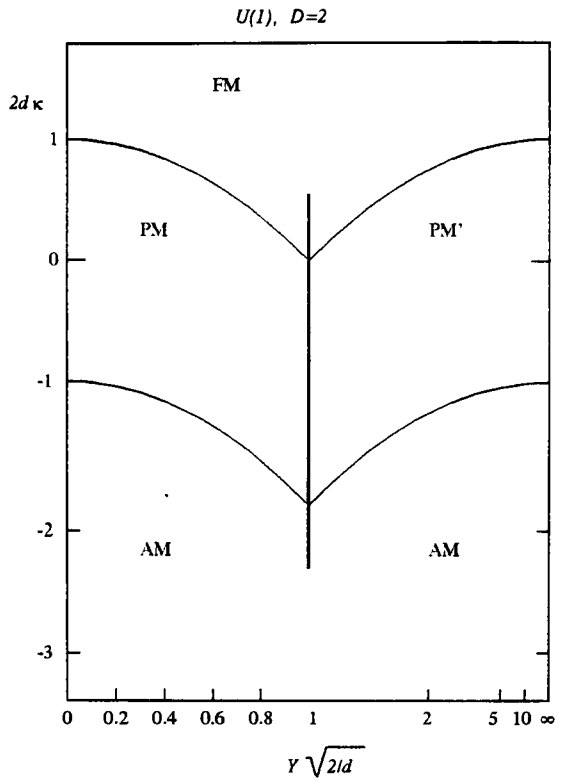

Figure 3.3: The phase diagram of the $U(1)$ model with 2 staggered fermions. See also the caption to fig. 3.2. The second order phase transition lines are given by equations: (2.80), (2.81), (2.83) and (2.84).

eqs. (2.54) and (2.107). It has opposite signs in these two models. The additional minus sign in this term comes from the equation (2.100). The situation with higher order terms is similar.

Now we return to the question of the region of applicability of the equations (2.107), (2.104), (2.108) and (2.109). We can find using the equations (2.107) and (2.108) that the PM–FM and PM–AM phase transition lines intersect at $Y^2 = d/\sqrt{D+1}$. Similarly, at large Y (2.104) and (2.109) give the intersection point: $Y^2 = d\sqrt{D+1}/4$. One can now distinguish two qualitatively different situations depending on the value of D.

If $D = 1, 2, 3$ the PM–FM and PM–AM lines do not intersect before $Y^2 = d/2$ and we can expect that the regions of applicability of (2.107) and (2.104) (and similarly of (2.108) and (2.109)) merge at $Y^2 = d/2$. This situation is the same as in the $Z(2)$ and $U(1)$ models.[4] Then there is a phase transition along the line $Y = \sqrt{d/2}$ separating two distinct symmetric $\langle \sigma \rangle = 0$ phases: PM with usual

[4]As in these models the value $Y = \sqrt{d/2}$ is remarkable because $\det M$ vanishes for some configurations of the field ϕ at $Y^2 = (d/2)(1 + O(1/d))$. See appendix C.

massless fermions and PM' with very heavy fermions. The line of this transition can also continue into FM and AM phases (see fig. 3.4a). The case $D = 3$ is marginal: all four phase transition lines come to the same point: $Y = \sqrt{d/2}$, $\kappa = -2/d$.

Similarly to the $Z(2)$ model the real phase diagram of the $U(1)$ and $O(4)$ models at $d = 4$ can have deviations from our large d diagram, e.g., the PM–FM and PM'–FM lines might not arrive to the same point on the PM–PM' line, there could be an intermediate region between the PM and PM' phases, etc.

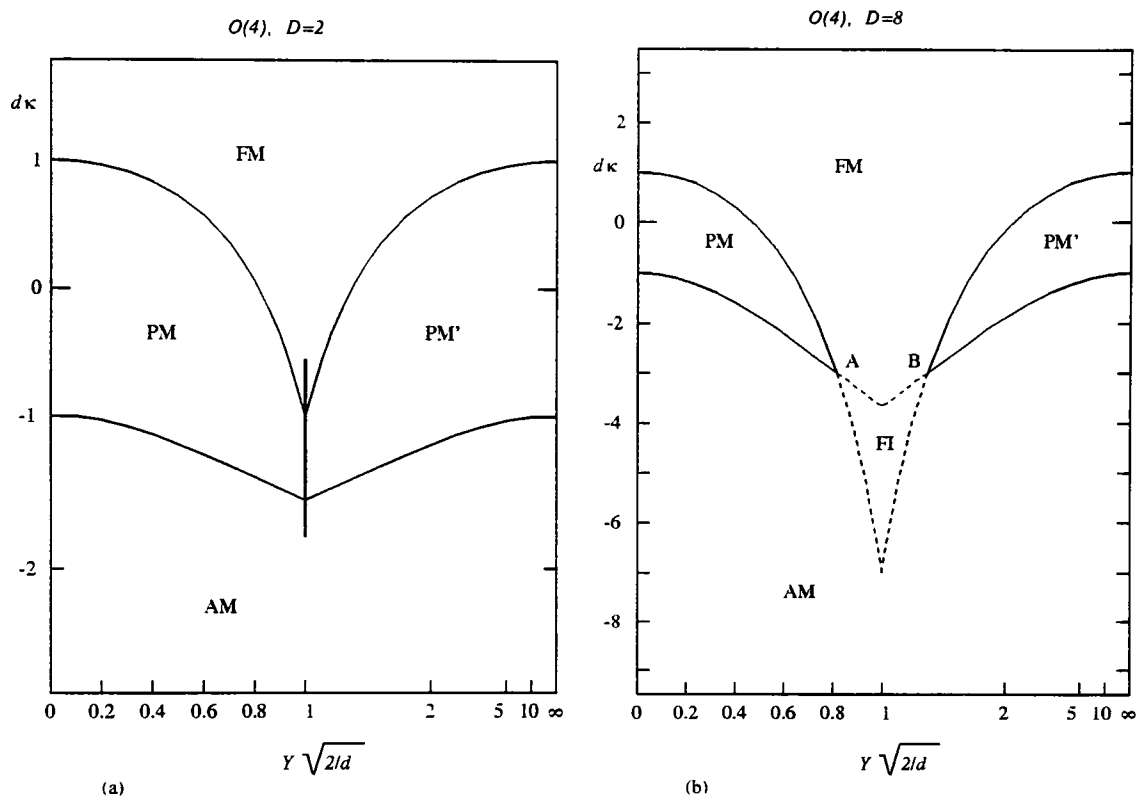

Figure 3.4: The phase diagram of the $O(4)$ model with D doublets of staggered fermions: (a) – with $D = 2$ — the situation is similar to fig. 3.2: and (b) – with $D = 8$. The second order phase transition lines are given by equations: (2.104), (2.107), (2.108) and (2.109). Dashed curves in (b) are only naive continuation of the PM–FM and PM–AM lines into the region between points A and B where these lines lose their meaning and are drawn to indicate very roughly the location of the FI domain.

If $D = 4, 5, \ldots$ then the PM–FM and PM–AM lines intersect *before* $Y^2 = d/2$ at points A and B (see fig. 3.4b). The lines obtained as the lines of the phase transition from PM to FM and AM phases certainly lose their meaning after the intersection in points A and B. Indeed, we could calculate the mean field free energy only for the values of the order parameters $\langle\phi\rangle$ and $\langle\phi_{st}\rangle$ close to zero. However one can expect that these lines describe the situation in the vicinity of the points A and B

where $\langle\phi\rangle$ and $\langle\phi_{\rm st}\rangle$ are still small. This means that we have four different phases meeting in the point A (and similarly for the point B):

PM - where $\langle\phi\rangle = \langle\phi_{\rm st}\rangle = 0$: totally symmetric;

FM - where $\langle\phi\rangle \neq 0$ but $\langle\phi_{\rm st}\rangle = 0$: ferromagnetic order only;

AM - where $\langle\phi_{\rm st}\rangle \neq 0$ but $\langle\phi\rangle = 0$: antiferromagnetic order only;

FI - a *ferrimagnetic* phase, where both order parameters are nonzero: $\langle\phi\rangle \neq 0$ and $\langle\phi_{\rm st}\rangle \neq 0$.

The domain of the FI phase lies somewhere down and to the right from the point A and down and to the left from the point B (see fig.3.4b).

3.2.3 The scalar–fermion models at $\kappa = 0$

In the limit $\kappa = 0$ one can integrate over the scalar variables in the partition function of the scalar–fermion models. Then one obtains a pure fermionic theory with local self interactions. The models with the minimum number of species of staggered fermions: $D = 2$ in the Z_2 and $U(1)$ models and $D = 1$ in the $O(4)$ model, have the simplest interaction: $(\bar\chi\chi)^2$, and can be related to each other. We can then check whether this exact relation is preserved by our approximations. Interestingly, it is.

First, consider the Z_2 model with D staggered fermions. The partition function at $\kappa = 0$ has the form:

$$Z|_{\kappa=0} = \sum_{\{\phi_x=\pm1\}} \int \prod_x d\chi_x\, d\bar\chi_x \, \exp\left\{ -\sum_{\alpha=1}^{D} \sum_{xy} \bar\chi_x^\alpha K_{xy} \chi_y^\alpha - \sum_{\alpha=1}^{D} \sum_x Y \bar\chi_x^\alpha \chi_x^\alpha \phi_x \right\}. \tag{3.25}$$

The sum over the scalar variables factorises:

$$\sum_{\{\phi_x=\pm1\}} \exp\left\{ -\sum_x h_x \phi_x \right\} = \prod_x 2\cosh(h_x). \tag{3.26}$$

Using this equation with $h_x = Y \sum_{\alpha=1}^{D} \bar\chi_x^\alpha \chi_x^\alpha$ we obtain:

$$Z|_{\kappa=0} = \int \prod_x d\chi_x\, d\bar\chi_x \, \exp\left\{ -\sum_{\alpha=1}^{D} \sum_{xy} \bar\chi_x^\alpha K_{xy} \chi_y^\alpha + \sum_x \ln\cosh(h_x) \right\}, \tag{3.27}$$

where we dropped the unimportant constant factor 2^N.

We can expand $\ln\cosh(h_x)$ in powers of h_x. In fact, this expansion contains only a finite number, $D/2$, terms. This is due to the property of the anticommuting variables χ, $\bar\chi$: $\chi\chi = \bar\chi\bar\chi = 0$. The last term (of the order Y^D) contains the product

of all $2D$ fields χ^α, $\bar{\chi}^\alpha$ in one site. Thus the model (3.27) is a pure fermionic theory with polynomial self interactions.

For $D = 2$ — the minimal number of staggered fermions — only the h^2 term survives:

$$\ln\cosh(h) = \frac{h^2}{2} = \frac{Y^2}{2}(\bar{\chi}^1\chi^1 + \bar{\chi}^2\chi^2)^2 = Y^2\bar{\chi}^1\chi^1\bar{\chi}^2\chi^2. \tag{3.28}$$

Thus we obtain a model with local four-fermion interaction between staggered fermion fields χ^1, χ^2 with the action:

$$S = \sum_{\alpha=1,2}\sum_{xy}\bar{\chi}^\alpha_x K_{xy}\chi^\alpha_y - Y^2\sum_x \bar{\chi}^1_x\chi^1_x\bar{\chi}^2_x\chi^2_x. \tag{3.29}$$

The $U(1)$ model has exactly the same kinetic term for the fermion fields as in the Z_2 model. The Yukawa term in the action for the model with $D = 2$ staggered fermions is:

$$Y\sum_x \bar{\chi}^1_x(\phi^0_x + i\zeta_x\phi^1_x)\chi^1_x + Y\sum_x \bar{\chi}^2_x(\phi^0_x - i\zeta_x\phi^1_x)\chi^2_x. \tag{3.30}$$

At $\kappa = 0$ we can integrate over the two component field $\phi^i_x = (\cos\theta_x, \sin\theta_x)$:

$$\int\prod_x d\theta_x \exp\left\{-\sum_x h^i_x\phi^i_x\right\} = \prod_x 2\pi I_0(|h_x|), \tag{3.31}$$

where $|h_x| = \sqrt{(h^0_x)^2 + (h^1_x)^2}$. Using this equation with:

$$h^0_x = Y(\bar{\chi}^1_x\chi^1_x + \bar{\chi}^2_x\chi^2_x);$$
$$h^1_x = i\zeta_x Y(\bar{\chi}^1_x\chi^1_x - \bar{\chi}^2_x\chi^2_x).$$

and expanding the Bessel function: $I_0(x) = 1 + x^2/4 + \ldots$. we obtain the fermion self interaction term in the action:

$$-\sum_x \ln I_0(|h_x|) = -\sum_x \frac{|h_x|^2}{4} = -Y^2\sum_x \bar{\chi}^1_x\chi^1_x\bar{\chi}^2_x\chi^2_x. \tag{3.32}$$

We see that the actions of the $U(1)$ $D = 2$ and the Z_2 $D = 2$ models at $\kappa = 0$ coincide. This means that the phase structure of these models along the line $\kappa = 0$ should be the same. Comparing the phase diagrams on fig. 3.2b and 3.3 we see that this is indeed true in our approximation. It is a rather nontrivial fact. The equation for the phase transition line in the Z_2 model is obtained by summing the expansion in powers of Y (or $1/Y$). The point $Y^2 = d/2$ is the furthest point from the origin of the expansion in the domain of convergence of the series. It is amusing that the phase transition line in the Z_2 model comes at $\kappa = 0$ to the same point, $Y^2 = d/2$, as it does in the $U(1)$ model. The higher order terms in the expansions in Y and $1/Y$ for the phase transition lines in the Z_2 model play an important role: without

them the line would cross the $\kappa = 0$ axis earlier, which would contradict the result in the $U(1)$ model.

Similarly, one can consider the $O(4)$ model with $D = 1$ doublets of staggered fermions. It has the same fermion content as the Z_2 and $U(1)$ models with $D = 2$:

$$\chi = \begin{pmatrix} \chi^1 \\ \chi^2 \end{pmatrix}.$$

The fermion kinetic form has the same form too. The Yukawa term is:

$$Y\bar{\chi}_x(\phi_x^0 + i\zeta_x \boldsymbol{\tau} \cdot \boldsymbol{\phi}_x)\chi_x.$$

We can integrate over the 4 component scalar field ϕ_x^k at $\kappa = 0$:

$$\int \prod_x d\mu_x \exp\left\{-\sum_x h_x^k \phi_x^k\right\} = \prod_x 2\pi^2 \{I_0(|h_x|) - I_2(|h_x|)\}, \tag{3.33}$$

where $|h_x| = \sqrt{h_x^k h_x^k}$. The components h_x^k are:

$$\begin{aligned} &h_x^0 = Y\bar{\chi}_x\chi_x = Y(\bar{\chi}_x^1\chi_x^1 + \bar{\chi}_x^2\chi_x^2); \\ &h_x^i = i\zeta_x Y\bar{\chi}_x\tau^i\chi_x; \\ &\text{e.g.,} \quad h_x^1 = i\zeta_x Y(\bar{\chi}_x^1\chi_x^2 + \bar{\chi}_x^2\chi_x^1). \end{aligned} \tag{3.34}$$

Only the term $|h^2|$ survives in the expansion of $\ln\{I_0(|h|) - I_2(|h|)\}$. Using (3.34) and anticommuting properties of χ's we find for each component of h^i:

$$\begin{aligned} &(h_x^0)^2 = Y^2(\bar{\chi}_x^1\chi_x^1 + \bar{\chi}_x^2\chi_x^2)^2 = 2Y^2\bar{\chi}_x^1\chi_x^1\bar{\chi}_x^2\chi_x^2; \\ &(h_x^1)^2 = Y^2(\bar{\chi}_x^1\chi_x^2 + \bar{\chi}_x^2\chi_x^1)^2 = 2Y^2\bar{\chi}_x^1\chi_x^1\bar{\chi}_x^2\chi_x^2; \\ &\text{etc.} \end{aligned} \tag{3.35}$$

Finally, we obtain for the fermion self interaction term in the action:

$$-\sum_x \ln\{I_0(|h_x|) - I_2(|h_x|)\} = -\sum_x \frac{|h_x|^2}{8} = -Y^2 \sum_x \bar{\chi}_x^1\chi_x^1\bar{\chi}_x^2\chi_x^2, \tag{3.36}$$

which is the same as in (3.32) and (3.29).

Thus the $O(4)$ model with $D = 1$ doublets of staggered fermions at $\kappa = 0$ is also equivalent to the Z_2 or $U(1)$ model with $D = 2$ at $\kappa = 0$. Comparing (2.107), (2.80) and (2.54) we see that the PM–FM phase transition line (similarly, PM'–FM) in all three models comes to the same point on the line $\kappa = 0$: $Y = \sqrt{d/2}$. We take this agreement as an additional argument for the consistency of our approximations.

3.3 Mean field vs Monte Carlo

In this section we compare the phase diagrams we obtained in the mean field (and large d) approximation with available Monte Carlo results.

3.3.1 The $U(1)$ model

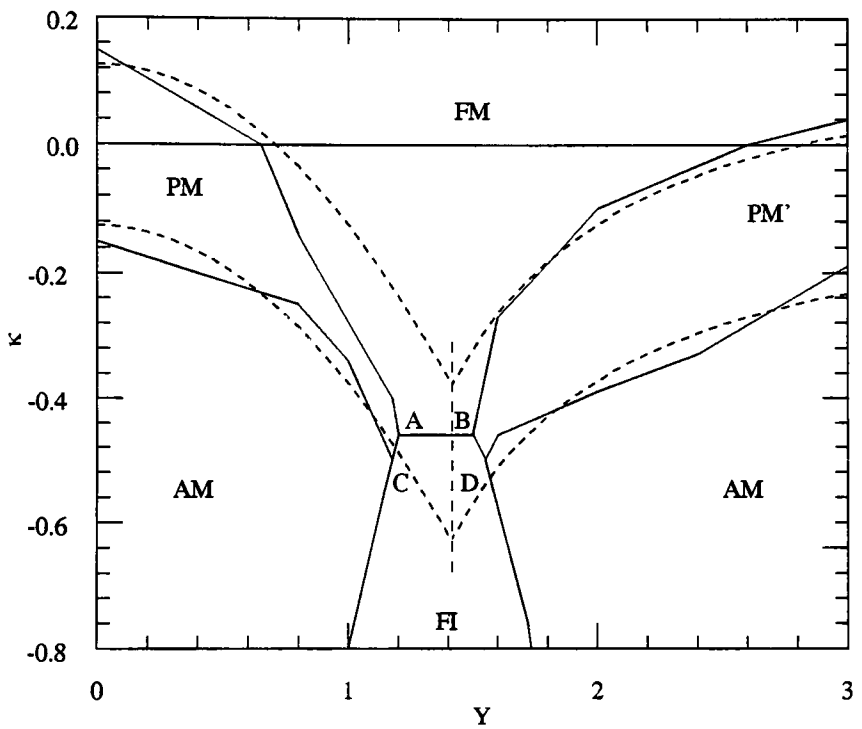

Figure 3.5: The phase diagram of the $U(1)$ model with 8 staggered fermions. The solid lines: Monte Carlo [41]; the dashed lines: the mean field approximation.

The phase diagram of the $U(1)$ model with 2 species of Dirac lattice fermions was computed numerically in [41]. This model is equivalent to our model (2.60) with $D = 8$ staggered fermions. The naive continuum limit of such a theory (see section 1.3.4) contains 32 continuum Dirac fields. The computation was done on a 6^4 lattice. In figure 3.5 we plotted the phase transition lines obtained in the mean field approximation: (2.80), (2.81), (2.83), (2.84), together with the phase diagram computed in [41] numerically.

First of all, we see a good agreement for the PM–AM, PM'–FM and PM'–AM lines. The agreement for the PM–FM line is worse. This can be explained by the crudeness of our approximations or by finite size or some other effects in the Monte Carlo simulation. Note that the PM–AM and PM–FM lines are *exactly* related by the transformation: $\kappa \to -\kappa$ and $Y^2 \to -Y^2$ (see section 2.5.2). As our approximate

PM–FM and PM–AM lines are related by this transformation it seems strange that one line agrees with the numerical result and another does not.

We do not find the FI phase in our approximation in this model. The FI phase found numerically in [41] occupies the region around $Y \approx 1.4$. This is the region where we assumed the domains of applicability of large and small Y expansions to merge. It is possible that this assumption is valid only in the large d limit and at finite d the PM and PM' phases are separated by a region of another, FI, phase. However, it is also possible that the FI phase found in [41] is a numerical artifact. The computation in the region of intermediate Y close to 1.4 is very difficult: the algorithm for the inversion of the fermion matrix involved in the procedure slows down considerably (see appendix C).

3.3.2 The $O(4)$ model

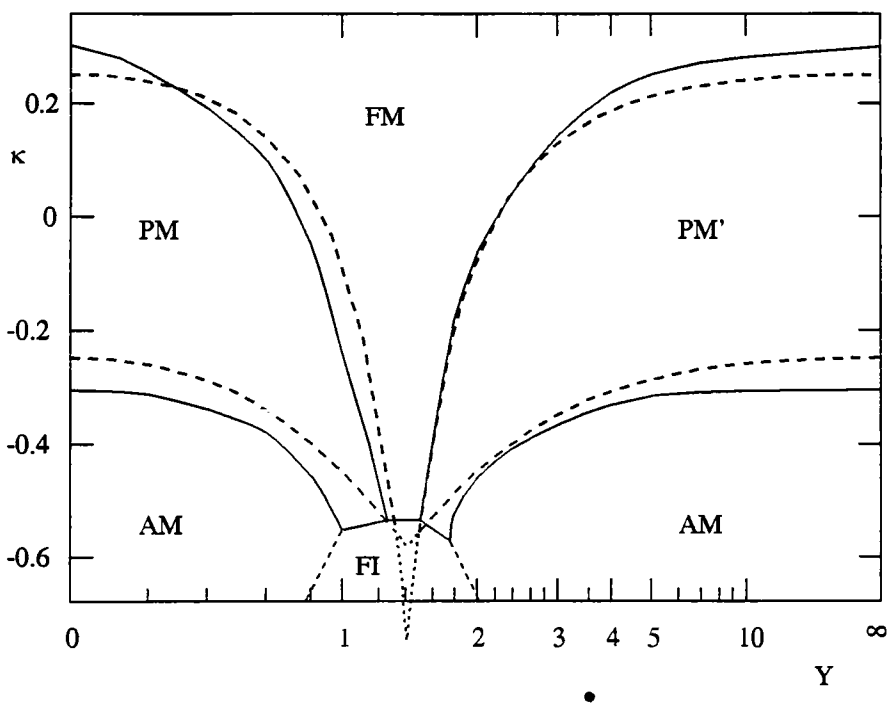

Figure 3.6: The phase diagram of the $O(4)$ model with 4 staggered fermions. The solid lines: Monte Carlo [50]; the dashed lines: the mean field approximation.

The phase diagram of the $SU(2) \otimes SU(2)$, or $O(4)$, theory with 4 staggered fermions was studied numerically in [50]. A $4^3 \times 8$ lattice was used. This phase diagram is compared in fig. 3.6 to our mean field results for the phase transition lines: (2.104), (2.107), (2.108), (2.109).

We see a reasonably good agreement. Similarly to fig. 3.5 the agreement is better for the PM'– lines than for the PM– lines. The FI phase is predicted by the

mean field method and its position agrees with the numerical result. Monte Carlo computations in this region are difficult (see appendix C) and the boundary of the FI phase is not determined very well.

The most accurate determination of the phase diagram of the $O(4)$ model was done in a series of papers by the Jülich group [51–53]. The theory with 2 lattice Dirac fermions was studied. This corresponds to the theory (2.85) with $D = 8$ staggered fermions. The lattices of the size 6^4 and 8^4 were used. In fig. 3.7 we compare the resulting phase diagram to our mean field predictions: (2.104), (2.107), (2.108), (2.109).

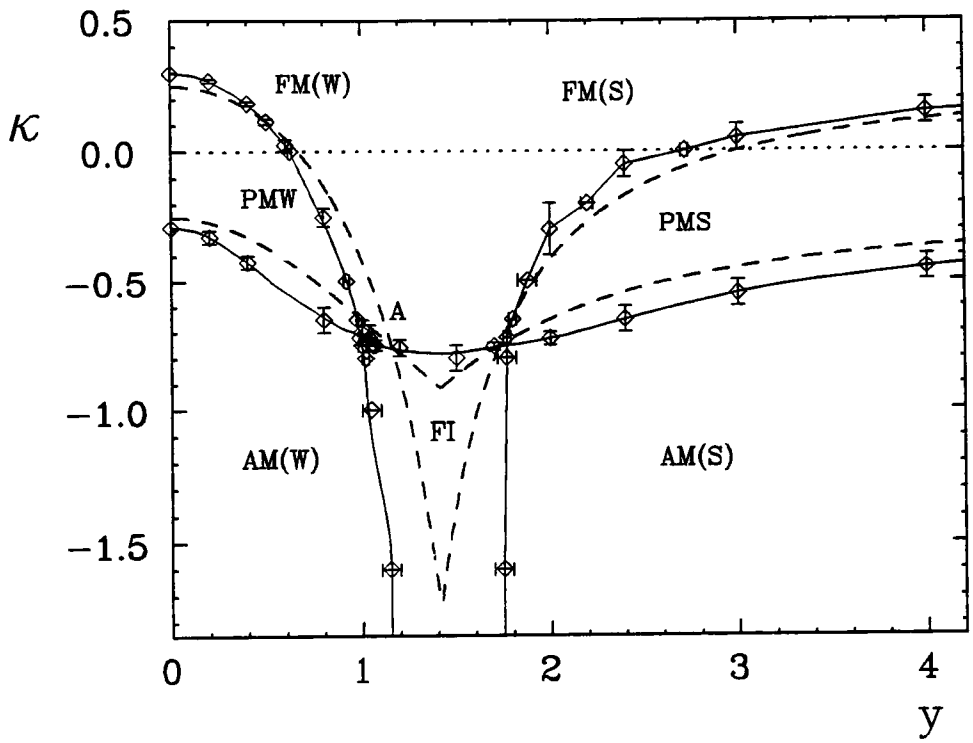

Figure 3.7: The phase diagram of the $O(4)$ model with 8 staggered fermions. Letters "W" and "S" stand for weak and strong Yukawa coupling regions: PMW=PM and PMS=PM'. The solid lines: Monte Carlo [52]; the dashed lines: the mean field approximation. The plot was presented to the author by C. Frick.

The agreement is as good as for figs. 3.5 and 3.6. For additional comparison we list in table 3.1 the coordinates of the point A where the PM–FM line meets the PM–AM line and the point B where the PM'–FM line meets the PM'–AM line (see also fig. 3.4b). The mean field predictions for the coordinates of these points are

given by the formulae (see section 3.2.2):

$$Y_A = \left(\frac{d}{\sqrt{D+1}}\right)^{1/2}; \qquad Y_B = \left(\frac{d\sqrt{D+1}}{4}\right)^{1/2};$$
$$\kappa_A = \kappa_B = -\frac{\sqrt{D+1}}{d}; \tag{3.37}$$

with $d = 4$ and $D = 8$. The Monte Carlo coordinates are from [52]. We find very good agreement for the point B and worse for the point A.

Table 3.1: The coordinates of the points A and B.

	A		B	
	Y	κ	Y	κ
Mean field: eq. (3.37)	1.115	−0.75	1.732	−0.75
Monte Carlo: [52]	1.000(5)	−0.78(5)	1.770(10)	−0.75(1)

One can see that the situation in fig. 3.7 is similar to figs. 3.5 and 3.6: the disagreement for the lines at small Y is larger than at large Y and has the same sign in all three models too (except for the PM–AM line in fig. 3.5). The most obvious reason for the deviations is the $1/d$ corrections. We conclude that these corrections are larger at small Y. The finite size effects in numerical simulations could be also enhanced in this region as compared to the large Y region due to the presence of light fermions.

3.4 Continuum limits

The mean field method is not suitable to discuss the critical behaviour of a system in detail. Indeed, at the critical point the correlations in the system grow large and the mean field approximation which neglects these correlations is not good. However, one can find the approximate *position* of the point of the phase transition using the mean field method up to corrections of order $1/d$ for large d. Also. the analysis of the spin systems (e.g., the Ising model, the XY model, etc.) shows that the mean field method predicts the critical exponents correctly for d greater than some d_c — the upper critical dimension (see, e.g., [23]). For the spin systems $d_c = 4$. The critical exponents control the behaviour of the order parameter, correlation length, susceptibility to the external field, etc. near the critical point. For example, the critical exponent β in the Ising model is defined as:

$$\sigma \equiv \langle \phi \rangle \sim (\kappa - \kappa_c)^{\beta}, \tag{3.38}$$

as $\kappa \to \kappa_c$. The mean field approximation gives $\beta = 1/2$ as is obvious from (2.6). In $d = 4$ mean field critical behaviour like (3.38) is modified by factors of $\ln(\kappa - \kappa_c)$ to some power. These logarithmic corrections are beyond the scope of the mean field approximation.

In this work we do not attempt to study continuum limits of the scalar–fermion theories in detail. What we can do, however, is to point out were on the phase diagram possible continuum limits can be defined and what the spectrum of the theory is. To study the continuum limit in greater detail, e.g., to address the questions of triviality, upper bounds on the masses, etc. one has to use more complicated methods such as, for example, lattice renormalisation group or numerical simulations by Monte Carlo.

The most obvious candidates for the points where a continuum limit can be taken lie on the PM–FM phase transition line. Indeed, there the mass of the scalar particle in lattice units goes to zero. This mass is proportional to the second derivative of the mean field free energy with respect to H in our approximation. The mass of the fermion: $m_F \approx Y\sigma$, also vanishes as $\sigma \to 0$.

The spectrum of the continuum theory, or the low energy degrees of freedom, if we take the limit from the FM phase consists of a massive scalar particle σ (the Higgs boson), $n - 1$ massless Goldstone particles π (where n is the number of the components of the scalar field) and 4D massive fermions (doublets in the $O(4)$ case). This theory is the most obvious candidate to describe the Higgs sector of the electroweak model.

This continuum limit taken form the FM side on the PM–FM line was studied

extensively by Monte Carlo [52,53]. It was found that all the points along this line belong to the same universality class: the universality class of the perturbative scalar–fermion theory with Yukawa interaction. One can show that in perturbation theory the continuum limit of the Yukawa model is a free (noninteracting) theory of scalars and fermions. Similarly to the pure scalar case one can derive perturbative triviality upper bounds on the scalar and fermion masses [22].

Note that the PM–FM line continues below the $\kappa = 0$ line in the models with large enough D. One can observe that at negative κ the relation between the continuum action and the lattice action breaks down. In other words, the lattice action in the limit $a \to 0$ does not correspond to any continuum classical action like (1.13). Indeed, to obtain the continuum action one needs to rescale the lattice field ϕ_x, which is real, by a factor $\sqrt{2\kappa}$, which becomes imaginary. If we rescale by $\sqrt{2|\kappa|}$ we obtain at negative κ the continuum limit *classical* action with *negative* sign in front of the gradient (kinetic) term. However, the continuum *quantum* theory is the same everywhere along the PM–FM line. There is nothing special in the critical behaviour near the point $\kappa = 0$ or at negative κ [53]. What happens is that quantum corrections to the kinetic term of the scalar field from virtual fermion loops make the kinetic term in the *effective* action (at long distance scales) positive everywhere along the PM–FM line (see also sect. 3.6).

The continuum limit taken from the PM side of the PM–FM line is a Yukawa theory in the symmetric phase. The spectrum consists of an n-plet of scalar particles and $4D$ massless fermions.

Another candidate for a continuum limit is the PM'–FM line. Here again the mass of the scalar particle in lattice units vanishes similar to the PM–FM line. The mass of the fermion does not vanish near the PM'–FM line. As we saw in section 3.1.2 the mass of the fermions is very large in lattice units in the symmetric phase PM'.

One can also estimate the behaviour of the fermion mass in the FM phase at large Y in the following way. Consider the fermion propagator $\langle (M^{-1})_{xy} \rangle$ (see section 3.1.2). To calculate it for large Y we expand it in powers of $1/Y$ as in (3.23). The problem with computing the average of each term in this expansion is the correlations between φ_x in different sites. We neglect these correlations in the mean field approximation. However, in the FM phase another problem is that $\langle \phi_x^2 \rangle \neq \langle \phi_x \rangle^2$ Such contributions appear if the chain of sites, connecting points x and y, i.e., $z_1, \ldots, z_n$ in (3.23), has self crossings. If we neglect such contributions we can calculate the fermion propagator. It seems plausible that the contribution of self crossings of the chain becomes relatively small in the large d limit. With this assumption we can compute each term in the expansion (3.23): we need simply to

substitute σ instead of all ϕ_x^*. Then summing the series we obtain:

$$\langle (M^{-1})_{xy} \rangle_H = \left(K + \frac{Y}{\sigma} \right)^{-1}_{xy}, \tag{3.39}$$

i.e. the mass of the fermions: $m_F \approx Y/\sigma$.

We can see that the mass of the fermions *grows* as we approach the PM'–FM phase transition line from the FM phase. Thus in the continuum limit taken near this line the fermions can not appear as low energy degrees of freedom. In other words, the spectrum of the continuum theory at the PM'–FM line consists of scalars only. All continuum theories along this line are in the same universality class: the universality class of the n component spin model.

In the next two sections we discuss the properties of the scalar–fermion theories near the PM–PM' line and near the PM–AM line.

3.5 Bound states in the scalar–fermion theories

One can expect that at some large Yukawa coupling the interaction between the fermions mediated by the scalar particles can become strong enough to produce bound states of these fermions.

In this section we study the lattice scalar–fermion models at large values of Y. A straightforward way to study bound states is to look at the poles in the scattering amplitudes. We calculate four–fermion amplitudes in the strong coupling symmetric phase PM' using the mean field approximation (i.e., neglecting correlations of the scalar field). We find that there are poles in these amplitudes which can be interpreted as bound states of the fermion–fermion or fermion–(anti)fermion pair [57].

3.5.1 The model

We demonstrate the calculation on a simple model. Consider the $U(1)$ model (2.60) with $D = 2$ staggered fermions. We write its action in the form:

$$\begin{aligned} S &= S_B + S_F; \\ S_B &= -2\kappa \sum_{x,\mu} \phi^k_x \phi^k_{x+\hat{\mu}}, \qquad \phi^k_x \phi^k_x = 1; \\ S_F &= \sum_{xy} \left\{ \bar{\chi}^1_x (K_{xy} + Y\phi_x \delta_{xy}) \chi^1_y + \bar{\chi}^2_x (K_{xy} - Y\phi^*_x \delta_{xy}) \chi^2_y \right\}, \end{aligned} \tag{3.40}$$

where

$$K_{xy} = \frac{1}{2} \sum_{\mu} \eta_{x,\mu} (\delta_{y,x+\hat{\mu}} - \delta_{y,x-\hat{\mu}})$$

is the matrix of the kinetic term for the staggered fermions. We use a new notation for the scalar field in the Yukawa term: $\phi_x = \phi^0_x + i\zeta_x \phi^1_x$. We changed the fields in the action (2.60):

$$\chi^2_x \to \zeta_x \chi^2_x \qquad \text{and} \qquad \bar{\chi}^2_x \to -\zeta_x \bar{\chi}^2_x,$$

to make our calculations more convenient. This resulted in the minus sign in front of the Yukawa term for χ^2 in (3.40) (see also footnote 1 on page 31).

Let us now consider the following four–fermion correlator in our lattice theory:

$$C_{xy} = \langle\, \chi^1_x \bar{\chi}^2_x \; \chi^2_y \bar{\chi}^1_y \,\rangle. \tag{3.41}$$

This correlator can be viewed as the propagator of the local composite field $\chi^1_x \bar{\chi}^2_x$ or, alternatively, as the amplitude of fermion–antifermion scattering. For example, the tree level contribution to such an amplitude comes from the diagram with ϕ

field exchange (see fig. 3.8). A bound state of $\chi^1\bar{\chi}^2$ could appear if the Yukawa interaction is sufficiently strong and the contributions with multiple ϕ exchanges in the t-channel become important. This bound state would then show up as a pole in the s-channel of the process in fig. 3.8 and in the correlator C_{xy}.

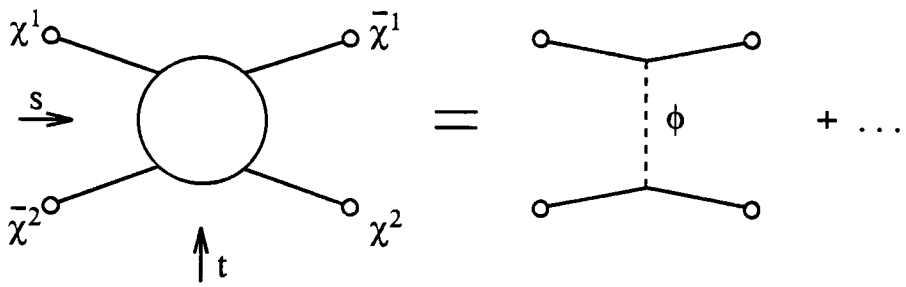

Figure 3.8: The amplitude of fermion-antifermion scattering and a tree level contribution to it.

3.5.2 Computing the four-fermion correlator

To study the correlator C_{xy} we integrate over the fermionic variables in (3.41). First, we introduce fermion sources: η^α, $\bar{\eta}^\alpha$. The partition function of the model is then:

$$Z[\eta,\bar{\eta}] = \int \prod_x d\theta_x \int \prod_{y,\alpha} d\chi_y^\alpha \, d\bar{\chi}_y^\alpha \, \exp\{-S + \textstyle\sum_{x,\alpha}(\bar{\eta}_x^\alpha \chi_x^\alpha + \bar{\chi}_x^\alpha \eta_x^\alpha)\} =$$
$$= \int \prod_x d\theta_x \, \exp\{-S_{\rm eff} + \bar{\eta}^1 (K + Y\phi)^{-1}\eta^1 + \bar{\eta}^2 (K - Y\phi^*)^{-1}\eta^2\}, \quad (3.42)$$

where

$$S_{\rm eff} = S_B - \ln\det(K + Y\phi)(K - Y\phi^*) = S_B - 2\,{\rm Re}\,\ln\det(K + Y\phi),$$

and $Y\phi$ denotes the diagonal matrix $Y\phi_x\delta_{xy}$.

Now we can write for the correlator C_{xy}:

$$C_{xy} = \langle\, \chi_x^1 \bar{\chi}_x^2 \; \chi_y^2 \bar{\chi}_y^1 \,\rangle = -\langle\, \chi_x^1 \bar{\chi}_y^1 \; \chi_y^2 \bar{\chi}_x^2 \,\rangle = -\frac{\delta}{\delta\bar{\eta}_x^1}\frac{\delta}{\delta\eta_y^1}\frac{\delta}{\delta\bar{\eta}_y^2}\frac{\delta}{\delta\eta_x^2} Z[\eta,\bar{\eta}]\Big|_{\eta=\bar{\eta}=0}. \quad (3.43)$$

Taking the derivatives of (3.42) we find:

$$C_{xy} = -\left\langle (K + Y\phi)^{-1}_{xy} \, (K - Y\phi^*)^{-1}_{yx} \right\rangle_{S_{\rm eff}}. \quad (3.44)$$

where the average on the right hand side is taken with respect to the pure bosonic weight $\exp(-S_{\rm eff})$.

In principle, the correlator (3.44) can be evaluated numerically by Monte Carlo very much like the fermion propagator $\langle (M^{-1})_{xy} \rangle$. The quenched approximation

could also give a good estimate. The contribution of the fermion determinant in S_{eff} is neglected in this approximation, which simplifies the numerical task. The main contribution to the expected pole comes from the diagrams with multiple scalar exchanges and the contribution of the fermion loops is, probably, not significant.

In our analytical study we use the mean field (and large d) approximation to estimate the correlator C_{xy}. This means that we neglect the correlations of the field σ_x when computing the average in (3.44). The correlator is then given by:

$$C_{xy} = -\left\langle\, (K + Y\phi)^{-1}_{xy}\, (K - Y\sigma^*)^{-1}_{yx} \,\right\rangle_H , \tag{3.45}$$

where the average is over the uncorrelated random field σ_x with the probability distribution $\exp(\sum_x H^i \phi^i_x)$ and H^i is the two component mean field (see (2.66)).

We shall consider the correlator C_{xy} in the symmetric phase of our model, i.e., when $\langle\phi\rangle = H = 0$. As we discussed in the sections 3.1.2 and 3.2 this phase consists of two distinct regions (phases): PM at small Y with massless fermions, and PM' at large Y with very heavy fermions. The two phases are separated by a phase transition along the line $Y^2 = d/2$. We shall be mainly interested in the phase at large Y: the PM' phase.

The mean field approximation works well if we are not very close to the critical points where the correlation length of the field σ_x becomes large. This means we can apply the mean field approximation inside the PM' phase not very close to the PM'–FM, PM'–AM lines.

We expand in powers of $1/Y$ in (3.45) to compute the correlator in the region $Y^2 > d/2$:

$$\begin{aligned} C_{xy} = \Bigg\langle \left(\frac{\phi^*}{Y} - \frac{\phi^*}{Y} K \frac{\phi^*}{Y} + \frac{\phi^*}{Y} K \frac{\phi^*}{Y} K \frac{\phi^*}{Y} - \dots \right)_{xy} \\ \left(\frac{\phi}{Y} + \frac{\sigma}{Y} K \frac{\phi}{Y} + \frac{\sigma}{Y} K \frac{\phi}{Y} K \frac{\sigma}{Y} + + \dots \right)_{yx} \Bigg\rangle_{H=0} , \end{aligned} \tag{3.46}$$

where we used the fact that $1/\phi = \phi^*$. Multiplying term by term the two series in parentheses we obtain the expansion for C_{xy}. One can represent each term in this expansion by a diagram. Each term is a product of two terms: one from each of the parentheses in (3.46). For example, the term of order $1/Y^{n+2}$ $(n > 1)$ in the last parenthesis is:

$$\left(\frac{\phi}{Y} K \frac{\sigma}{Y} \cdots K \frac{\phi}{Y} \right)_{yx} = \frac{1}{Y^{n+2}} \sum_{z_1 \dots z_n} \phi_y K_{yz_1} \sigma_{z_1} K_{z_1 z_2} \cdots K_{z_n x} \varphi_x . \tag{3.47}$$

It can be depicted as a chain of the lattice sites: $x, z_1, \dots, z_n, y$. The links of the chain connect neighbouring sites because matrix elements of K are nonzero only

then. Each term in the first parenthesis is depicted by a similar diagram. Each term in the expansion for C_{xy} is then a product of two chains. Using the property of the average (see (2.75)):

$$\langle(\phi_x)^k\rangle_{H=0} = 0 \qquad \text{for } k = 1.2.3\ldots, \tag{3.48}$$

we conclude that only the diagrams with all sites passed equal number of times by the two chains (so that each ϕ_x is paired with ϕ_x^*) contribute to C_{xy}. It is sensible to expect that of these diagrams the *double chains* (i.e., when the two chains coincide) give the leading contribution in the large d limit (see fig.3.9). Other types of diagrams contain self crossings and their contribution is small at large d.

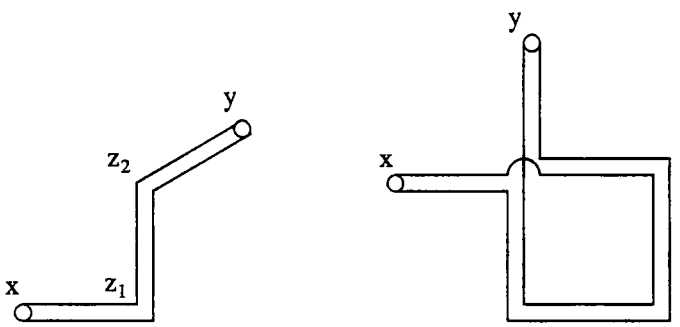

Figure 3.9: Typical diagrams representing the terms in the $1/Y$ expansion of the correlator C_{xy}. Links of the chains connect neighbouring sites. Diagram (a) – a typical double chain diagram in the order $1/Y^8$ ($n = 2$ term in (3.49)); (b) – an example of a diagram which we neglect in the large d limit.

In this approximation we can sum up the expansion for the C_{xy}:

$$C_{xy} = \frac{1}{Y^2} + \frac{1}{Y^4}(K_{xy})^2 + \ldots + \frac{1}{Y^{2n+4}} \sum_{z_1\ldots z_n} (K_{xz_1})^2 (K_{z_1z_2})^2 \ldots (K_{z_ny})^2 = \\ = \frac{1}{Y^2}\left(1 - \frac{1}{Y^2}A\right)^{-1}_{xy}. \tag{3.49}$$

where the matrix elements of A are:

$$A_{xy} = (K_{xy})^2 = \frac{1}{4}\sum_{\mu}(\delta_{y,x+\hat{\mu}} + \delta_{y,x-\hat{\mu}}). \tag{3.50}$$

If we denote the lattice Laplacian by Δ, then we can write:

$$4A_{xy} = \Delta_{xy} + 2d\delta_{xy}.$$

Substituting this into (3.49) we find for the correlator in our approximation:

$$C_{xy} = 4\left(4Y^2 - 2d - \Delta\right)^{-1}_{xy}. \tag{3.51}$$

We see that C_{xy} is proportional to the (Euclidean) lattice propagator of a free massive boson with the mass μ: $\mu^2 = 4Y^2 - 2d$. The residue, 4, in the corresponding pole in C_{xy} is the square of the coupling of this composite boson to the fermions.

The mass μ (in lattice units) of the bound state vanishes as we approach the line $Y^2 = d/2$, which coincides with the boundary of the PM' phase in our approximation. This means that the correlation length of the composite field $\chi^1_x \bar{\chi}^2_x$ becomes large and one can define a continuum theory with physical composite particle in the spectrum at this boundary.

The result (3.51) for the four-fermion correlator is obtained in the large d limit. We do not know the behaviour of this correlator at finite $d = 4$. It is possible that the mass of the bound state remains finite in the PM' phase and on its boundary. However, one can expect that this mass becomes small in lattice units near $Y^2 \approx d/2$, so that one can define *effective* continuum theory with composite bosonic particle in the low energy spectrum. An interesting possibility is that the mass of the bound state in lattice units vanishes near $Y^2 \approx d/2$ (e.g., on the boundary of the PM' phase) also in the real case $d = 4$. It would be very interesting to do a numerical Monte Carlo computation in that region which could clarify this question.

Note also that the composite particle is stable as it can not decay into fermion–antifermion pair due to large mass of the fermions. The decay into ϕ particles is forbidden by the simple symmetries of (3.40) which correspond to the separate conservation of the fermion number of each of the fermion species. Such a particle cannot be stable in the PM phase: it can always decay into massless fermion and antifermion.

Let us consider other channels in our four-fermion amplitude. Looking for possible bound states in the t-channel on fig. 3.8 we calculate the following correlator:

$$\langle \chi^1_x \bar{\chi}^1_x \chi^2_y \bar{\chi}^2_y \rangle = \left\langle (K + Y\phi)^{-1}_{xx} (K - Y\phi^*)^{-1}_{yy} \right\rangle_{S_{\text{eff}}} . \tag{3.52}$$

If we neglect correlations of the field ϕ_x we can calculate this correlator in the large d limit. Similarly to (3.46) we expand in powers of $1/Y$ in (3.52). Each term in the expansion is a product of two chains. Now, however, both chains are closed: one chain begins and ends in the site x, another in the site y. Using (3.48) we conclude that the two chains should pass each site equal number of times. If we neglect self crossings, which is sensible in the large d limit, then the contribution of the diagrams is nonzero only when x and y coincide: both chains visit this point twice. Thus the correlator $\langle (K + Y\phi)^{-1}_{xx} (K - Y\phi^*)^{-1}_{yy} \rangle_{H=0}$ is proportional to δ_{xy} in the large d limit. We see that there are no poles in this correlator.

Where is the σ particle itself then? The answer is that the correlator $\langle (K + Y\phi)^{-1}_{xx} (K - Y\phi^*)^{-1}_{yy} \rangle_H$ is the mean field estimate for the one particle irreducible

part of the correlator (3.52). The situation is similar to the one already discussed in the footnote 1 on page 56. We conclude that the only pole in the t-channel of the amplitude in fig. 3.8 corresponds to the ϕ particle.

We can assign fermion number $+1$ to the fields χ^1 and χ^2 and -1 to the fields $\bar{\chi}^1$ and $\bar{\chi}^2$. Then the s and t channels of our amplitude (fig. 3.8) have fermion number 0. There is also a channel with fermion number 2: the u-channel on the fig. 3.8. There is a pole in this channel too. Indeed:

$$\begin{aligned}
&\langle\ \chi^1_x \zeta_x \chi^2_x\ \bar{\chi}^2_y \zeta_y \bar{\chi}^1_y\ \rangle = \\
&\quad = -\Big\langle\ (K + Y\phi)^{-1}_{xy}\ \zeta_x\ (K - Y\phi^*)^{-1}_{xy}\ \zeta_y\ \Big\rangle_{S_{\rm eff}} = \\
&\quad = -\Big\langle\ (K + Y\phi)^{-1}_{xy}\ (K - Y\phi^*)^{-1}_{yx}\ \Big\rangle_{S_{\rm eff}} = C_{xy},
\end{aligned} \tag{3.53}$$

where we used the fact that $\zeta_x K_{xy} \zeta_y = K_{yx}$. The correlator of the composite field $\chi^1_x \zeta_x \chi^2_x$ is the same as the correlator of the field $\chi^1_x \bar{\chi}^2_x$, i.e., it has a pole.

3.5.3 Discussion

We studied four–fermion correlators in the $U(1)$ scalar-fermion theory in the mean field (and large d) approximation. We found that in the symmetric phase PM' at $Y^2 > d/2$, where the fermions are very massive, there are poles in certain channels of the four–fermion amplitude which do not correspond to fundamental particles of the theory. Here we make some comments about the properties of the corresponding composite particles.

(i) Note that the bound states created by the operators $\chi^1_x \bar{\chi}^2_x$ and $\chi^1_x \zeta_x \chi^2_x$ are neutral with respect to the $U(1)$ charge which is carried by the field ϕ and the fermion fields. This charge corresponds to the $U(1)$ symmetry transformation of the model:

$$\begin{aligned}
&O_x \to e^{i2\theta\zeta_x} O_x, \quad \chi^1_x \to e^{-i\theta\zeta_x} \chi^1_x, \quad \chi^2_x \to e^{+i\theta\zeta_x} \chi^2_x, \\
&\qquad\qquad \bar{\chi}^1_x \to e^{-i\theta\zeta_x} \bar{\chi}^1_x, \quad \bar{\chi}^2_x \to e^{+i\theta\zeta_x} \bar{\chi}^2_x.
\end{aligned} \tag{3.54}$$

The fields $\chi^1_x \bar{\chi}^2_x$ and $\chi^1_x \zeta_x \chi^2_x$ are invariant under this transformation.

(ii) The composite operators $\chi^1_x \bar{\chi}^2_x$ and $\chi^1_x \zeta_x \chi^2_x$ do not necessarily create scalars in the continuum limit. Indeed, our two staggered fermions give $2 \cdot 2^{d/2}$ Dirac fermions in the naive continuum limit due to the fermion doubling. The components of the continuum Dirac $2^{d/2}$–spinors are given by linear combinations of the χ fields living in 2^d corners of the unit lattice hypercube (see section 1.3.4). Thus the composite operators are products of spinor components and can also create components of (pseudo)vector or tensor.

(iii) It is easy to see that these results would be the same in the theory (2.60) with any number D of staggered fermions. The method and the results obtained in this paper can be easily generalised to the $Z(2)$ and the $O(4)$ theories. Similarly to the $U(1)$ case one finds $Z(2)$ or $O(4)$ "neutral" bound states.[5]

(iv) In the phase FM with broken symmetry: $H \neq 0$, and the computation of the correlator (3.45) is complicated. However, due to the continuity of the transition from the symmetric to the broken phase one can expect that there are still corresponding poles in the correlator C_{xy} at least in some vicinity of the phase transition line in the FM phase.

(v) Note that the bosonic particle content in the FM phase near $Y^2 = d/2$ resembles the one in the Nambu-Jona-Lasinio (NJL) model: an effective continuum theory with four-fermion interaction [58]. Namely, there are poles in the four-fermion amplitude in the NJL model corresponding to a massless Goldstone and a massive scalar (t-channel in our approach), a massive vector (s-channel) and a massive scalar difermion (u-channel).

The similarity with NJL model is not a surprise because one can integrate out the scalar degrees of freedom in the model (3.40) and for $\kappa = 0$ obtain a theory with local four–fermion coupling $\bar{\chi}^1_x \chi^1_x \bar{\chi}^2_x \chi^2_x$ (see section 3.2.3). One can also observe that the diagrams that contribute to C_{xy} in our approximation have the same topology as the bubble diagrams in the NJL approach.

(vi) At $\kappa = 0$ in the theory (3.40) one can establish a duality relation between the channels in the four–fermion amplitude:

$$A(a, b, c, d) \equiv \langle \bar{\chi}^1_a \chi^1_b \; \bar{\chi}^2_c \chi^2_d \rangle, \tag{3.55}$$

where a, b, c, d are some sites of the lattice. As we show in appendix D, this amplitude for even distances between the sites a, b, c, d is invariant under a permutation of any of its legs or, in other words, under permutations of the channels s, t, u. For example, see (D.4): $A(a, b, c, d) = A(a, c, b, d)$. This is an exact result.

Turn now to the original theory with the scalar field and arbitrary κ (3.40). We know that there is a pole in the t–channel of the four-fermion amplitude corresponding to the ϕ particle. From duality we derive that there are the same poles in the s– and u– channels at $\kappa = 0$. One can expect by continuity that in some region of nonzero κ the four-fermion amplitude still has poles in the s and u channels. These are obviously the poles that we find in the mean field approximation.

(vii) Consider the (effective) continuum theory defined near $Y^2 \approx d/2$ in the

[5] Remember, however, that the PM-PM boundary at $Y^2 = d/2$ in the $O(4)$ model exists only for the theory with $D < 3$ $SU(2)$ doublets of staggered fermions.

PM' phase. The fermions in this theory do not appear in the low energy spectrum: their masses are larger than the lattice cutoff. However, bound states of fermion–(anti)fermion pairs may have masses smaller than the lattice cutoff and thus remain in the physical spectrum. This resembles the situation with quarks which, being fundamental fermions in the theory, do not appear in the spectrum, but form white ($SU(3)$ *neutral*) bound states.

Pushing this analogy further one can say that fermions at large Y are "confined"[6] in $U(1)$ neutral bosonic states by strong attractive Yukawa forces caused by ϕ particle exchanges. The correlation length of a single fermion has then the meaning of some characteristic size of the bound state. Using this analogy one could give the following heuristic description of the behaviour of the fermion correlation length (or inverse mass) in the region of large Y.

As indicated by earlier Monte Carlo and analytical investigations [34] the fermion correlation length becomes smaller at fixed Y as κ approaches the FM-PM' line from above (see also (3.39)). One can see from the computation of the fermion propagator (3.23) that the fluctuations of the scalar field ϕ are responsible for trapping single fermions. Indeed, it is the property $\langle\phi\rangle_{H=0} = 0$ that makes the fermion propagator vanish in the PM' phase. For the same reason a nonzero contribution to the propagator of the composite field $\chi^1\bar{\chi}^2$ comes only from the terms in (3.46) where two fermion chains are glued together. As we decrease κ the fluctuations of the scalar field become stronger (they are frozen near $\langle\phi\rangle = 1$ at $\kappa = \infty$) and the binding force effectively increases. Then the characteristic size of the bound state becomes smaller. The fermion correlation length also becomes smaller as Y grows. This happens because the binding due to the Yukawa attraction becomes stronger.

[6] Bearing in mind the considerable difference with confinement in the case of QCD we use quotes here.

3.6 Unitarity and the PM–AM line

In this section we discuss the continuum limit at the PM–AM phase transition line. We argue that one cannot define a physical theory in this limit.

We use the $O(4)$ theory as an example. This theory in $d = 4$ is the most realistic approximation of the Higgs–fermion sector of the electroweak theory and it was extensively studied by the Monte Carlo method in [51–53]. In particular, the behaviour near the point A on the phase diagram (see fig. 3.7) attracted considerable interest [17,52.53]. The results are the same in the Z_2 and $U(1)$ models. We shall omit the index of the scalar field components in the following as it does not play any role here.

We can use the transformation (2.82):

$$\begin{array}{lll} \kappa \to -\kappa, & & \phi_x \to \zeta_x \phi_x, \\ Y \to -iY, & \chi_x \to \exp(i\zeta_x \frac{\pi}{4})\chi_x, & \bar{\chi}_x \to \exp(i\zeta_x \frac{\pi}{4})\bar{\chi}_x. \end{array} \tag{3.56}$$

to relate the continuum theory at the PM–AM line at small Y to the continuum theory at the PM–FM line at small Y. The action of the model (2.85) is invariant under this transformation.

The fluctuations that acquire long correlation length near the PM–AM line are the fluctuations of the staggered scalar field: $\phi^{\rm st}_x = \zeta_x \phi_x$, where, as usual, $\zeta_x = (-1)^{x_1+\ldots+x_4}$. In other words, the soft modes of the field $\phi^{\rm st}_x$ define the continuum scalar field at the PM–AM line. The transformation (3.56) shows that the lattice theory for the field $\phi^{\rm st}_x$ is the same as the lattice theory for ϕ_x with $\kappa \to -\kappa$ and $Y \to -iY$. In particular, the continuum limit for the soft modes of the field $\phi^{\rm st}_x$ at $\kappa \approx -\kappa_c$ and small Y (at the PM–AM line) is the same as the continuum limit for the soft modes of the field ϕ_x at $\kappa \approx \kappa_c$ and small *imaginary* Y.

The continuum limit at the point $\kappa \approx \kappa_c$ and small *real* Y (at the PM-FM line) is a scalar–fermion theory with weak Yukawa coupling.[7] The same theory with imaginary Yukawa coupling is not physical. Indeed, the Lagrangian of such a theory (back in the Minkowski space) is complex. This means that this theory is not unitary: the sum of the probabilities of all outcomes of a process is not unity.

To see this more explicitly one can use the optical theorem: one of the manifestations of the unitarity. This theorem relates the imaginary part of the forward scattering amplitude (the loss of the probability from the forward channel due to the scattering) to the total cross section (the probability of all final scattering states).

[7] This continuum limit is discussed in the section 3.4. Due to the triviality of the theory what we actually mean by the continuum limit is in fact an *effective* theory with remote but finite cutoff: $\Lambda \gg m$ (see also 1.3.2).

Formally, one can apply this theorem to the propagator of the scalar field ϕ. To lowest order in the Yukawa coupling the optical theorem for the scalar propagator has the form which is represented in fig. 3.10 by Feynman diagrams.[8] If we replace the real Yukawa coupling y by iy the left hand side changes sign while the right hand side does not. Thus the unitarity relation for the scalar propagator is violated for imaginary Yukawa couplings (for the small couplings at least).

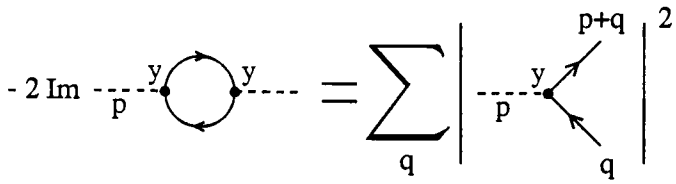

Figure 3.10: The unitarity relation for the scalar propagator in the lowest order in the Yukawa coupling y.

There is another, rather instructive, way to see that something is wrong with the unitarity of the theory in the continuum limit at the PM–AM line. One can look at the wave function renormalisation constant of the field ϕ^{st}.

In a physical theory one would expect the wave function renormalisation constant of a given field $\phi(x)$ to obey: $Z \leq 1$ [59]. This is again a consequence of unitarity. To see this one can use the dispersion relation (Källén - Lehmann spectral representation [59]) for the propagator of the field ϕ:

$$G(p) = \frac{Z}{p^2 - m^2 + i\epsilon} + \int d\mu^2 \frac{\rho(\mu^2)}{p^2 - \mu^2 + i\epsilon}, \tag{3.57}$$

where the integral is over all possible invariant masses squared of the states in the continuum spectrum: many particle states created by ϕ acting on the vacuum (e.g., fermion–antifermion pairs). The spectral function $\rho(\mu^2)$ is the probability density of creating multiparticle states with a given invariant mass μ by the field ϕ. Indeed, using a formal relation:

$$\mathrm{Im}\,\frac{1}{x + i\epsilon} = -\pi\delta(x), \tag{3.58}$$

one can find:

$$-\frac{1}{\pi}\,\mathrm{Im}\,G(p) = Z\delta(p^2 - m^2) + \rho(p^2), \tag{3.59}$$

which is the optical theorem for the propagator. We conclude that $\rho(\mu^2)$ is nonnegative.

[8]The imaginary part of the propagator exists for the off–shell values of momentum of the scalar field: $p^2 > 4m_F^2$, when the creation of a fermion–antifermion pair is kinematically allowed: see also (3.59). There is also a δ-function contribution at $p^2 = m^2$ from the one ϕ particle state. We refer here to the momentum in Minkowski space. In Euclidean space the corresponding values of the momenta are imaginary: $p_E^2 < -4m_F^2$ and $p_E^2 = -m^2$

The field $\phi(x)$ is the bare field: its normalisation is fixed by the condition that the kinetic term in the bare Lagrangian is $(1/2)\partial_\mu\phi\partial^\mu\phi$. In the continuum theory this means that at very high momenta p the propagator: $G(p) \to 1/p^2$. Taking this limit in (3.57) we arrive at:

$$1 = Z + \int d\mu^2\, \rho(\mu^2). \tag{3.60}$$

— the relation for Z found by Källén and Lehmann [59].[9] In essence, this is a sum rule for the probabilities of creating all possible states by the operator $\phi(x)$. It tells us that Z — the probability of creating the one ϕ particle state — is unity for the free field and receives a strictly negative contribution from any additional state (e.g., the fermion–antifermion pair) which can be created by the field ϕ due to the interaction.

Now we apply these ideas to study the continuum limit of the lattice theory near the PM–AM line and compare it to the continuum limit at the PM–FM line. One can find the wave function renormalisation constant of the scalar field numerically by Monte Carlo. One computes the propagator $\langle\phi_x\phi_y\rangle$ and finds its Fourier transform $G(p)$. If we are interested in the continuum limit near the PM–FM line we need to look at the behaviour of $G(p)$ at small p, which corresponds to the soft modes of the field ϕ_x. For the continuum limit near the PM–AM line we are interested in the behaviour of $G(p)$ at p close to the opposite corner of the Brillouin zone: $(\pi, \pi. \pi, \pi)$. This corresponds to the soft modes of the field $\phi^{\rm st}_x = \zeta_x\phi_x$.

The renormalisation constant of the field ϕ_x is the residue in the pole near $p = 0$. The renormalisation constant of the field $\phi^{\rm st}_x$ is the residue in the pole near $p = (\pi, \pi. \pi, \pi)$. These constants were computed numerically in [53]. The authors of [53] use a clever fit to the propagator $G(p)$. It includes the contributions of the poles near $p = 0$ and $(\pi, \pi. \pi. \pi)$ with residues Z and $Z^{\rm st}$ and also a contribution of the two particle fermion–antifermion states. The parameters Z. $Z^{\rm st}$ are fitted then (together with the renormalised Yukawa coupling and the particle masses).

To use the Källén–Lehmann relation (3.60) we have to normalise the fields ϕ and $\phi^{\rm st}$ first. We recall from sections 1.3.1 and 1.4.1 that to obtain the lattice model we rescaled the scalar field by a factor 2κ. In other words, the lattice version of the kinetic term $(1/2)\partial_\mu\phi(x)\partial^\mu\phi(x)$:

$$\frac{1}{2}\sum_\mu(\varphi_{x+\hat\mu} - \varphi_x)^2. \tag{3.61}$$

[9]The equations (3.57) and (3.60) might not be very well defined due to the ultraviolet divergences (the integrals over μ^2 diverge). We neglect this problem here, assuming that the theory is made finite by some suitable regularisation.

would give the hopping term in the lattice action:

$$-\sum_{x,\mu} \phi_x \phi_{x+\hat{\mu}},$$

while our action has additional factor 2κ in front. This means that the residue in the pole of the propagator $\langle \phi_x \phi_y \rangle$ should be multiplied by 2κ to obtain the wave function renormalisation constant of the continuum field $\phi(x)$. Near the PM–FM line the continuum field $\phi(x)$ is given by the soft modes of $\sqrt{2\kappa}\phi_x$ and the wave function renormalisation constant is $Z_{\rm cont} = 2\kappa Z$. Near the PM–AM line the continuum field $\phi(x)$ is given by the soft modes of $\sqrt{-2\kappa}\,\zeta_x \phi_x$. This is because the theory of the field $\zeta_x \phi_x$ is the same as the theory of ϕ_x with $\kappa \to -\kappa$. The wave function renormalisation constant of the continuum field near the PM–AM line is then $Z^{\rm st}_{\rm cont} = -2\kappa Z^{\rm st}$.

In table 3.2 we show the Monte Carlo data for the constant Z near the PM–FM line and in table 3.3 — for the constant $Z^{\rm st}$ near the PM–AM line. We see that near the PM–FM line the constant $Z_{\rm cont}$ is less than unity as we expected from (3.60).

Table 3.2: The Monte Carlo data [60] for the constant Z and the renormalisation constant $Z_{\rm cont}$ of the continuum field $\phi(x) = \sqrt{2\kappa}\,\phi_x$ near the PM–FM line in the theory (2.85) with $D = 8$. The two sets of 3 points are taken on two vertical lines at constant Y approaching the critical line from the FM phase (compare with the phase diagram in fig. 3.7). The measure of the distance from the critical line is the mass of the scalar particle in lattice units. For the first set of 3 points it is: m =(0.08, 0.05, 0.02), and for the second set: (0.20, 0.16, 0.12). The data in the tables 3.2 and 3.3 are from 8^4 lattice.

Y	κ	Z	$Z_{\rm cont} = 2\kappa Z$
0.2	0.30	1.47(4)	0.88(2)
0.2	0.28	1.59(6)	0.89(3)
0.2	0.26	1.57(14)	0.82(7)

Y	κ	Z	$Z_{\rm cont} = 2\kappa Z$
0.4	0.24	1.23(10)	0.59(5)
0.4	0.22	1.27(7)	0.56(3)
0.4	0.20	1.42(9)	0.57(4)

An interesting observation: the wave function renormalisation constant $Z_{\rm cont} = 2\kappa Z$ becomes negative at negative κ as we follow the PM–FM line! We already discussed the problem of relating the continuum and lattice *classical* theories at negative κ in 3.4. Here we can add that from the point of view of the Källén–Lehmann relation (3.60) negative $Z_{\rm cont}$ corresponds to the situation when the spectral integral $\int d\mu^2\, \rho(\mu^2)$ becomes larger than unity and oversaturates the left hand side of (3.60). This happens at some point as the Yukawa coupling grows. However, one can smoothly continue to larger Yukawa couplings using a *negative* kinetic term for the scalar field in the bare (classical) Lagrangian: $\kappa < 0$. The physical theory at low energy–momentum scale will be the same as for positive κ (see section 3.4).

Now we turn to the continuum theory for the staggered scalar field ϕ^{st} at the PM–AM line. Here we see that the constant Z^{st}_{cont} is *greater* than unity (table 3.3). This agrees with our perturbative considerations earlier in this section. The contribution of the spectral integral in (3.60) has the wrong sign. This means that the continuum theory at the PM–AM line contains states with negative norm, for which the probability of being created by the field $\phi(x)$ is negative.

Table 3.3: The Monte Carlo data [60] for the constant Z^{st} and the renormalisation constant Z^{st}_{cont} of the continuum field $\phi(x) = \sqrt{-2\kappa}\,\phi^{st}_x$ near the PM–AM line. The points lie on the horizontal line $\kappa = -0.72$ just above the point A on the phase diagram (see fig.3.7). The first two points are in the PM phase, the last two are in the FM phase. The distance from the continuum limit is characterised by the mass of the staggered scalar. It was measured very approximately: $m^{st} = 0.4 \div 0.8$.

Y	κ	Z^{st}	$Z^{st}_{cont} = -2\kappa Z^{st}$
0.95	−0.72	1.78(14)	2.56(20)
0.98	−0.72	1.96(9)	2.82(13)
1.02	−0.72	1.65(26)	2.38(37)
1.06	−0.72	1.61(10)	2.32(14)

Unitarity of a Euclidean (in particular, lattice) theory is closely related to reflection positivity [61]. Reflection positivity requires that if we divide the Euclidean space by a hyperplane $x_4 = 0$ (x_4 is the Euclidean time) and consider observables that depend on the field variables from one half of the Euclidean space only, then the vacuum expectation values of all quantities which can be written as products of such two observables related to each other by reflection of the Euclidean time axis are positive. For example, in the scalar theory the simplest quantity of this sort is: $\langle\phi(x_4, \boldsymbol{x})\phi(-x_4, \boldsymbol{x})\rangle$. In more complicated theories the time reflection can be accompanied by a suitable conjugation–like transformation of the fields. In some sense reflection positivity is the condition that all probabilities in the theory are positive. Unitarity of a theory follows from reflection positivity.

It is possible to prove reflection positivity in scalar–fermion theories at positive κ [44]. It means that the theory at positive κ is unitary. However, at negative κ no proof has been found, to our knowledge. The nonunitarity of the theory near the PM–AM line means that no such proof should exist. Reflection positivity is *not* a necessary condition for unitarity. The existence of a unitary theory in the continuum limit at the PM–FM line at $\kappa < 0$ does not contradict the absence of reflection positivity.

Chapter 4

Summary and conclusions

The scalar–fermion theory with Yukawa interaction was first introduced to describe the low energy properties of hadrons [62]. In the context of the electroweak theory the scalar–fermion Yukawa model can be an approximation for the Higgs–fermion sector. Such an approximation is good in the case when the masses of the Higgs particle and of some fermions are large compared to the electroweak scale. This is because the mass of the Higgs is proportional to the (square root of) the effective scalar ϕ^4 coupling and the mass of the fermion to the effective Yukawa coupling. When these masses are large the corresponding couplings are large also and one can neglect the interactions governed by the small electroweak gauge couplings and the Yukawa couplings to light fermions.

In the pure scalar theory, which is an approximation to the Higgs sector in the absence of heavy fermions, one finds that the mass of the Higgs can not exceed some 700 GeV. The scalar self coupling gets screened by a cloud of virtual scalar particles very much like the electric charge is screened in quantum electrodynamics by a cloud of electron–positron pairs. The effective coupling λ_{eff} measured at the physical scale m_H as a function of the bare coupling λ at a given scale $\Lambda > m_H$ is saturated at some finite value as $\lambda \to \infty$. The largest possible λ_{eff} one obtains for the lowest Λ/m_H and $\lambda \to \infty$. From the lowest sensible cutoff, $\Lambda/m_H \approx 3$ one then obtains an upper bound on λ_{eff}. This bound due to the relation: $m_H = \sqrt{8\lambda_{\text{eff}}}(246$ GeV) translates into the bound on the Higgs mass.

It would be interesting to understand how the presence of a heavy fermion can affect the upper bound on the Higgs mass. If the Yukawa theory is also trivial then similar arguments would lead to a bound on the effective Yukawa coupling y_{eff} and consequently on the fermion mass $m_F = y_{\text{eff}}(246$ GeV). Assuming the applicability of perturbation theory one can estimate this bound which turns out to be of the order of 500 GeV [22]. To establish this bound properly one needs to study the

scalar–fermion Yukawa theory nonperturbatively. The lattice regularisation is the most powerful method suitable for this purpose.

Another interesting question is whether the introduction of the Yukawa interaction can solve the triviality problem of the Higgs sector of the electroweak theory. The problem is that one cannot remove the cutoff in the theory while keeping finite the interaction between particles. In other words, the electroweak theory can exist only as an effective theory applicable only in the range of energies up to some cutoff Λ. This is not very disastrous, as this only means that at the energy scale around Λ some new physics should exist. However, it would be very appealing from the conceptual point of view if the theory with Yukawa interaction could be applicable for arbitrarily high energy scales. In the lattice regularisation this would mean that there is another universality class of lattice theories, different from the universality class of the free theory. This universality class would describe the interacting scalar–fermion continuum theory. The search for such a possibility is another task for nonperturbative (in particular, lattice) studies.

The present work aims at more moderate goals. We study the phase structure of the scalar–fermion models. We are mainly interested in finding critical points on the phase diagram where physically interesting continuum limits can be defined. This knowledge is crucial for a more detailed investigation which could determine the upper bounds on the Higgs and fermion masses and which might tell us if the Yukawa theories can be nontrivial.

Besides the realistic model with four component scalar field we consider also somewhat simplified models with one and two component scalar fields. We choose one of the most straightforward discretisations of the Yukawa model. We use staggered fermions to reduce the number of fermion species in the continuum theory. The lattice approximation for the Yukawa term is given by the product of lattice fermion, antifermion and scalar fields in one lattice site. Other discretisations are possible. The dependence on the choice of the lattice action is studied, for example, in [36].

We also do not attempt to make our models chiral. In other words, our models contain equal numbers of left– and right–handed fermion fields which interact in the same way. This is not the case for the known fermions in the Standard Model. The problem of discretising a chiral theory is very fundamental and is still unsolved [16,18,26–28]. We expect, however, that for the questions we are interested in, such as the upper bounds on the Higgs and fermion masses and the triviality of the Yukawa theory, the chirality of the theory is not crucial.

We apply a mean field approximation to study the phase diagrams of the scalar–

fermion models. In the Ising and similar spin models it is known that one can calculate the phase transition point with about 20% error. To apply the mean field approximation to scalar–fermion models we integrate over the fermionic variables in the partition function of the model. This leads to a pure bosonic theory with the action containing the contribution of the fermion determinant:

$$S_{\text{eff}} = S_B - \ln \det M.$$

To compute the partition function Z (or the free energy $NW = -\ln Z$, N is the number of the lattice sites) of the model we approximate the average over the configurations of the scalar field ϕ_x with the weight

$$\exp(-S_B + \ln \det M)$$

by the average over the configurations of the uncorrelated random field with the weight:

$$\exp(\sum_x H\phi_x).$$

The mean field H is a parameter which is determined by the condition that the mean field free energy $\tilde{W}(H)$ is minimal.

In the Ising model one can compute the mean field free energy exactly and obtain the (self consistency) equation for the mean field H. Depending on the value of the hopping parameter the minimum of the mean field free energy $\tilde{W}(H)$ is at the origin, $H = 0$. or at nonzero values of H. The point where the minimum at the origin becomes unstable and nonzero minima appear is the phase transition point from the symmetric to the broken phase.

In the scalar–fermion models we cannot compute the mean field free energy exactly. The problem is in computing the average over the configurations of the random field ϕ_x of $\ln \det M$. We can expand this quantity in powers of the Yukawa coupling Y or in powers of $1/Y$. One can compute only the first few terms in this expansion exactly. We recall, however, that the mean field approximation should become exact in the limit $d \to \infty$. Thus we can obtain the leading behaviour in this limit by keeping only the leading contributions in the $1/d$ expansion of the terms in $\ln \det M$. We also notice that one needs to know $\tilde{W}(H)$ only up to powers H^2 or, which is the same, $\sigma^2 \equiv \langle \phi_x \rangle_H = O(H)$, to study the *local* stability of the symmetric phase. With this in mind we take every order in the Y or $1/Y$ expansion of the $\ln \det M$ and compute it in the large d limit up to the power σ^2 Then we sum these contributions.

In such a way we obtain the mean field free energy $\tilde{W}(H)$ to the order H^2 in the large d limit. The origin $H = 0$ is always an extremum of $\tilde{W}(H)$ due to the

symmetry of the model. It is a *local* minimum or maximum depending on the sign of the H^2 term. This term vanishes at the second order phase transition between the symmetric and the broken phases. Thus the condition

$$\left.\frac{\partial^2 \tilde{W}(H)}{\partial H^2}\right|_{H=0} = 0$$

determines the critical points on the phase diagram of the scalar–fermion model.

In this way we obtain the lines of second order phase transitions in Chapter 2. We cannot firmly establish how far from the points $Y = 0$ and $Y = \infty$ these equations are applicable. However, one obtains a self consistent picture in the large d limit if the regions of applicability of the Y and $1/Y$ expansions merge along the vertical line $Y = \sqrt{d/2}$.

A somewhat similar approach to calculating the phase transition lines at large d is used in [46]. It is also based on the $1/d$ expansion. It is useful to compare the two approaches. The authors of [46] perform a systematic expansion in powers of $1/d$ of the $\ln\det M$. An important difference is that the $1/d$ order of each term in this expansion is determined by fixing $Y = O(d)$ in the large d limit. Such an expansion gives a better estimate at large Y of order d. However, it does not tell us anything about the behaviour of the system at the intermediate values of Y of order $\sqrt{d}$. This is the region where the most interesting phase structure is observed. The limit $d \to \infty$ in our approach corresponds to keeping $Y = O(\sqrt{d})$. This comes about naturally when we find that the leading term in the limit $d \to \infty$ in each given order $1/Y^{2n}$ is proportional to d^n.

We observe that the transition from the symmetric (paramagnetic) to the antiferromagnetic phase can be related to the para–ferro transition by a transformation: $\kappa \to -\kappa$ and $Y^2 \to -Y^2$. For example, the phase transition lines are related by such a transformation. Note, however, that this transformation is not a simple geometrical mapping between the lines. It involves analytical continuation to imaginary Y. We also study the continuum limit near the PM–AM line and find that the theory defined in this limit is not unitary.

We compare our results to available Monte Carlo data for the phase diagrams of the scalar–fermion theory. The agreement is a strong argument for the validity of our methods. In particular, one can see that the higher powers in Y and $1/Y$ expansions are essential to this agreement.

In Chapter 3 we extend our methods to study the properties of different phases. We find that there are two distinct symmetric phases. In both of them the vacuum expectation value $\langle\phi\rangle$ of the scalar field vanishes. The fermions, however, behave differently.

In the symmetric phase at small Y the fermions are massless. This agrees with the expectation from perturbation theory: $m_F = y\langle\phi\rangle$. Also, one can notice that the explicit mass term $m\bar{\psi}\psi$ violates the (chiral) symmetry of the model: the term $\bar{\psi}\psi$ is an isovector under this symmetry (in the Z_2 model it changes sign under the Z_2 transformation). Thus it is natural to expect fermions to be massless in the symmetric phase.

From this point of view the symmetric phase PM' at large Y is very interesting. The fermions are massive in this phase. More precisely, their masses are very large in lattice units. This means that the continuum limit taken on the critical line separating this phase from the FM phase does not contain fermions as physical degrees of freedom. Such a situation is often called decoupling of the fermions. This phase was first described independently in [36,37].

The nature of the PM' phase is still not understood completely. There is no contradiction between the symmetry of the model and the existence of the fermion mass. In principle, the symmetry of the model allows to build mass terms which mix different fermion species. In other words, one can realise the chiral symmetry in the fermion spectrum in two ways: massless fermions or parity doublets with equal masses. However, it is not clear how to write down the corresponding mass terms explicitly. Such a point of view also does not explain why the fermions are *so* massive.

We study the properties of the PM' phase in somewhat more detail. We compute the four–fermion correlator in the mean field approximation and find that it has poles in channels with quantum numbers different from the fundamental scalar field ϕ. This means that the fermions can form bosonic bound states.

It is quite natural to expect bound states to appear when the Yukawa coupling is large enough. For relatively small Yukawa couplings one can illustrate this on a simple example. Consider a nonrelativistic problem of two massive fermions interacting via exchange of a massive scalar (Yukawa interaction).[1] If the scalar is light and the Yukawa coupling is small one can estimate that the binding energy is of order $y^4 m_F$ and the size of the bound state is of order $(y^2 m_F)^{-1}$. These estimates are the same as in the nonrelativistic Coulomb system. For this approximation to be valid the Yukawa potential should be close to the Coulomb one at the distances where the bound state wave function is not small. This means the mass of the scalar mediating the interaction should be small enough: $m \ll y^2 m_F$. The Yukawa coupling should be also small for the nonrelativistic approximation to be valid: the typical velocity of the fermion is of order y^2. On the other hand, if the typical size of

[1]The author thanks P. Hasenfratz for suggesting this example.

the bound state, $(y^2 m_F)^{-1}$, is too large compared to the range of the Yukawa interaction m^{-1} the potential is not wide enough to hold a bound state. The condition for the bound state to exist can be written as a condition on the Yukawa coupling: $y^2 > \text{const}\,(m/m_F)$. However, the bound states which we observe in our lattice approach occur at large values of the Yukawa coupling when such approximations are not possible.

Another important observation is that the mass μ of the bound state *in lattice units* vanishes at $Y^2 = d/2$. In our approximation this coincides with the boundary between the PM' and PM phases. If this remains true outside the mean field approximation one can define a continuum theory at the PM–PM' line. The physical spectrum will consist of the bound state bosonic particles. The fermions will not appear in the continuum limit in the PM' phase: their masses are very large in lattice units.

One can then imagine another possible interpretation of the PM' phase. The fermions in this phase are not physical degrees of freedom but form bosonic states which appear in the physical spectrum. The binding of fermions into bosonic states and their disappearance from the spectrum could be part of the same phenomenon. The situation is similar to QCD in some respects. In both cases a single fermion (a quark) can not propagate but a bound state of two quarks with opposite color charges (white, or color neutral, state) can propagate. However an important difference is that QCD is an asymptotically free theory: the interaction becomes small at small distances. The confinement of quarks in QCD is a large distance (infrared) phenomenon. The Yukawa interaction, in contrast, grows at smaller distance scales. The binding that we observe in the Yukawa theory is an ultraviolet phenomenon. It could be even that the scale of it is intrinsically the scale of the lattice cutoff.[2] It would be interesting to study this phenomenon in greater detail and understand what physical situations (if any) it could describe. For example, it could play a role in possible scenarios of a strongly interacting Higgs sector or in composite Higgs boson models.

The fact that the behaviour of the fermions is different at small and large Yukawa couplings in the FM phase near the critical line separating broken and symmetric phases was first observed in [34] using the quenched approximation. The fermion mass vanishes at this line at small Y and grows as one approaches this line at large Y. The authors of [34] conjectured that the change from one behaviour to the other

[2]Strong dependence on the regularisation can be seen from the fact that there is no PM' phase if one discretises the Yukawa interaction in another way, taking the product of fermion, antifermion fields in one site and the average of the scalar field over the 16 sites on a hypercube near this site [33,36].

could happen at some point along this line at intermediate values of Y. This point could then have nontrivial properties. If we assume that the real phase diagram in $d = 4$ at $Y \approx \sqrt{d/2}$ is qualitatively the same as the mean field phase diagram, then this point is where the lines FM–PM, FM–PM' and PM–PM' meet. The points to the left, on the critical line FM–PM at small Y, are in the universality class of the free scalar–fermion theory — the same as in the point $\kappa = \kappa_c$, $Y = 0$. The points to the right, on the FM-PM' line, are in the universality class of the pure scalar model (the fermions decouple). It is possible that the point at $Y \approx \sqrt{d/2}$ defines another universality class. However, we do not see a way to study this question analytically. This could be a task for a Monte Carlo simulation.

In conclusion, the scalar–fermion theories are interesting physical systems. It is very encouraging that some analytical techniques such as, for example, the mean field approximation can be used successfully to study the phase structure of corresponding lattice models. Some of the properties of the scalar–fermion theories are still not understood and deserve further study. This eventually could help us to understand how the masses of the particles of matter are generated.

Appendix A

Gamma matrices

Chiral representation for the Dirac 4×4 γ-matrices in Minkowski space can be chosen in such a way:

$$\gamma_0 = \begin{pmatrix} 0 & 1 \\ 1 & 0 \end{pmatrix}; \qquad \gamma_i = \begin{pmatrix} 0 & -\sigma_i \\ \sigma_i & 0 \end{pmatrix}, \qquad \text{for } i = 1, 2, 3. \tag{A.1}$$

The entries in the matrices are 2×2 matrices themselves. The Pauli 2×2 matrices are as usual:

$$\sigma_1 = \begin{pmatrix} 0 & 1 \\ 1 & 0 \end{pmatrix}; \qquad \sigma_2 = \begin{pmatrix} 0 & -i \\ i & 0 \end{pmatrix}; \qquad \sigma_3 = \begin{pmatrix} 1 & 0 \\ 0 & -1 \end{pmatrix}. \tag{A.2}$$

The γ_5-matrix is:

$$\gamma_5 = i\gamma_0\gamma_1\gamma_2\gamma_3 = \begin{pmatrix} 1 & 0 \\ 0 & -1 \end{pmatrix}. \tag{A.3}$$

The γ_5-matrix is diagonal in this representation. The upper components of a Dirac spinor describe states with chirality $+1$ (right), the down components describe states with chirality -1 (left).

Appendix B

Positivity of $\det M$

Here we argue that the determinant of the fermion matrix in the $O(4)$ model is positive. This is not a proof.

The fermion matrix M is given by:

$$M_{xy} = \frac{1}{2}\sum_{\mu} \eta_{x,\mu}(\delta_{y,x+\hat{\mu}} - \delta_{y,x-\hat{\mu}}) + Y(\phi_x^0 + i\zeta_x \boldsymbol{\tau}\cdot\boldsymbol{\phi}_x)\delta_{xy}. \tag{B.1}$$

This matrix satisfies the identity:

$$M^* = \tau_2 M \tau_2 \tag{B.2}$$

First of all, one can see that the determinant of M is real:

$$(\det M)^* = \det M^* = \det \tau_2 M \tau_2 = \det M. \tag{B.3}$$

Further, one can see that all the eigenvalues of M are either real, or come in complex conjugate pairs. Indeed, if λ is an eigenvalue, i.e.,

$$\det(M - \lambda) = 0.$$

then

$$\det(M - \lambda^*) = \det(\tau_2 M^* \tau_2 - \lambda^*) = \det(M^* - \lambda^*) = (\det(M - \lambda))^* = 0,$$

i.e. λ^* is also an eigenvalue. The degeneracy of these eigenvalues must also coincide because the characteristic equations: $\det(M-\lambda) = 0$ and $\det(M-\lambda^*) = 0$, coincide.

The determinant is a product of the eigenvalues. We see that complex eigenvalues present no problem for the positivity of the determinant. Negative real eigenvalues could make the determinant negative. It seems plausible that one can vary the parameters of the matrix M like Y, ϕ_x^i infinitesimally or add some other small

perturbation which does not destroy the property (B.2) so as to make a given real eigenvalue complex. Then this eigenvalue must split into a complex conjugate pair (or pairs) of eigenvalues. This suggests, that all real eigenvalues have even degeneracy. Then the determinant is positive.

Appendix C

Exact $\det M$ for some configurations of ϕx

Here we calculate the determinant of the fermion matrix M *exactly* for some configurations of the scalar field ϕ_x. We show that this determinant vanishes for some values of Y for these configurations.

The matrix M is given by the equation (1.40):

$$M_{xy} = \frac{1}{2}\sum_{\mu}\gamma_{\mu}(\delta_{y,x+\hat{\mu}} - \delta_{y,x-\hat{\mu}}) + Y\phi_x\delta_{xy}. \tag{C.1}$$

First, we consider the configuration when all the variables ϕ_x are equal to 1 except for one in the site x_0, which is equal to -1:

$$\phi_x = \begin{cases} 1, & x \neq x_0; \\ -1. & x = x_0. \end{cases} \tag{C.2}$$

We choose the coordinates of x_0 to be $(0,0,\ldots,0)$. We denote the matrix M on such a configuration by M_1.

The Fourier transform $(\hat{M}_1)_{pq}$ of the matrix $(M_1)_{xy}$ can be calculated:

$$(\hat{M}_1)_{pq} \equiv \frac{1}{N}\sum_{xy} e^{ipx}(M_1)_{xy}e^{-iqy} = (-i\sum_{\mu}\gamma_{\mu}\sin p_{\mu} + Y)\delta_{pq} - \frac{2}{N}Y \tag{C.3}$$

The first term on the right hand side is a diagonal matrix with indices p and q, the second one is a matrix with *all* matrix elements equal to $-\frac{2}{N}Y$.[1]

It is convenient to normalise $\det M_1$ by $\det M_0$, where M_0 is the matrix M for the homogeneous configuration $\phi_x = 1$:

$$(M_0)_{xy} = \frac{1}{2}\sum_{\mu}\gamma_{\mu}(\delta_{y,x+\hat{\mu}} - \delta_{y,x-\hat{\mu}}) + Y\delta_{xy}. \tag{C.4}$$

[1]The momentum indices p and q are discrete for lattices with finite number of sites N

It is obvious that:

$$\frac{\det M_1}{\det M_0} = \frac{\det \hat{M}_1}{\det \hat{M}_0} = \exp \text{ tr } \ln(\hat{M}_1 \hat{M}_0^{-1}), \tag{C.5}$$

where $\hat{M}_0$ is the Fourier transform of $(M_0)_{xy}$. It coincides with the first term on the right hand side of (C.3). Therefore:

$$(\hat{M}_1 \hat{M}_0^{-1})_{pq} = \delta_{pq} - \frac{2}{N} Y(-i\textstyle\sum_\mu \gamma_\mu \sin q_\mu + Y)^{-1}. \tag{C.6}$$

The tr $\ln(\hat{M}_1 \hat{M}_0^{-1})$ can be now computed expanding around tr $\ln \delta_{pq}$. Finally we obtain using (C.5):

$$\det M_1 = [1 - 2Y^2 F(Y)]^D \det M_0, \tag{C.7}$$

where in the limit $N \to \infty$:

$$F(Y) = \int_{-\pi}^{+\pi} \frac{d^d p}{(2\pi)^d} (\textstyle\sum_\mu \sin^2 p_\mu + Y^2)^{-1} = \int_0^\infty d\alpha \, e^{-\alpha(\frac{d}{2}+Y^2)} \, [I_0(\alpha/2)]^d. \tag{C.8}$$

One can see that $\det M_1$ vanishes at some finite value of Y. In the large d limit (and Y^2 of order d):

$$F(Y) \approx \left(\frac{d}{2} + Y^2\right)^{-1}. \tag{C.9}$$

Thus

$$\det M_1 \approx \left[\frac{d - 2Y^2}{d + 2Y^2}\right]^D \det M_0 \tag{C.10}$$

is zero at $Y^2 = d/2$. Numerically from (C.7), (C.8), for $d = 4$, $\det M_1$ vanishes at $Y \approx 1.3647$.

One can also calculate the determinant of the matrix M^{st} for staggered fermions (1.43) for the configuration (C.2). Actually, one can use the equation (1.42) to deduce from (C.7) that:

$$\det M_1^{\text{st}} = [1 - 2Y^2 F(Y)] \det M_0^{\text{st}}. \tag{C.11}$$

We can not compute the fermion determinant for arbitrary configuration. However, this example suggests that the value $Y^2 \approx d/2$ is singled out and one can expect some change in the properties of the model to occur near it. Also, Monte Carlo simulations in the region $Y \approx 1.4$ ($d = 4$) are very difficult due to the fact that the algorithm of inversion of the matrix M slows down considerably. This is probably due to the fact that for some configurations the $\det M$ vanishes or becomes very small in this region.

Similarly, one can compute the fermion determinant for the totally antiferromagnetically ordered configuration: $\phi_x = \zeta_x$. One can use the transformation of the matrix M which is equivalent to the transformation of the fermion fields in (2.57):

$$M_{xy} \to \exp(i\zeta_x \frac{\pi}{4}) M_{xy} \exp(i\zeta_y \frac{\pi}{4}). \tag{C.12}$$

This transformation does not change the value of $\det M$. The matrix for antiferromagnetic configuration becomes the matrix for the homogeneous configuration $\phi_x = 1$ but with iY instead of Y. One can then compute the determinant using the relation $\det M = \exp \operatorname{tr} \ln M$:

$$\det M_{xy}|_{\phi_x=\zeta_x} = \exp\left\{ D \int_{-\pi}^{+\pi} \frac{d^d p}{(2\pi)^d} \ln |\textstyle\sum_\mu \sin^2 p_\mu - Y^2| \right\}. \tag{C.13}$$

One can notice that there are singularities in the integrand for $0 < Y^2 < d$. They are integrable. However, if one considers a *finite* lattice then the integral is replaced by the sum over the discrete momenta p allowed by the boundary conditions on the fermion fields. In this case the $\det M$ for the antiferromagnetic configuration vanishes at some discrete values of Y. These values are determined by the condition that there is an allowed momentum $p = (p_1, \ldots, p_d)$ for which $\sum_\mu \sin^2 p_\mu = Y^2$. This phenomenon was observed in the study of the $O(4)$ model [51]. This is obviously an artifact of the finite lattice size. It can create problems in Monte Carlo simulations in the region of Y of order $\sqrt{d/2}$ at negative values of κ when the antiferromagnetic configuration is favoured by the bosonic part of the action: S_B. In particular, the FI phase observed in [41] (see fig. 3.5) could be such an artifact.

Appendix D

Duality of the four–fermion amplitude

Here we show that in the theory (3.40) at $\kappa = 0$ the four–fermion amplitude:

$$A(a,b,c,d) \equiv \langle \bar{\chi}^1_a \chi^1_b \; \bar{\chi}^2_c \chi^2_d \rangle, \tag{D.1}$$

is invariant under permutation of any of its legs. This is provided that the sites a, b, c, d are living on the same, even or odd, sublattice.[1]

At $\kappa = 0$ the integration over the field ϕ_x in the partition function is simple and the result is a pure fermionic theory with four–fermion local interaction (sect. 3.2.3). The action of this theory is given by (see (3.29)):

$$S = \sum_{\alpha=1,2} \sum_{xy} \bar{\chi}^\alpha_x K_{xy} \chi^\alpha_y - Y^2 \sum_x \bar{\chi}^1_x \chi^1_x \bar{\chi}^2_x \chi^2_x. \tag{D.2}$$

To prove the duality property take, for example, the permutation $b \leftrightarrow c$ (if $ab \to cd$ is the t–channel and $ac \to bd$ is the u–channel, then the permutation $b \leftrightarrow c$ is equivalent to $t \leftrightarrow u$). Consider the transformation of staggered fermion fields (index x is suppressed for simplicity):

$$\left.\begin{array}{l} \bar{\chi}^1 \to \chi^2 \\ \chi^2 \to -\bar{\chi}^1 \end{array}\right\} \text{for even } x \qquad \text{and} \qquad \left.\begin{array}{l} \chi^1 \to \bar{\chi}^2 \\ \bar{\chi}^2 \to -\chi^1 \end{array}\right\} \text{for odd } x. \tag{D.3}$$

This performs the permutation $b \leftrightarrow c$ in (D.1) (if we take a, b, c, d to be even sites, for definiteness) and leaves, as one can check[2], the action (D.2) of our theory with four–fermion interaction invariant.

[1] A given site x is even, i.e., belongs to the even sublattice, if $x = x_1 + \ldots + x_d$ is even ($\zeta_x \equiv (-1)^x = +1$). All other sites form the odd sublattice.

[2] One should take into account that the fermion variables anticommute.

Thus

$$A(a,b,c,d) = A(a,c,b,d). \tag{D.4}$$

Note that there is no approximation involved. Other permutations could be considered in a similar way.

Bibliography

[1] S.L. Glashow, Nucl. Phys. 22 (1961) 769;
A. Salam, in: Elementary Particle Theory, Eds. N. Svartholm, Almquist & Wiksell, Stockholm 1968, p. 367;
S. Weinberg, Phys. Rev. Lett. 19 (1961) 1264.

[2] P.W. Higgs, Phys. Lett 12 (1964) 132; Phys Rev. Rev. Lett. 13 (1964) 508; Phys. Rev. 145 (1966) 1156;
R. Brout and F. Englert, Phys. Rev. Lett. 13 (1964) 321;
G.S. Guralnik, C.R. Hagen and T.W.B. Kibble, Phys. Rev. Lett. 13 (1964) 585;
T.W.B. Kibble, Phys. Rev. 155 (1967) 773.

[3] J. Goldstone, Nuovo Cimento 19 (1961) 154;
J. Goldstone, A. Salam and S. Weinberg, Phys. Rev. 127 (1962) 965.

[4] M. Veltman Nucl. Phys. B123 (1977) 89;
M.S. Chanovitz, M.A. Furman, I. Hinchliffe, Phys. Lett. B78 (1978) 285;
for a more recent review and experimental data see, e.g., [5,6].

[5] Particle Data Group, Phys. Rev. D45 (1992) 1.

[6] R. Tanaka, in: Proceedings of the XXXI International Conference on High Energy Physics, Ed. J.R. Sanford, AIP Conf. Proc. 1993, p. 681.

[7] R. Dashen and H. Neuberger, Phys. Rev. Lett. 50 (1983) 1897.

[8] For a general introduction into the lattice field theory and Monte Carlo method see, e.g.,
M. Creutz, Quarks, Gluons and Lattices, Cambridge University Press 1983.

[9] The earliest Monte Carlo results on the Higgs mass upper bound from the ϕ^4 model:
C. Whitmer, Ph.D. Thesis, Princeton University, 1983 (unpublished);
M.M. Tsypin, Lebedev Inst. Preprint No.280 (1985); in: Lattice Higgs Workshop, Eds. B. Berg et al, World Scientific, Singapore 1988. p. 258.

This was followed by a number of larger scale and more detailed studies. Some of the papers are listed in refs. [10–13]. For further references see reviews [14–19].

[10] A. Hasenfratz, K. Jansen, C.B. Lang, T. Neuhaus and H. Yoneyama, Phys. Lett. B199 (1987) 531;
A. Hasenfratz, K. Jansen, J. Jersák, C.B. Lang, T. Neuhaus and H. Yoneyama, Nucl. Phys. B317 (1989) 81;
K. Jansen, Nucl. Phys. B (Proc. Suppl.) 4 (1988) 422;

[11] J. Kuti, L. Lin and Y. Shen, Phys. Rev. Lett. 61 (1988) 678; Nucl. Phys. B (Proc. Suppl.) 4 (1988) 397

[12] Monte Carlo methods used together with high temperature expansion in:
M. Lüscher and P. Weisz, Nucl. Phys. B290 (1987) 25; Nucl. Phys. B295 (1988) 65; Phys. Lett. B212 (1988) 472; Nucl. Phys. B318 (1989) 705.

[13] The dependence of the Higgs mass upper bound on the lattice discretisation is studied, e.g., in:
G. Bhanot, K. Bitar, Phys. Rev. Lett. 61 (1988) 798;
G. Bhanot, K. Bitar, U.M. Heller and H. Neuberger, Nucl. Phys. B343 (1990) 467; Nucl. Phys. B353 (1991) 551;
U.M. Heller, H. Neuberger and P. Vranas, Phys. Lett. B283 (1992) 335.

[14] P. Hasenfratz, Nucl. Phys. B (Proc. Suppl.) 9 (1989) 3.

[15] H. Neuberger, Nucl. Phys. B (Proc. Suppl.) 17 (1990) 17.

[16] J. Shigemitsu, Nucl. Phys. B (Proc. Suppl.) 20 (1991) 515

[17] I. Montvay, Nucl. Phys. B (Proc. Suppl.) 26 (1992) 57.

[18] D.N. Petcher, Nucl. Phys. B (Proc. Suppl.) 30 (1993) 50

[19] U.M. Heller, Nucl. Phys. B (Proc. Suppl.) 34 (1994) 101.

[20] B. Freedman, P. Smolensky and D. Weingarten, Phys. Lett. B113 (1982) 481.

[21] N. Cabibbo, L. Maiani, G. Parisi and R. Petronzio, Nucl. Phys. B158 (1979) 295.

[22] M. Lindner, Z. Phys. C31 (1986) 295;
M. Lindner and B. Grzadkowski, Phys. Lett. 178B (1986) 81.

[23] K.G. Wilson and J. Kogut, Phys. Rep. 12C (1974) 75.

[24] A review on triviality of the ϕ^4 see in:
D.J.E. Callaway, Phys. Rep. 167 (1988) 241.

[25] Original papers of Landau et al. (1954) on the triviality of quantum electrodynamics are reprinted in:
L.D. Landau, Collected Papers of L.D. Landau, ed. D. ter Haar, Gordon and Breach, New York 1965.

[26] L.H. Karsten and J. Smit, Nucl. Phys. B183 (1981) 103.

[27] J. Smit, Nucl. Phys. B (Proc. Suppl.) 17 (1990) 3;
M.F.L. Golterman, Nucl. Phys. B (Proc. Suppl.) 20 (1991) 528.

[28] H. Nielsen and M. Ninomiya, Nucl. Phys. B185 (1981) 20; Nucl. Phys. B193 (1981) 173.

[29] N. Kawamoto and J. Smit, Nucl. Phys. B192 (1981) 100.

[30] A discussion of staggered fermions can be found in the review:
J.B. Kogut, Rev. Mod. Phys. 55 (1983) 775.

[31] J. Shigemitsu, Phys. Lett. B189 (1987) 164; B226 (1989) 364.

[32] J. Polonyi and J. Shigemitsu, Phys. Rev D38 (1988) 3231.

[33] J. Shigemitsu, Nucl. Phys. B (Proc. Suppl.) 9 (1989) 96.

[34] A. Hasenfratz and T. Neuhaus, Phys. Lett. B220 (1989) 435.

[35] I-H. Lee, J. Shigemitsu and R.E. Shrock Nucl. Phys. B330 (1990) 225.

[36] I-H. Lee, J. Shigemitsu and R.E. Shrock Nucl. Phys. B334 (1990) 265.

[37] M.A. Stephanov and M.M. Tsypin, Sov. Phys. JETP 70 (1990) 228; Phys. Lett. B236 (1990) 344.

[38] S. Aoki, I-H. Lee, D. Mustaki, J. Shigemitsu and R.E. Shrock, Phys. Lett. B244 (1990) 301.

[39] J. Berlin, A. Hasenfratz, U.M. Heller and M. Klomfass, Phys. Lett. B249 (1990) 485.

[40] D. Stephenson and A. Thornton, Phys. Lett. B212 (1988) 479;
A. Thornton, Phys. Lett. B214 (1988) 577; B221 (1989) 151.

[41] A. Hasenfratz, W. Liu and T. Neuhaus, Phys. Lett. B236 (1990) 339.

[42] M.A. Stephanov and M.M. Tsypin, Phys. Lett. B242 (1990) 432.

[43] L. Lin, I. Montvay and H. Wittig, Phys. Lett. B264 (1991) 407.

[44] L. Lin, I. Montvay, G. Münster and H. Wittig, Nucl. Phys. B355 (1991) 511.

[45] S. Aoki, J. Shigemitsu and J. Sloan, Nucl. Phys. B372 (1992) 361;
J. Shigemitsu, Nucl. Phys. B (Proc. Suppl.) 26 (1992) 507;
J. Sloan and J. Shigemitsu, Nucl. Phys. B (Proc. Suppl.) 30 (1993) 639.

[46] M.F.L. Golterman and D.N. Petcher, Phys. Lett. B247 (1990) 370; Nucl. Phys. B359 (1991) 91.

[47] A. Hasenfratz, K. Jansen and Y. Shen, Nucl. Phys. B394 (1993) 527.

[48] I. Montvay, Phys. Lett. B199 (1987) 89; Nucl. Phys. B307 (1988) 389.

[49] Y. Shen, J. Kuti, L. Lin and P. Rossi, Nucl. Phys. B (Proc. Suppl.) 9 (1989) 26.

[50] J. Berlin and U.M. Heller, Nucl. Phys. B (Proc. Suppl.) 20 (1991) 597.

[51] W. Bock, A.K. De, K. Jansen, J. Jersák, T. Neuhaus and J. Smit, Nucl. Phys. B344 (1990) 207.

[52] W. Bock, A.K. De, C. Frick, K. Jansen and T. Trappenberg, Nucl. Phys. B371 (1992) 683.

[53] W. Bock, A.K. De, C. Frick, J. Jersák and T. Trappenberg, Nucl. Phys. B378 (1992) 652.

[54] M.A. Stephanov and M.M. Tsypin, Phys. Lett. B261 (1991) 109.

[55] A.K. De and J. Jersák, in: Heavy Flavours, eds. A. Buras and M. Lindner, World Scientific, Singapore 1992, p. 732.

[56] R. Balian, J.M. Drouffe and C. Itzykson, Phys. Rev. D10 (1974) 3376;
C. Itzykson, in: Structural Elements in Particle Physics and Statistical Mechanics, New York, Plenum, 1983, p. 61.

[57] M.A. Stephanov, Phys. Lett. B266 (1991) 447.

[58] Y. Nambu and G. Jona-Lasinio, Phys. Rev. 122 (1961) 345, 124 (1961) 246.

[59] G. Källén, Helv. Phys. Acta 25 (1952) 417;
H. Lehmann, Nuovo Cimento 1 (1954) 342;
a good discussion of the spectral representation is in:
D.J. Bjorken and S.D. Drell, Relativistic Quantum Fields. McGraw–Hill 1965.

[60] W. Bock, A.K. De, C. Frick, J. Jersák and T. Trappenberg, private communication.

[61] K. Osterwalder and R. Schrader, Commun. Math. Phys. 31 (1973) 83; 42 (1975) 281.

[62] H. Yukawa, Proc. Phys. Math. Soc. Japan 17 (1935) 48.